DOI:
10.1161/CIRCGENETICS.117.001808

Document Version
Publisher's PDF, also known as Version of record

Original Article

Plasma Proteomics for Epidemiology
Increasing Throughput With Standard-Flow Rates

Xiaoke Yin, PhD; Ferheen Baig, MSc; Eloi Haudebourg, MSc; Richard T. Blankley, PhD; Tejas Gandhi, PhD; Sebastian Müller, PhD; Lukas Reiter, PhD; Helmut Hinterwirth, PhD; Raimund Pechlaner, MD, PhD; Sotirios Tsimikas, MD; Peter Santer, MD; Johann Willeit, MD; Stefan Kiechl, MD; Joseph L. Witztum, MD; Anthony Sullivan, PhD; Manuel Mayr, MD, PhD

Background—Mass spectrometry is selective and sensitive, permitting routine quantification of multiple plasma proteins. However, commonly used nanoflow liquid chromatography (LC) approaches hamper sample throughput, reproducibility, and robustness. For this reason, most publications using plasma proteomics to date are small in study size.

Methods and Results—Here, we tested a standard-flow LC mass spectrometry (MS) method using multiple reaction monitoring for the application to large epidemiological cohorts. We have reduced the LC-MS run time to almost a third of the nanoflow LC-MS approach. On the basis of a comparison of the quantification of 100 plasma proteins in >1500 LC-MS runs, the SD range of the retention time during continuous operation was substantially lower with the standard-flow LC-MS (<0.05 minutes) compared with the nanoflow LC-MS method (0.26–0.44 minutes). In addition, the standard-flow LC method also offered less variation in protein measurements. However, 5× more sample volume was required to achieve similar sensitivity. Two different commercial multiple reaction monitoring kits and an antibody-based multiplexing kit were used to compare the apolipoprotein measurements in a subset of samples. In general, good agreement was observed between the 2 multiple reaction monitoring kits, but some of the multiple reaction monitoring–based measurements differed from antibody-based assays.

Conclusions—The multiplexing capability of LC-MS combined with a standard-flow method increases throughput and reduces the costs of large-scale protein measurements in epidemiological cohorts, but protein rather than peptide standards will be required for defined absolute proteoform quantification. **(*Circ Cardiovasc Genet*. 2017;10:e001808. DOI: 10.1161/CIRCGENETICS.117.001808.)**

Key Words: apolipoprotein ■ cardiovascular disease ■ mass spectrometry ■ precision medicine ■ proteomics

The plasma proteome is among the most challenging biological matrices to analyze.[1] An untargeted proteomics approach results in oversampling of abundant proteins, leaving peptides from low abundant proteins undetected.[2] The selectivity of multiple reaction monitoring (MRM) on the triple quadrupole (QqQ) mass spectrometer (MS) ensures that lower abundant proteins can be targeted using stable isotope-labeled standards (SIS) for absolute quantification.[3,4] MRM has been used as the gold standard in small molecule quantification for decades[5] and has recently been explored for measuring plasma proteins.[6–10] Other MS approaches for plasma proteomics have also been described, including Stable Isotope Standards and Capture by Anti-Peptide Antibodies[6] and data-independent acquisition,[7] but these can add several steps to the work flow and increase data analysis time, limiting the application for epidemiological studies. Instead, throughput and costs are critical considerations for applications in clinical research. The latest high sensitive QqQ MS combined with high-performance liquid chromatography (HPLC) offers the potential to eliminate the need for protein enrichment or fractionation, which limits throughput and also introduces technical variability.[7,11–14] A recent study demonstrated robust analytic performance for MRM analyses across laboratories and instrument platforms,[15] a prerequisite for the advancement of MS-based protein quantification for routine clinical applications.

See Clinical Perspective

Among the numerous potential biomarkers cited in the proteomics literature, only few have obtained regulatory approval.[16] Several clinical studies using targeted plasma proteomics have been published, including both nanoflow[8,17] and

Received April 30, 2017; accepted October 3, 2017.

From the King's British Heart Foundation Centre, King's College London, United Kingdom (X.Y., F.B., E.H., H.H., M.M.); Agilent Technologies Ltd, Cheadle, United Kingdom (R.T.B., A.S.); Biognosys AG, Schlieren, Switzerland (T.G., S.M., L.R.); Department of Neurology, Medical University of Innsbruck, Austria (R.P., J.W., S.K.); School of Medicine, University of California San Diego (S.T., J.L.W.); and Department of Laboratory Medicine, Bruneck Hospital, Italy (P.S.).

The Data Supplement is available at http://circgenetics.ahajournals.org/lookup/suppl/doi:10.1161/CIRCGENETICS.117.001808/-/DC1.

Correspondence to Manuel Mayr, MD, PhD, King's British Heart Foundation Centre, King's College London, 125 Coldharbour Ln, London SE5 9NU, United Kingdom. E-mail manuel.mayr@kcl.ac.uk

standard-flow methods,[9,18,19] but the sample numbers are low (<100). Currently, the preferred high-sensitivity proteomics workflows use nanoflow LC, which is slow in nature and hampered by poor robustness during continuous operation. A previous comparison of standard-flow and nanoflow LC-MRM was limited to 30 samples.[10] The need for validating the applicability of standard-flow MRM method to larger cohorts is apparent.[3,20]

In this study, we have applied a standard-flow LC-MS method to quantify 100 proteins in plasma samples from the community-based, prospective Bruneck cohort (n=668 samples, >1500 injections), which is, to our knowledge, the largest targeted proteomics study on human plasma samples to date.

Methods

The data, analytic methods, and study materials will not be made available to other researchers for purposes of reproducing the results or replicating the procedure because of the limited availability of plasma samples. However, the raw files (a subset of 44 samples) and transition list from both nanoflow and standard-flow platforms were deposited into the PeptideAtlas SRM Experiment Library (Data set Identifier: PASS00949). The MRM data are also deposited into Panorama Public: https://panoramaweb.org/labkey/plasmadive1.url (MacCoss Laboratory Software).

Human Plasma Samples

The human plasma samples were from the year 2000 evaluation of the prospective, community-based Bruneck Study.[21,22] The Bruneck Study protocol conformed to the Declaration of Helsinki and was approved by the Local Ethics Committee (Bolzano, Italy). All participants provided their written informed consent before entering the study. Blood samples were drawn after an overnight fast and 12 hours of abstinence from smoking. Citrate plasma samples were divided into aliquots and stored at −80°C. In this study, the plasma samples (n=668) were used for observation purposes only. The serotransferrin (TRFE) clinical measurement was conducted using a Behring BNA II nephelometer system immediately after the plasma sample collection.

Sample Preparation Using PlasmaDive

Plasma samples were analyzed using the PlasmaDive MRM Panel (beta test version; Biognosys AG, CH). Sample processing was semi-automated on a Bravo liquid handling system (Agilent Technologies). In brief, 10 µL of plasma was denatured, reduced, and alkylated according to the manufacturer's instruction, followed by spiking-in of SIS peptides and an in-solution digestion overnight using trypsin (Thermo Fisher Scientific). After solid-phase extraction cleanup with a 96-well C18 spin plate (Harvard apparatus), the eluted peptides were dried using a SpeedVac (Thermo Fisher Scientific) and resuspended in 40 µL of LC solution with addition of indexed retention time (RT) peptides (Biognosys, CH) to adjust the RT variability across different LC-MS runs. A pooled sample was used as quality control (QC) sample with repeated injections during continuous operation.

Nanoflow HPLC-MRM

On the nanoflow platform (Thermo U3000 RSLCnano; Thermo Fisher Scientific), 2 µL of digested sample was directly injected onto a 15-cm column (Acclaim PepMap 100, C18, 15 cm×75 µm, 3 µm, 100 Å) and separated over a 32-minute gradient at 300 nL/min (0–30 min, 5%–35% B; 30–32 min, 35%–99% B; 32–40 min, 99% B; 40–70 min, 2% B; A=1% acetonitrile, 0.1% formic acid; B=97% acetonitrile, 0.1% formic acid). The nanoflow HPLC was interfaced to a TSQ Vantage MS (Thermo Fisher Scientific). Analysis was performed using the following parameters: Q1 resolution 0.7 Th, Q2 collision gas pressure 1 mTorr, Q3 resolution 0.7 Th. Eight hundred fifty transitions were exported from SpectroDive software version 6 (Biognosys AG, CH) and scheduled with a cycle time of 3 s and a RT window of 4 minutes. The transition list is shown in Table I in the Data Supplement. The SIS peptides were labeled with heavy lysine (+8 Da) or arginine (+10 Da), and the cysteines were carbamidomethylated (+57 Da).

Standard-Flow HPLC-MRM

The same samples were also analyzed on a standard-flow platform (Agilent 1290 Infinity II LC). Ten microliters of digest was directly injected onto a 25-cm column (AdvanceBio Peptide Mapping, C18, 2.1 mm×250 mm, 2.7um, 120 Å) and separated over a 23-minute gradient at 350 µL/min (0–0.5 min, 5%–7.5% B; 0.5–18 min, 7.5%–28% B; 18–20 min, 28%–95% B; 20–23 min, 95% B; 23–27 min, 5% B; A=0.1% formic acid in H_2O; B=0.1% formic acid in acetonitrile) at 50°C. The standard-flow LC was interfaced to an Agilent 6495 QqQ MS, and both were controlled by MassHunter Workstation software (version B.08.00). Both Q1 and Q3 were set at unit resolution (0.7 Th), and the following parameters were used: Delta EMV 350, Frag 380 V, Cell Acc 4 V, Gas Temp 200°C, Gas Flow 11 L/min, Nebulizer 35 psi, Sheath Gas Heater 250°C, Sheath Gas Flow 12 L/min, Capillary 4 kV, VCharging 300, Ion Funnel Pos High-Pressure RF 180 V, and Pos Low-Pressure RF 90 V. Seven hundred sixty-five transitions were scheduled using Dynamic MRM with a cycle time of 0.5 s and a RT window of 0.8 minutes. The transition list is provided in Table II in the Data Supplement.

PlasmaDive MRM Data Analysis

The data were analyzed using SpectroDive, and protein concentrations were calculated using the light/heavy ratio and the concentration of spiked-in SIS peptides. The data with a Q value <0.01 were included in the final results.

Sample Preparation for Standard Curve

Pooled human plasma was digested using the PlasmaDive protocol (Biognosys, CH) without SIS peptides. Then 2 pools were made: pool 1, 90 µL of digested plasma +30 µL of SIS peptides; and pool 2, 450 µL of digested plasma+100 µL of LC solution (5% acetonitrile, 0.1% formic acid)+50 µL of 10x iRT standard (Biognosys, CH). Pool 1 represents 1× SIS in plasma matrix, and pool 2 is the background plasma matrix. Serial dilutions of SIS peptides were performed in plasma matrix (1:10, 1:100, 1:1000, 1:10 000, 1:100 000). The same procedure was followed to make serial dilutions of SIS peptides in LC solution (5% acetonitrile, 0.1% formic acid) only. On the nanoflow HPLC system, the injection volume was 3 µL. On the standard-flow HPLC system, the injection volume was 15 µL. The limit of detection was calculated by using the mean response of the blank samples+3×SD. The limit of quantification was calculated by using the mean response of the blank samples+10×SD.

Enzyme-Linked Immunosorbent Assays

The levels of platelet factor 4 (PLF4) were measured using the DuoSet ELISA Development kits (DY795) and the DuoSet Ancillary Reagent Kit 2 (DY008, R&D Systems, Minneapolis) according to the manufacturer's instructions. Absorbance at 450 nm was measured on a Tecan Infinite 200 Pro plate reader (Tecan Group Ltd, Männedorf, Switzerland) using 570 nm as a reference wavelength. Results were calculated using a 4-parameter logistic fit.

PeptiQuant MRM Assay Biomarker Assessment Kit (BAK-76, MRM Proteomics)

The plasma samples were processed according to the manufacturer's instruction. In brief, the individual plasma samples were diluted 1:10 using 25 mmol/L ammonium bicarbonate first, and pooled plasma was used as reference sample. Thirty microliters of diluted plasma sample or pooled plasma (×4 wells) was mixed with 177 µL of 25 mmol/L ammonium bicarbonate and 37 µL of 10% sodium deoxycholate to denature proteins. The proteins were reduced by 5 mmol/L

tris(2-carboxyethyl) phosphine and alkylated by 10 mmol/L iodoacetamide. The remaining iodoacetamide was quenched by adding 10 mmol/L dithiothreitol. Trypsin solution (23.3 μL; 0.9 mg/mL; Affymetrix) was added and the samples incubated at 37°C for 16 hours. Six dilutions (from 0.5 to 250 fmol/μL) of the SIS peptide mixture for reference samples were prepared for the reference samples. Fifty microliters of the SIS peptide mixture for reference samples was added to 227 μL pooled reference plasma digest and 277 μL of 1% formic acid. Next, 227 μL of each plasma digest was mixed with 50 μL of 25 fmol/μL SIS peptide mixture for the experimental samples and 277 μL of 1% formic acid. After centrifugation at 12 000*g* for 10 minutes, 444 μL of peptide supernatant was desalted and concentrated by solid phase extraction (Oasis HLB Extraction Cartridge, Waters). The eluted peptides were freeze-dried and resuspended in 100 μL of 0.1% formic acid. Each reference sample (standard A–F) was injected 3× using 15 μL per injection, and each experimental sample was injected once using 15 μL per sample. The samples were run on the standard-flow platform (Agilent 1290 Infinity II LC with 6495 QqQ MS) and analyzed using MassHunter Quantitative Analysis (Agilent) and Qualis-SIS (University of Victoria, Canada) following the manufacturer's instructions.

Milliplex Map Human Apolipoprotein Magnetic Bead Panel Kit

Apolipoproteins (apo) were measured using Milliplex Map Human Apolipoprotein Magnetic Bead Panel Kit, 96-well plate assay (Cat No. APOMAG-62K, Millipore) following the manufacturer's instructions. In brief, plasma samples were diluted 1:4000 in the assay buffer in duplicate, and 10 μL of diluted plasma was used per well. One hundred fifty microliters of each antibody-immobilized bead for apoA1, apoA2, apoC2, apoC3, and apoE was mixed and topped up to 3 mL with Bead diluent. QC1, QC2, and the apolipoprotein calibrator cocktail were reconstituted with 250 μL deionized water and mixed thoroughly. The calibrator was further diluted to 1:5, 1:25, 1:125, 1:625, 1:3125, 1:15 625, in Assay buffer. After washing and drying the plate, 65 μL of Assay buffer, 10 μL of Assay buffer/serial dilution of calibrators/QC1/QC2/diluted samples, and 25 μL of the premixed beads were added to each well before the plate was sealed, wrapped in foil, and incubated at 700 rpm for 1 hour at room temperature. A handheld magnetic plate was used to gently remove well contents, and the plate was washed 3× using the Washing buffer. Subsequently, 50 μL of detection antibodies mixture was added to each well, and the plate was incubated at 700 rpm for 30 minutes at room temperature. The wash step was repeated before adding 50 μL of streptavidin–phycoerythrin per well for a final incubation of 30 minutes. After a third wash step, the plate was prepared for analysis on FlexMap 3D by resuspending the beads in 100 μL of sheath fluid on a plate shaker for 5 minutes. The median fluorescent intensity data were analyzed to calculate apolipoprotein concentrations in the samples. A dilution factor of 4000 was applied to the concentrations to correct for the sample dilution, and an average of the 2 technical replicates of each sample was calculated.

Statistics

Agreement of nanoflow and standard-flow measurements for all proteins measured was described graphically by overlaying 95% data ellipses on the x=y line indicating perfect agreement. Agreement of nanoflow and standard-flow measurements with independent reference measurements for 2 exemplary proteins (TRFE and PLF4) was analyzed by means of Bland–Altman plots,[23] and the dependence of measurement difference on measurement mean was summarized by ordinary least squares regression lines. Both proteins were log transformed toward normality beforehand. Agreement between PlasmaDive, PeptiQuant BAK-76, and Luminex measurements was analyzed using scatter plots, Pearson correlation, and Deming regression, which in contrast to ordinary least squares regression considers error in both x and y. Comparative performance of nanoflow and standard-flow methodology in a clinical context was evaluated by comparing associations with the same clinical variables of measurements produced by either method. Significance of association was derived from Pearson correlation analysis, except for the categorical clinical variables sex and diabetes mellitus, for which Student *t* tests were used. Analyses were conducted using R 3.3.2.

Results

Plasma Proteomics in a Community-Based Cohort

MRM-MS was applied to plasma samples of the prospective, community-based Bruneck study (n=668, year 2000 evaluation) using nanoflow LC-MS (Ultimate3000 RSLCnano interfaced to a TSQ Vantage QqQ MS; Thermo Fisher Scientific) as recommended by the manufacturer (PlasmaDive; Biognosys, CH). The raw files were analyzed using SpectroDive software, which calculated concentrations for the majority of the 100 proteins.

When using the nanoflow LC-MS platform, each sample required a 32-minute gradient for separation of the peptides and a further 38 minutes for washing and reequilibrating the column. The total run time for the entire cohort (n=668) was 2 months because of the inherent complications of nanoflow LC, for example, blockage of column or spray emitter, prolonged purging/calibration of the nanoflow pump, and shifts in RT.

To further the application of plasma proteomics to larger cohorts, we transferred the nanoflow LC-MS method onto a standard-flow platform consisting of an Agilent 1290 Infinity II HPLC interfaced to an Agilent 6495 QqQ MS. A 27-minute LC method was successfully established to measure the same 200 peptides (light and heavy peptides for 100 proteins) with a minimum of 3 transitions for each peptide. The lower limit of detection and the lower limit of quantification were evaluated on both the nanoflow and the standard-flow platform (Table III in the Data Supplement and Figure I in the Data Supplement). To obtain a similar sensitivity to the nanoflow method, 5× more sample volume (10 μL) had to be injected using the standard-flow approach compared with nanoflow (2 μL). With the larger sample load, a similar detection range could be achieved despite the switch to standard-flow LC-MS with higher ion suppression. When using the nanoflow system, median SIS peptide intensities in plasma samples were only decreased by one third compared with the intensities in the LC solution (Figure II in the Data Supplement). Using the standard-flow system, the median lower limit of detection was about 2-fold higher in the SIS diluted with plasma than with LC solution (Table III in the Data Supplement).

Among the proteins quantified by both methods, the results showed a high correlation (r=0.998) in all 668 samples (Figure 1 and Table IV in the Data Supplement) apart from few notable exceptions: for β-2-glycoprotein 1 (APOH_HUMAN) because of chromatography issues with the SIS peptide after digestion, for fibrinogen β chain (FIBB_HUMAN) and for serum paraoxonase/arylesterase 1 (PON1_HUMAN) because of a RT window error, and for α-2-macroglobulin (A2MG_HUMAN) because of a manufacturing error with a missing SIS peptide.

To demonstrate that both high and less abundant proteins were measured reliably, we selected TRFE and PLF4 as examples to be compared with a reference measurement from a routine clinical assay for TRFE or ELISA for PLF4. The high abundant TRFE displayed similar agreement with the reference measurement for both the nanoflow and standard-flow LC-MS measurements (Figure 2A). For less abundant

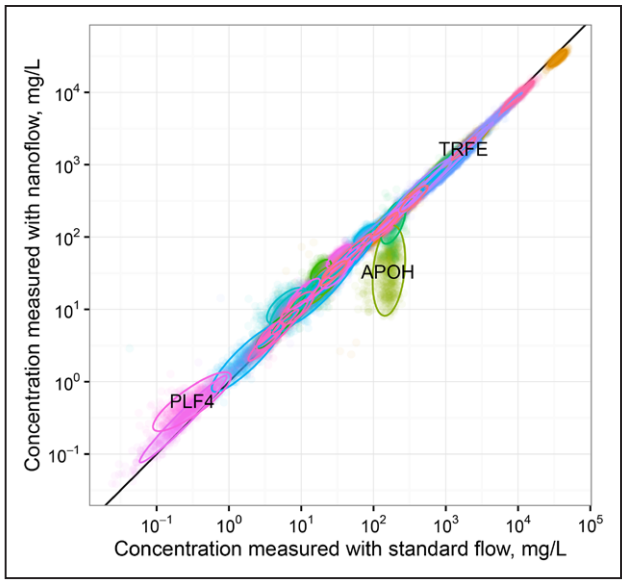

Figure 1. Comparison between nanoflow and standard-flow liquid chromatography (LC) method. Plasma samples from the Bruneck Study (year 2000 evaluation, n=668) were digested, and 100 proteins were measured using multiple reaction monitoring (MRM) with stable isotope-labeled standards (SIS) peptides as spike-in standards. Samples were denatured, reduced, alkylated, and digested with trypsin using PlasmaDive MRM Panel kit (Biognosys, CH) on an automated liquid handling robot (BRAVO, Agilent) following the manufacturer's instruction. The SIS peptides were spiked-in before tryptic digestion. The digested peptides were purified and analyzed on both nanoflow high-performance liquid chromatography (HPLC) mass spectrometry (MS) and standard-flow HPLC-MS. The results were analyzed using SpectroDive software (Biognosys, CH). Protein concentrations measured by nanoflow and standard-flow LC-MS are highly correlated with the exception of β-2-glycoprotein 1 (APOH_HUMAN) because of a splitting of the chromatographic peak for the reference peptide.

PLF4, standard-flow LC-MS displayed closer agreement with the reference measurement, whereas nanoflow LC-MS measured higher values than the reference measurement in the low concentration range and lower values in the high concentration range, resulting in higher overall deviation from the reference measurement compared with standard-flow method (Figure 2B).

To evaluate the performance of the 2 LC-MS platforms, a pooled QC sample was injected periodically during continuous operation while analyzing hundreds of samples on both platforms. For the peptides quantified on both platforms, the relative SD of the light or heavy peptide peak area on the nanoflow platform was much higher (light 38.07%–83.80%, heavy 37.92%–80.88%) compared with the standard-flow platform (light 5.12%–28.51%, heavy 5.59%–28.14%) with P <0.001. After adjustment to heavy peptides, the variations of the light:heavy ratio in both platforms were more comparable (nanoflow 1.68%–16.56%, standard flow 1.34%–18.52%; P=0.651; Figure 3). Nonetheless, the nanoflow LC-MS system showed higher variation for the absolute signal intensities between different runs.

When comparing the stability of the RT, in the nanoflow system, the SIS peptides eluted from 3.62 to 27.56 minutes. The SD of the RT of each peptide ranged from 0.26 to 0.44 minutes over 700 injections (Figure 4A). The standard peptides eluted in the standard-flow system from 3.22 to 19.99 minutes but with substantially less variation: the SD range was within 0.003 to 0.05 minutes (Figure 4B).

Comparison of Commercial MRM Kits for Plasma Proteomics

A different MRM kit (PeptiQuant MRM Assay Biomarker Assessment Kit BAK-76, MRM Proteomics) was used to compare the apolipoprotein measurements with the PlasmaDive (Biognosys, CH) results (n=44). The plasma samples were processed and analyzed on the standard-flow platform with 15 µL injection volume according to the manufacturer's instructions. The target peptide concentrations were calculated using both single-point calibration and relative response–relative concentration standard curve. The results derived from the single-point calibration for apolipoprotein measurements were compared with the PlasmaDive (Biognosys, CH) method (Figure 5). In general, the results were highly correlated between the 2 commercial kits when using the same proteotypic peptide (apo(a) r=0.928, apoC2 r=0.922, apoE r=0.930). For the same protein with different proteotypic peptides, the MRM-based measurements still showed good correlation (r>0.7). However, the absolute concentrations varied between the 2 kits with extreme ratios for apo(a) (6.01) and apoB (3.22). In both kits, a peptide (GTYSTTVTGR) within the Kringle repeat was selected for the measurement of apo(a) (APOA_HUMAN). The number of Kringle repeats, however, greatly varies between individuals.[24,25] Although the peptide is readily detectable in plasma digests, this peptide is not a suitable target for measuring apo(a) concentrations. Instead, both commercial MRM kits provide a readout for Kringle size (Kringle mass). For this reason, apo(a) was excluded from the final version of the PlasmaDive kit (Biognosys, CH).

Comparison to Antibody-Based Assays

Next, to evaluate the compatibility of MS-based methods with the traditional antibody-based method, we compared PlasmaDive (n=44) with an antibody-based Luminex assay (Milliplex MAP Human Apolipoprotein Magnetic Bead Panel kit, Millipore) for 5 apolipoproteins (apoA1, apoA2, apoC2, apoC3, and apoE). The PlasmaDive and the Luminex results showed very high correlation for apoC2 (r=0.917), apoC3 (r=0.944), and apoE (r=0.886; Figure 6). However, the MRM measurements returned lower concentrations compared with the antibody-based analysis. This difference was particularly pronounced for apoA2: the concentration of apoA2 was ≈27.7% of that of apoA1 using the Luminex kit. The MRM data, however, estimated apoA2 concentration to be just 3.7% of that of apoA1 (Figure III in the Data Supplement).

Association of Protein Measurements With Clinical Variables

Figure 7 shows the associations of protein measures with clinical variables. As expected, most proteins showed a similar strength of association when using either the nanoflow or standard-flow method, and the measurements of apoA1 and apoB were strongly associated with HDL-C and LDL-C, respectively (Figure IV in the Data Supplement). Nonetheless, 51.1% of comparisons returned lower P values with the

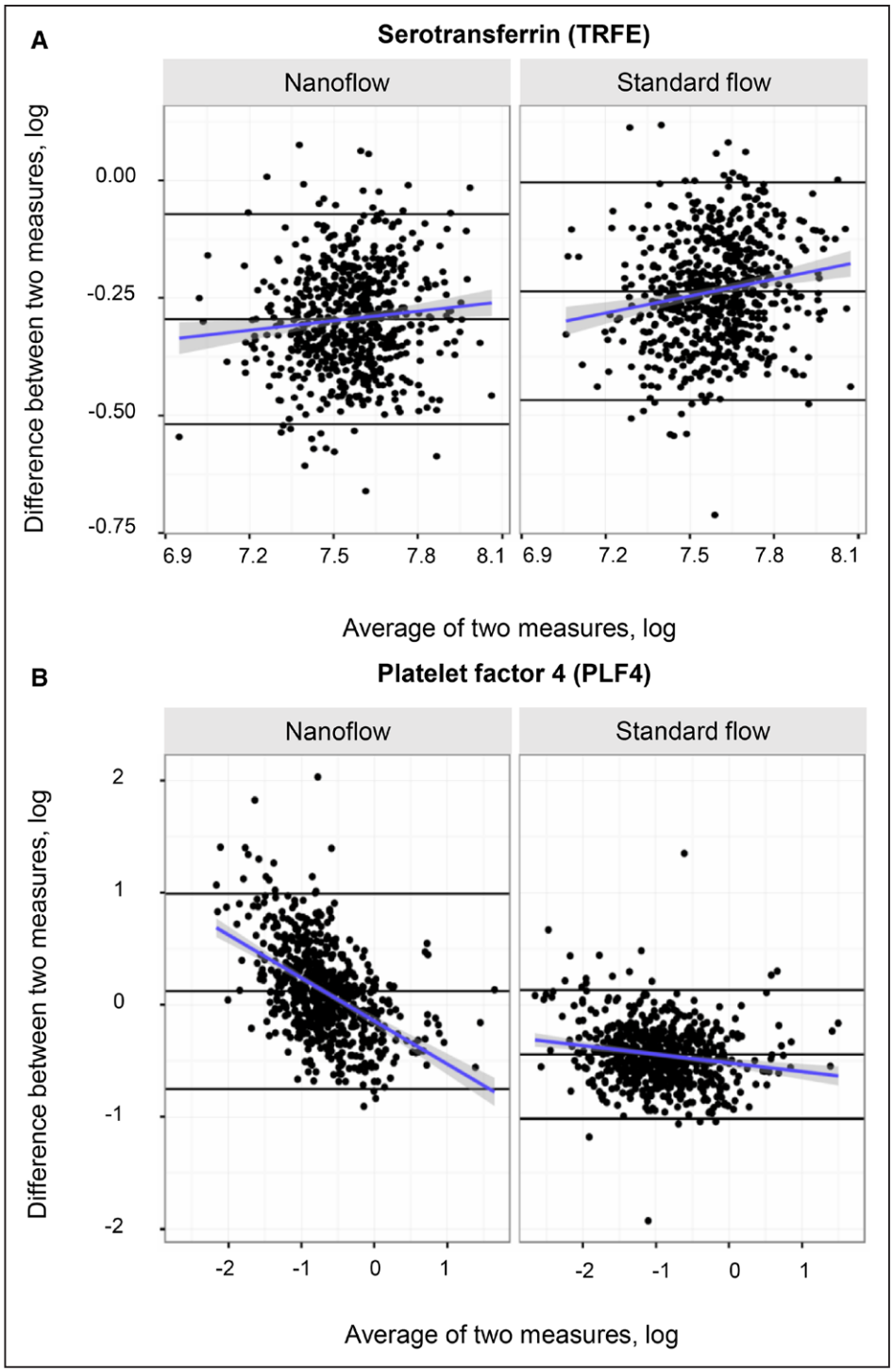

Figure 2. Comparison for high and low abundant plasma proteins. For the high abundant plasma protein TRFE, the nanoflow and standard-flow results were similar when compared with traditional measurements (**A**). For the less abundant plasma protein PLF4, nanoflow measurements are higher at low concentration end and lower at high concentration end compared with traditional measurements. The standard-flow measurements showed lower variation than nanoflow liquid chromatography (LC) mass spectrometry (MS; **B**). In the Bland–Altman plots, *x* axis is the mean of log-transformed protein concentration of subject-wise multiple reaction monitoring (MRM) and clinical measurement; *y* axis is the difference between these 2 measurements.

standard-flow method, but this was not significant (P=0.5 with t test und P=0.4 with Wilcoxon test). Importantly, there was less interference with the MRM transitions in the standard-flow method. The most discordant protein measurements are highlighted in Figure V in the Data Supplement.

Discussion

In this study, we have developed a standard-flow LC-MS workflow to analyze 100 proteins in plasma samples from a community-based, prospective cohort (n=668 samples, >1500 injections). The optimized standard-flow LC-MS method

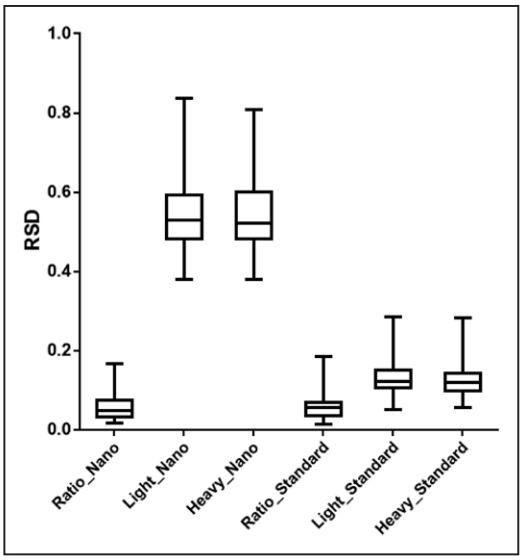

Figure 3. Comparison of relative SD (RSD) between nanoflow and standard-flow liquid chromatography (LC). The quality control samples on the nanoflow and standard-flow system showed similar RSD of the light/heavy ratio, but the light or heavy peptide peak area showed a higher variation on the nanoflow system.

improved reproducibility, robustness, and throughput in comparison to the traditional proteomics method using nanoflow LC. Using the standard-flow LC-MS method, the Bruneck cohort (n=668) could be analyzed in just over 2 weeks rather than 2 months without the need for enrichment, protein depletion, or fractionation of peptides.

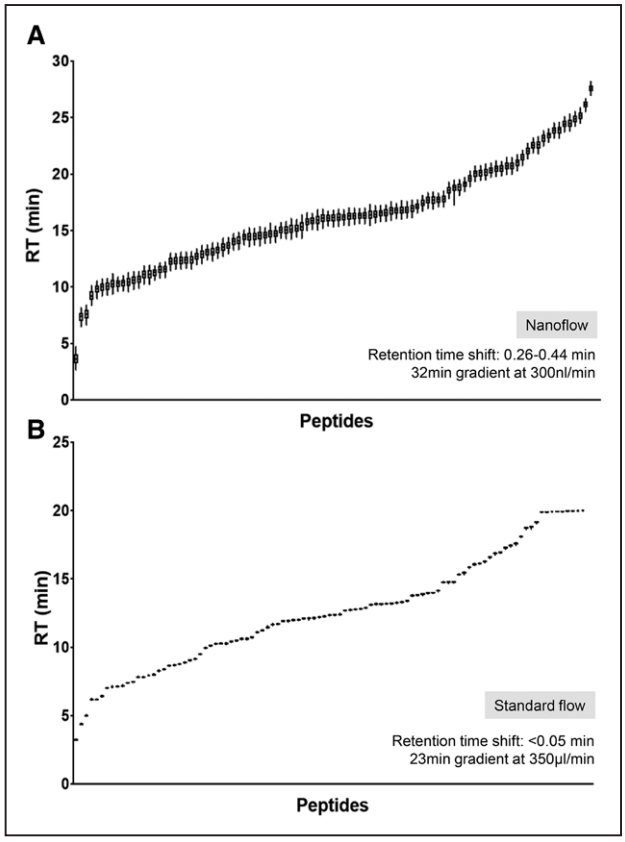

Figure 4. Comparison of retention time (RT) between nanoflow and standard-flow liquid chromatography (LC). The RT of each peptide showed higher variation across 668 samples using nanoflow LC (**A**) compared with standard-flow LC (**B**).

The PlasmaDive LC-MS method recommended by the manufacturer is based on a nanoflow LC method, and the protocol requires minimal user optimization. For large cohorts, however, analysis time becomes prohibitive. For example, for the samples of the Bruneck study, the total run time extended to 2 months because of the inherent complications that arose from nanoflow LC applications. The extended run time also required cleaning and calibration of the QqQ MS in between. Thus, nanoflow LC-based workflows did not allow the throughput required for clinical research applications. On the other hand, standard-flow LC offers greater stability and robustness and thus less variability but has only been described in small-scale studies.[6–10,17] By applying MRM-MS to a community-based cohort, we demonstrate the advantages of shifting from a nanoflow LC to a standard-flow LC method, ideally suited to epidemiological studies: The HPLC run time was shortened from 70 minutes in nanoflow LC-MS to 27 minutes. Accordingly, the cycle time was reduced to 0.5 s, and 3 transitions per peptide were used to accommodate the 200 peptides into the narrower peak width (0.2 minutes) and maintain a reasonable peak shape (≈15 data points). Because of the different ionization properties between the nanospray source and Jet Stream ESI source, the most abundant precursor charge state of some peptides had to be changed to get the best signal intensity. These transitions were also optimized independently using a quadrupole time-of-flight MS/MS (Agilent) system, which confirmed that the selection of the 3 transitions did not decrease the accuracy or sensitivity for reliable MRM quantification (data not shown). In fact, some of the peptide measurements were even improved by removal of transitions with a saturated peak or of an interfering peak.

Reduced sensitivity and increased ion suppression are the main limitations of standard-flow LC compared with nanoflow LC.[26,27] We have tested the limit of detection and ion suppression on both platforms. With the increased injection volume (5×), the standard-flow LC system reached the same sensitivity as the nanoflow LC system. However, this may also be in part because of the better sensitivity of the QqQ MS coupled to standard LC. The increased injection volume on the standard-flow platform is not problematic when the sample source is plasma, as the high protein concentration means that only a small volume (10 µL) is required to perform the analysis. Our ion suppression test revealed that some of the SIS peptides have a lower limit of quantification in LC solution compared with plasma, whereas others are not influenced as much. The ion suppression depends in part on the ionization properties of the peptides and coeluting abundant peptides. For low abundant proteins, the effects of ion suppression can be compensated by increasing the concentrations of spike-in SIS peptides as long as they remain with similar concentration to the target peptides.

Once the standard-flow LC-MS method was optimized, we analyzed 668 samples plus regular QCs, back-to-back with a total run time of 15 days. Overall, we demonstrate the advantages of shifting from a nanoflow LC to a standard-flow LC method. This is because of 2 main reasons:

1. The 2.1 mm inner diameter column had no blockages during continuous operation for a few months.
2. The better RT stability means smaller and less overlapping RT windows in a scheduled MRM, therefore, longer

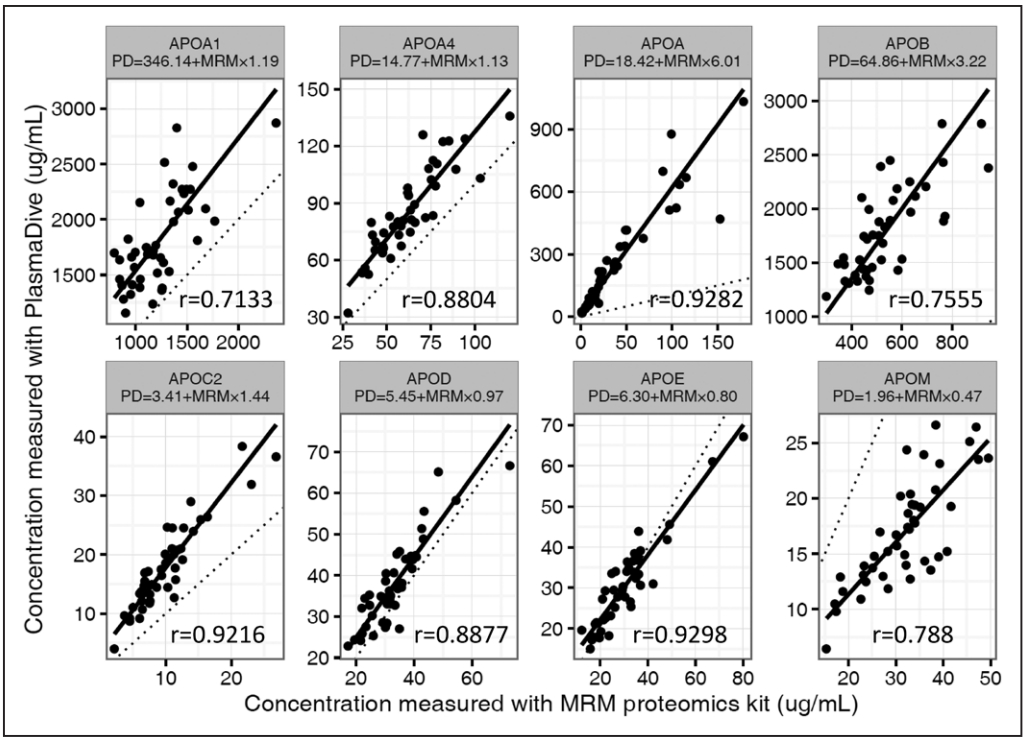

Figure 5. Comparison between multiple reaction monitoring (MRM)–based kits from 2 different vendors. When comparing the concentration of the same apolipoproteins measured by PlasmaDive (PD) and PeptiQuant BAK-76 (MRM), we observed a high correlation between the 2 kits, especially for those apolipoproteins measured using the same peptide (apo(a) *r*=0.928, apoC2 *r*=0.922, apoE *r*=0.930). However, the absolute concentrations varied between 2 kits with extreme ratios for apo(a) (6.01) and apoB (3.22). The linear regression formula is shown as PD=a+MRM×b on top of each graph.

dwell times for each transition resulting in better signal intensities and less missing data.

We have recently applied this standard-flow method to compare the associations of the different apolipoproteins with cardiovascular risk.[22] We also measured the same apolipoproteins in an intervention study using antisense therapy for apoC3. Plasma apoC3 levels were decreased by 75%, whereas apoC2 and apoE levels showed a 50% drop on antisense treatment. These apolipoproteins are predominantly associated with very-low-density lipoproteins, and there is increasing evidence for a role of very-low-density lipoproteins in addition to low-density lipoproteins in atherosclerosis.[28]

MRM Versus Alternative MS Quantification Methodologies

Different MS approaches for plasma proteomics have been described in recent years. Stable Isotope Standards and Capture by Anti-Peptide Antibodies uses antipeptide antibodies to enrich peptides of interest after addition of stable isotope-labeled internal peptide standards to the protein digest. Light and heavy peptides are enriched simultaneously, resulting in a sensitive and accurate quantification of the peptides of interest.[29,30] Data-independent acquisition analysis offers a hypothesis-free approach and allows the analysis of a larger number of proteins. The samples are converted into digital archive as all detectable peptides in the samples are fragmented and MS/MS spectra are acquired. However, sensitivity and dynamic range are limited in nondepleted plasma samples. In a subcohort of the UK Twin registry (n=232), 342 plasma proteins could be analyzed by Sequential Windowed Acquisition of All Theoretical Fragment Ion Mass Spectra analysis, but essential steps including depletion of the 14 most abundant proteins and fractionation into 6 fractions were needed.[7] Complicated analytic workflows or demanding data analysis will limit the wider application of proteomics in epidemiology. Throughput and costs are critical considerations for applications in clinical research. Thus, we focused on a standard-flow LC-MRM method for plasma proteomics to meet the requirements for epidemiological studies in terms of reducing costs and increasing throughput. Further improvements may include parallel reaction monitoring with comparable linearity, dynamic range and precision compared with MRM,[31,32] and less method development time for new targets as only the accurate precursor masses of the target peptides are required. For all MS-based methods, the choice of the proteotypic peptide is critical for meaningful quantification of a protein and must not only be based on criteria for LC-MS analysis, such as peptide length, uniqueness, post-translational modifications, physiochemical properties, and abundance, but also biological function as exemplified by the reference peptide selected for apo(a).

LC-MRM-MS Versus Antibody-Based Protein Measurements

Antibody-based methods require lower investment in equipment and offer automation and high throughput. Compared with LC-MS, however, immunoassays rely on the specificity and selectivity of the binders. The necessity of good antibodies results in high running costs, gives rise to batch to batch inconsistencies, and limits the multiplexing capability. Moreover,

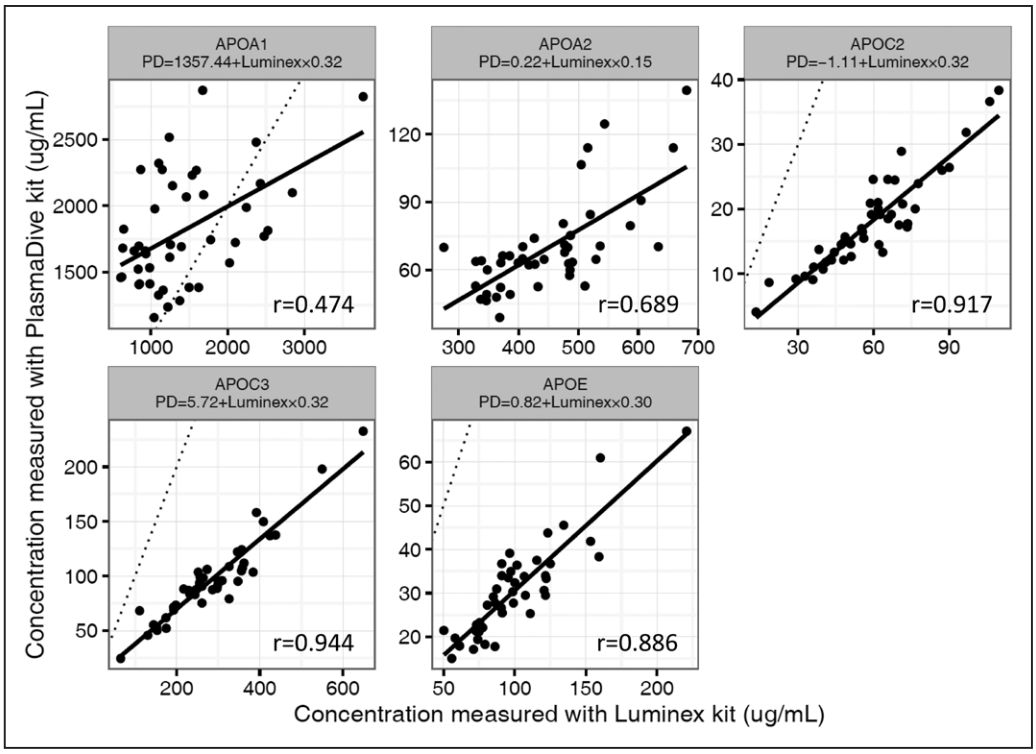

Figure 6. Comparison of mass spectrometry (MS)–based measurements (PlasmaDive [PD]) with antibody-based assays (Luminex). Measurements for apoC2, and apoE revealed a good correlation between the MS- and antibody-based measurements, but the absolute concentration is lower when measured using liquid chromatography (LC) MS (PD; Biognosys, CH). A poor correlation was observed for apoA1, and apoA2 concentrations were substantially lower compared with antibody-based measurements. The linear regression formula is shown as PD=a+Luminex×b on top of each graph.

only external standard but no internal standards are used. LC-MS has a higher initial cost for instrumentation and maintenance and offers a lower throughput at this moment. However, LC-MS methods are faster and cheaper to develop; they offer high multiplexing capability within a dynamic range for the simultaneous detection of low and high abundant analytes over 4 to 5 orders of magnitude; and stable isotope-labeled internal standards reduce variability while increasing robustness.[3]

Both MRM- and antibody-based absolute quantification methods rely on the accuracy of the standard. In general, lower concentrations were detected by the MRM method than the antibody-based method. We have investigated the digestion efficiency by measuring known amount of human TRFE in a fetal bovine serum background using the PlasmaDive kit. The PlasmaDive results returned about 88% of the spike-in concentration when the transferrin concentration is high and dropped to 60% when the concentration is low (data not shown). These differences may come from the weighting error, the incomplete digestion, the peptide loss during the experiment procedure, and the ion suppression especially when measuring at low concentrations. An inherent risk of using peptide standards in a relatively low concentration is that every sample preparation step may cause losses, that is, because of the hydrophobic peptides binding to the surface of plastic ware.[33] This may also be the reason for the variation of the late eluting peptides (eg, VSFLSALEEYTK from apoA1). Ideally, SIS proteins should be used instead of SIS peptides for MRM-based measurements. Stable isotope-labeled proteins, however, are significantly more expensive than using SIS peptides.[34] On the other hand, ELISA kits tend to use protein standards in physiological buffers or in reference samples but without the biological matrix of the actual sample. Differences in the matrix between samples may interfere with the binding of the antibody to the antigen and thus influence the results. With MRM-MS, proteins can be measured directly and the multiplexing capability allows for measurements of biomarker panels in a single run. Although MRM-MS is routinely applied clinically for measuring small molecules,[35–37] the use of MRM-MS could be expanded to protein measurements in future.

Conclusions

For large epidemiological studies, experimental variation has to be well controlled. We have successfully applied a standard-flow LC-MRM method to obtain tens of thousands of protein measurements in a community-based cohort. The standard-flow LC-MRM method resulted in significant time savings and offered higher precision and better reproducibility. Although the limitations of antibodies are well recognized, questions should also be raised about discordance between peptide measurements using LC-MS and the true protein concentration. For absolute quantification, protein standards may be required to adjust for tryptic digestion efficiency and to account for peptide losses, which might not always be similar for spike-in SIS and endogenous peptides.

Acknowledgments

Luminex Analysis was performed using Luminex FlexMap 3D at The iLab, Flow Cytometry Core, the National Institute of Health Research

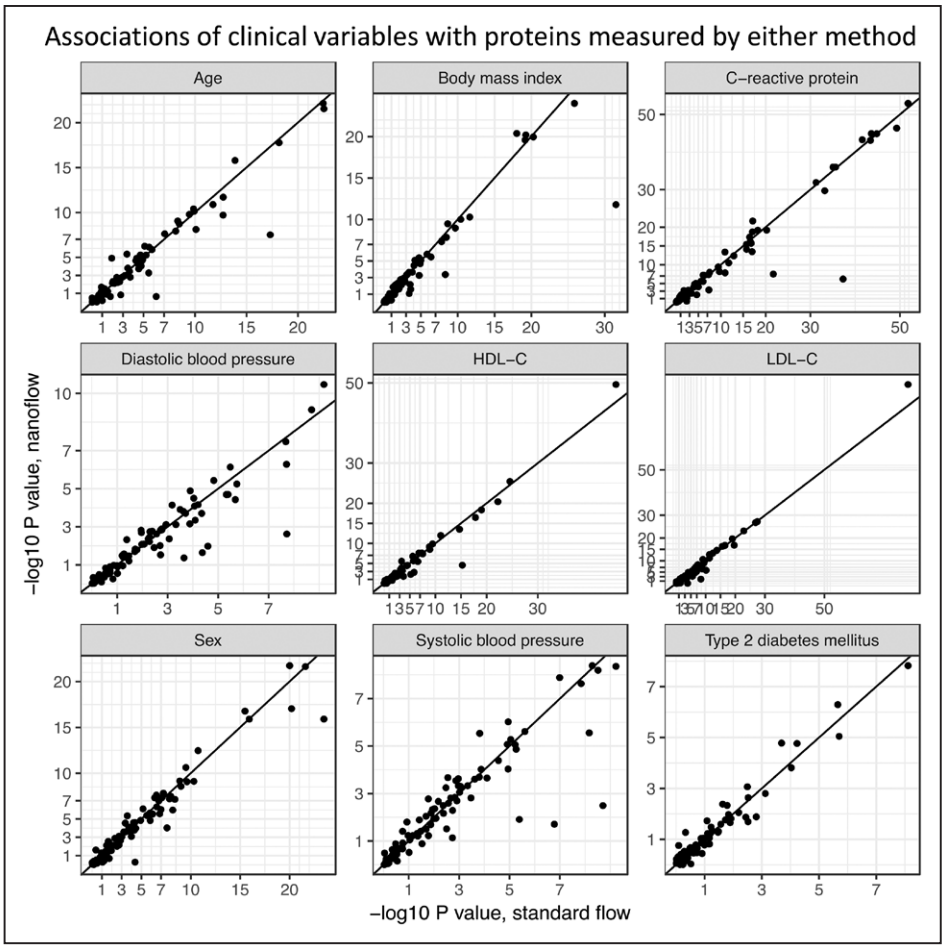

Figure 7. Associations of clinical variables with proteins measured by either nanoflow or standard-flow liquid chromatography (LC) method. The associations of protein measurements from both the nanoflow and standard-flow LC method were compared with clinical variables including age, body mass index, C-reactive protein, diastolic blood pressure, high-density lipoprotein cholesterol (HDL-C), low-density lipoprotein cholesterol (LDL-C), sex, systolic blood pressure, and type 2 diabetes mellitus.

(NIHR) Biomedical Research Centre based at Guy's and St Thomas' NHS Foundation Trust, and King's College London in partnership with King's College Hospital.

Sources of Funding

Dr Mayr holds a British Heart Foundation (BHF) Chair with programme grant support (CH/16/3/32406, RG/16/14/32397). The research was funded/supported by the National Institute of Health Research (NIHR) Biomedical Research Centre based at Guy's and St Thomas' NHS Foundation Trust and King's College London in partnership with King's College Hospital. Drs Kiechl, Willeit, Mayr, and Pechlaner are supported by an excellence initiative (Competence Centers for Excellent Technologies [COMET]) of the Forschungsförderungsgesellschaft/Austrian Research Promotion Agency: Research Center of Excellence in Vascular Ageing—Tyrol, VASCage (K-Project Nr. 843536) funded by the Bundesministerium für Verkehr, Innovation und Technologie/Austrian Ministry for Transport, Innovation and Technology, Bundesministerium für Wissenschaft, Forschung und Wirtschaft/Federal Ministry of Science, Research and Economy, the Wirtschaftsagentur Wien, and the Standortagentur Tirol. Dr Mayr is part of a transatlantic network supported by the Fondation Leducq (MiRVAD: MicroRNA-based Therapeutic Strategies in Vascular Disease).

Disclosures

Drs Kiechl, Willeit, and Mayr are named inventors on patents for cardiometabolic biomarkers. Drs Gandhi, Müller, and Reiter are employees of Biognosys AG. Drs Blankley and Sullivan are employees of Agilent. Drs Tsimikas and Witztum are coinventors and receive royalties from patents owned by the University of California at San Diego (UCSD) on oxidation-specific antibodies and on biomarkers related to oxidized lipoproteins. Dr Tsimikas currently has a dual appointment with UCSD and as an employee of Ionis Pharmaceuticals. Dr Witztum is a consultant to Ionis Pharmaceuticals, CymaBay, Intercept, and Prometheus and has stock in Ionis Pharmaceuticals. The other authors report no conflicts.

References

1. Anderson NL, Anderson NG. The human plasma proteome: history, character, and diagnostic prospects. *Mol Cell Proteomics*. 2002;1:845–867.
2. Gillette MA, Carr SA. Quantitative analysis of peptides and proteins in biomedicine by targeted mass spectrometry. *Nat Methods*. 2013;10:28–34. doi: 10.1038/nmeth.2309.
3. Carr SA, Abbatiello SE, Ackermann BL, Borchers C, Domon B, Deutsch EW, et al. Targeted peptide measurements in biology and medicine: best practices for mass spectrometry-based assay development using a fit-for-purpose approach. *Mol Cell Proteomics*. 2014;13:907–917. doi: 10.1074/mcp.M113.036095.
4. Kusebauch U, Campbell DS, Deutsch EW, Chu CS, Spicer DA, Brusniak MY, et al. Human SRMAtlas: a resource of targeted assays to quantify the complete human proteome. *Cell*. 2016;166:766–778. doi: 10.1016/j.cell.2016.06.041.
5. Grebe SK, Singh RJ. LC-MS/MS in the clinical laboratory - where to from here? *Clin Biochem Rev*. 2011;32:5–31.
6. Razavi M, Leigh Anderson N, Pope ME, Yip R, Pearson TW. High precision quantification of human plasma proteins using the automated

SISCAPA Immuno-MS workflow. *N Biotechnol*. 2016;33(5 pt A):494–502. doi: 10.1016/j.nbt.2015.12.008.
7. Liu Y, Buil A, Collins BC, Gillet LC, Blum LC, Cheng LY, et al. Quantitative variability of 342 plasma proteins in a human twin population. *Mol Syst Biol*. 2015;11:786.
8. Hüttenhain R, Soste M, Selevsek N, Röst H, Sethi A, Carapito C, et al. Reproducible quantification of cancer-associated proteins in body fluids using targeted proteomics. *Sci Transl Med*. 2012;4:142ra94. doi: 10.1126/scitranslmed.3003989.
9. Domanski D, Percy AJ, Yang J, Chambers AG, Hill JS, Freue GV, et al. MRM-based multiplexed quantitation of 67 putative cardiovascular disease biomarkers in human plasma. *Proteomics*. 2012;12:1222–1243. doi: 10.1002/pmic.201100568.
10. Percy AJ, Chambers AG, Yang J, Domanski D, Borchers CH. Comparison of standard- and nano-flow liquid chromatography platforms for MRM-based quantitation of putative plasma biomarker proteins. *Anal Bioanal Chem*. 2012;404:1089–1101. doi: 10.1007/s00216-012-6010-y.
11. Anderson L, Hunter CL. Quantitative mass spectrometric multiple reaction monitoring assays for major plasma proteins. *Mol Cell Proteomics*. 2006;5:573–588. doi: 10.1074/mcp.M500331-MCP200.
12. Anderson NL, Anderson NG, Haines LR, Hardie DB, Olafson RW, Pearson TW. Mass spectrometric quantitation of peptides and proteins using Stable Isotope Standards and Capture by Anti-Peptide Antibodies (SISCAPA). *J Proteome Res*. 2004;3:235–244.
13. Martosella J, Zolotarjova N, Liu H, Nicol G, Boyes BE. Reversed-phase high-performance liquid chromatographic prefractionation of immunodepleted human serum proteins to enhance mass spectrometry identification of lower-abundant proteins. *J Proteome Res*. 2005;4:1522–1537. doi: 10.1021/pr050088l.
14. Geyer PE, Kulak NA, Pichler G, Holdt LM, Teupser D, Mann M. Plasma proteome profiling to assess human health and disease. *Cell Syst*. 2016;2:185–195. doi: 10.1016/j.cels.2016.02.015.
15. Addona TA, Abbatiello SE, Schilling B, Skates SJ, Mani DR, Bunk DM, et al. Multi-site assessment of the precision and reproducibility of multiple reaction monitoring-based measurements of proteins in plasma. *Nat Biotechnol*. 2009;27:633–641. doi: 10.1038/nbt.1546.
16. Polanski M, Anderson NL. A list of candidate cancer biomarkers for targeted proteomics. *Biomark Insights*. 2007;1:1–48.
17. Cohen Freue GV, Borchers CH. Multiple reaction monitoring (MRM): principles and application to coronary artery disease. *Circ Cardiovasc Genet*. 2012;5:378. doi: 10.1161/CIRCGENETICS.111.959528.
18. Razavi M, Anderson NL, Yip R, Pope ME, Pearson TW. Multiplexed longitudinal measurement of protein biomarkers in DBS using an automated SISCAPA workflow. *Bioanalysis*. 2016;8:1597–1609. doi: 10.4155/bio-2016-0059.
19. Blankley RT, Fisher C, Westwood M, North R, Baker PN, Walker MJ, et al. A label-free selected reaction monitoring workflow identifies a subset of pregnancy specific glycoproteins as potential predictive markers of early-onset pre-eclampsia. *Mol Cell Proteomics*. 2013;12:3148–3159. doi: 10.1074/mcp.M112.026872.
20. Anderson L. Six decades searching for meaning in the proteome. *J Proteomics*. 2014;107:24–30. doi: 10.1016/j.jprot.2014.03.005.
21. Stegemann C, Pechlaner R, Willeit P, Langley SR, Mangino M, Mayr U, et al. Lipidomics profiling and risk of cardiovascular disease in the prospective population-based Bruneck study. *Circulation*. 2014;129:1821–1831. doi: 10.1161/CIRCULATIONAHA.113.002500.
22. Pechlaner R, Tsimikas S, Yin X, Willeit P, Baig F, Santer P, et al. Very-low-density lipoprotein-associated apolipoproteins predict cardiovascular events and are lowered by inhibition of APOC-III. *J Am Coll Cardiol*. 2017;69:789–800. doi: 10.1016/j.jacc.2016.11.065.
23. Altman DG, Bland JM. Measurement in medicine - the analysis of method comparison studies. *Statistician*. 1983;32:307–317.
24. Marcovina SM, Albers JJ, Scanu AM, Kennedy H, Giaculli F, Berg K, et al. Use of a reference material proposed by the International Federation of Clinical Chemistry and Laboratory Medicine to evaluate analytical methods for the determination of plasma lipoprotein(a). *Clin Chem*. 2000;46:1956–1967.
25. Kronenberg F, Utermann G. Lipoprotein(a): resurrected by genetics. *J Intern Med*. 2013;273:6–30. doi: 10.1111/j.1365-2796.2012.02592.x.
26. Annesley TM. Ion suppression in mass spectrometry. *Clin Chem*. 2003;49:1041–1044.
27. Gangl ET, Annan MM, Spooner N, Vouros P. Reduction of signal suppression effects in ESI-MS using a nanosplitting device. *Anal Chem*. 2001;73:5635–5644.
28. Khetarpal SA, Zeng X, Millar JS, Vitali C, Somasundara AVH, Zanoni P, et al. A human APOC3 missense variant and monoclonal antibody accelerate apoC-III clearance and lower triglyceride-rich lipoprotein levels. *Nat Med*. 2017;23:1086–1094. doi: 10.1038/nm.4390.
29. Whiteaker JR, Zhao L, Anderson L, Paulovich AG. An automated and multiplexed method for high throughput peptide immunoaffinity enrichment and multiple reaction monitoring mass spectrometry-based quantification of protein biomarkers. *Mol Cell Proteomics*. 2010;9:184–196. doi: 10.1074/mcp.M900254-MCP200.
30. Whiteaker JR, Zhao L, Lin C, Yan P, Wang P, Paulovich AG. Sequential multiplexed analyte quantification using peptide immunoaffinity enrichment coupled to mass spectrometry. *Mol Cell Proteomics*. 2012;11:M111.015347. doi: 10.1074/mcp.M111.015347.
31. Ronsein GE, Pamir N, von Haller PD, Kim DS, Oda MN, Jarvik GP, et al. Parallel reaction monitoring (PRM) and selected reaction monitoring (SRM) exhibit comparable linearity, dynamic range and precision for targeted quantitative HDL proteomics. *J Proteomics*. 2015;113:388–399. doi: 10.1016/j.jprot.2014.10.017.
32. Gallien S, Kim SY, Domon B. Large-scale targeted proteomics using Internal Standard Triggered-Parallel Reaction Monitoring (IS-PRM). *Mol Cell Proteomics*. 2015;14:1630–1644. doi: 10.1074/mcp.O114.043968.
33. Goebel-Stengel M, Stengel A, Taché Y, Reeve JR Jr. The importance of using the optimal plasticware and glassware in studies involving peptides. *Anal Biochem*. 2011;414:38–46. doi: 10.1016/j.ab.2011.02.009.
34. Lebert D, Dupuis A, Garin J, Bruley C, Brun V. Production and use of stable isotope-labeled proteins for absolute quantitative proteomics. *Methods Mol Biol*. 2011;753:93–115. doi: 10.1007/978-1-61779-148-2_7.
35. Tang WH, Wang Z, Levison BS, Koeth RA, Britt EB, Fu X, et al. Intestinal microbial metabolism of phosphatidylcholine and cardiovascular risk. *N Engl J Med*. 2013;368:1575–1584. doi: 10.1056/NEJMoa1109400.
36. Chen Z, Caulfield MP, McPhaul MJ, Reitz RE, Taylor SW, Clarke NJ. Quantitative insulin analysis using liquid chromatography-tandem mass spectrometry in a high-throughput clinical laboratory. *Clin Chem*. 2013;59:1349–1356. doi: 10.1373/clinchem.2012.199794.
37. Zoller M, Maier B, Hornuss C, Neugebauer C, Döbbeler G, Nagel D, et al. Variability of linezolid concentrations after standard dosing in critically ill patients: a prospective observational study. *Crit Care*. 2014;18:R148. doi: 10.1186/cc13984.

CLINICAL PERSPECTIVE

Despite the ongoing genetic sequencing efforts, the impact of most genetic variation on cardiovascular disease is still poorly understood. Attention has shifted to postgenomic technologies, including proteomics and lipidomics, to refine the cardiovascular disease phenotypes at a molecular level. For omics measurements in epidemiological cohorts, experimental variation has to be well controlled to assure data comparability over time and between studies. We have successfully applied mass spectrometry to obtain plasma protein measurements in a community-based cohort using a standard-flow liquid chromatography method. The standard-flow method resulted in significant time savings and offered higher precision and better reproducibility. The multiplexing capability of mass spectrometry combined with the standard-flow liquid chromatography method increased throughput and reduced the costs of large-scale protein measurements in epidemiological cohorts. For example, apolipoproteins can be measured with high specificity and precision using mass spectrometry. Our study demonstrates the use of mass spectrometry for simultaneously measuring a broader panel of apolipoproteins than the current antibody-based apolipoprotein measurements used in the clinic.

Circulation
Genomic and Precision Medicine

Plasma Proteomics for Epidemiology: Increasing Throughput With Standard-Flow Rates

Xiaoke Yin, Ferheen Baig, Eloi Haudebourg, Richard T. Blankley, Tejas Gandhi, Sebastian Müller, Lukas Reiter, Helmut Hinterwirth, Raimund Pechlaner, Sotirios Tsimikas, Peter Santer, Johann Willeit, Stefan Kiechl, Joseph L. Witztum, Anthony Sullivan and Manuel Mayr

Circ Cardiovasc Genet. 2017;10:
doi: 10.1161/CIRCGENETICS.117.001808
Circulation: Cardiovascular Genetics is published by the American Heart Association, 7272 Greenville Avenue, Dallas, TX 75231

Print ISSN: 1942-325X. Online ISSN: 1942-3268

SUPPLEMENTAL MATERIAL

Supplemental Figure 1. The standard curve of 13 apolipoproteins. The standard curve of apolipoproteins using both nanoflow system with 3ul injection volume (left) and standard flow system with 15ul injection volume (right). LOD response = mean of blank response + 3*SD, LOQ response =mean of blank response + 10*SD.

Supplemental Figure 2. The box plot of SIS peptides intensities in LC solution or in plasma digest. The SIS peptides intensities were lower in the plasma digest because of the ion suppression effect.

Supplemental Figure 3. The ApoA1 and ApoA2 concentrations showed different ratios when measured using different methods. The scatter plot using the PlasmaDive^{TM} measurements estimated apoA2 to be only 3.7% of the apoA1 concentration (A). In the antibody-based measurements (Luminex), the ratio is 27.7% (B).

Supplemental Figure 4. Associations with clinical variables of proteins measured by either nanoflow or standard flow method. The protein measurement from both nanoflow and standard flow method were associated with age, body mass index, C-reactive protein, diastolic blood pressure, high-density lipoprotein cholesterol (HDL-C), low-density lipoprotein cholesterol (LDL-C), sex, systolic blood pressure, and type 2 diabetes mellitus.

Supplemental Figure 5. Most discordant proteins between the nanoflow or standard flow method. The most discordant proteins were APOH, C1QB, C1QC, C1S, CFAH, CFAI, FCN3, and SEPP1. The nanoflow SIS peak areas showed much higher variation compared to those with standard flow and some of the low abundant light peaks were not detectable. Nf, nanoflow method; Sf, standard flow method.

Supplemental Table 1. Transition list used in nanoflow method on TSQ Vantage MS (Thermo). These proteins were part of the beta test version of the PlasmaDive™ kit. Proteins with grey background were omitted in the released PlasmaDive™ panel.

Supplemental Table 2. Transition list used in standard flow method on 6495 QqQ MS (Agilent). These proteins were part of the beta test version of the PlasmaDive™ kit. Proteins with grey background were omitted in the released PlasmaDive™ panel.

Supplemental Table 3. The LOD/LOQ and linear range in the nanoflow and standard flow system. The LOD/LOQ were expressed as ug/mL and were calculated based on 3ul injection volume in the nanoflow system and 15ul injection volume in the standard flow system. Please note that APOA_HUMAN (with grey background) was removed and ALS_HUMAN was added in the final PlasmaDive™ panel.

Supplemental Table 4. Protein concentration ranges measured by either nanoflow method and standard flow method. Most of the concentrations were similar in both methods.

Supplemental Figure 1

Standard Curve for APOA_HUMAN

Nano flow

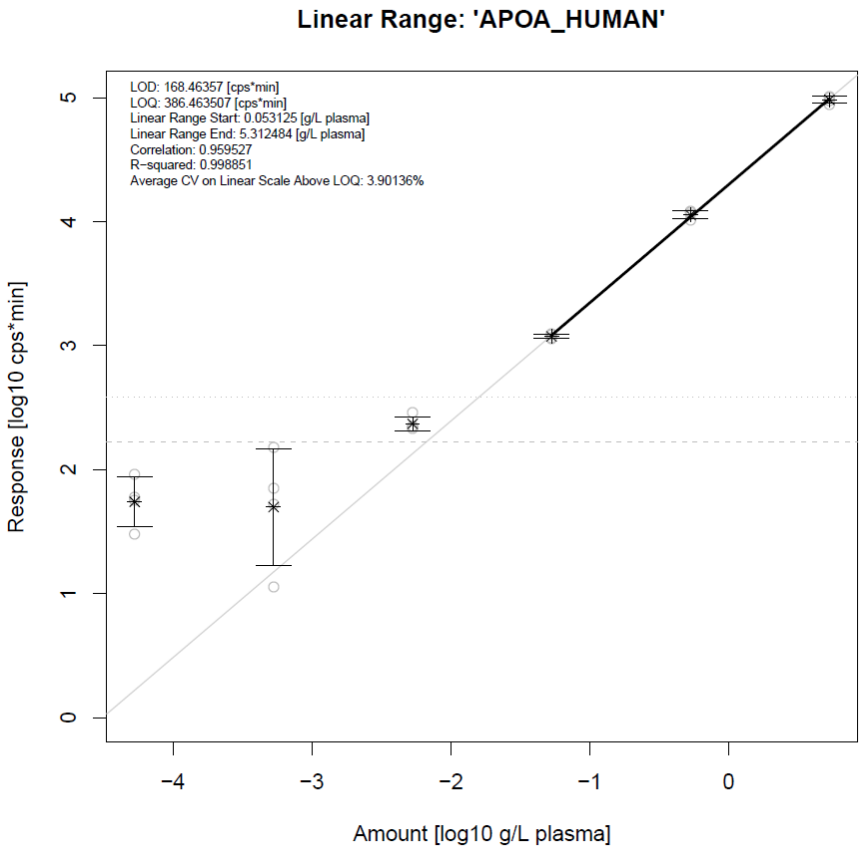

Standard flow

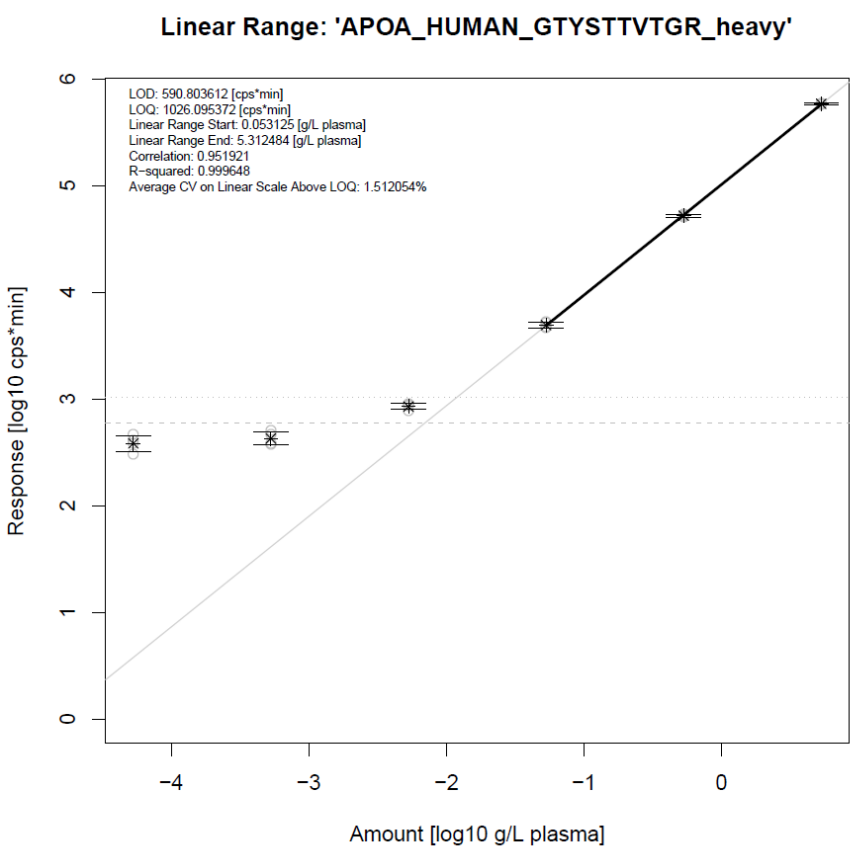

Supplemental Figure 1

Standard Curve for APOA1_HUMAN

Nano flow

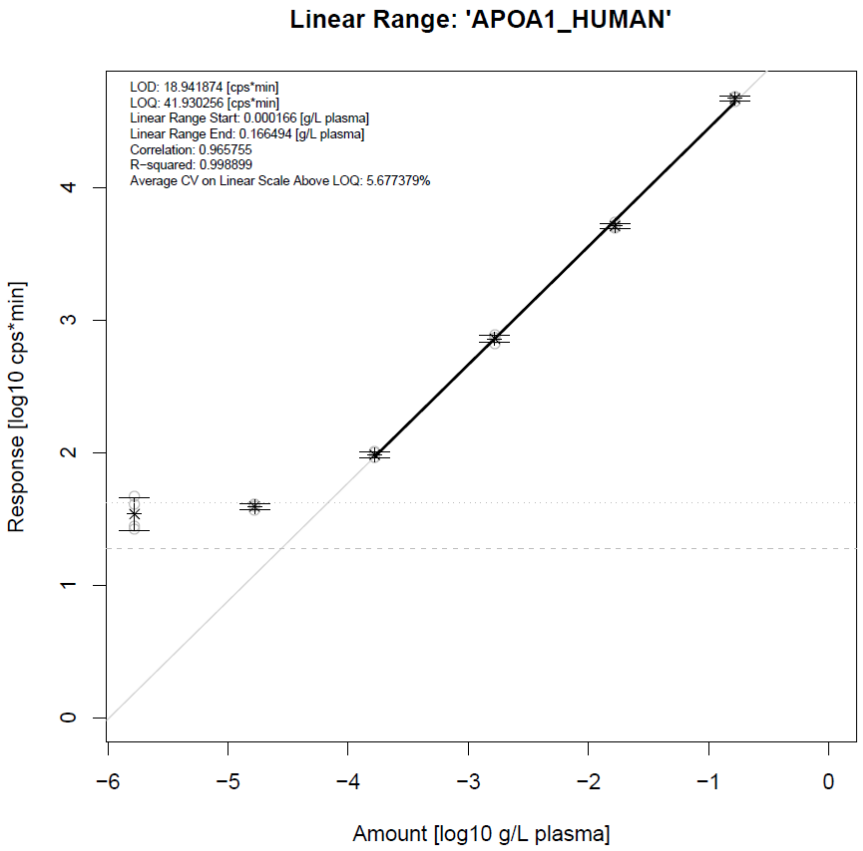

Standard flow

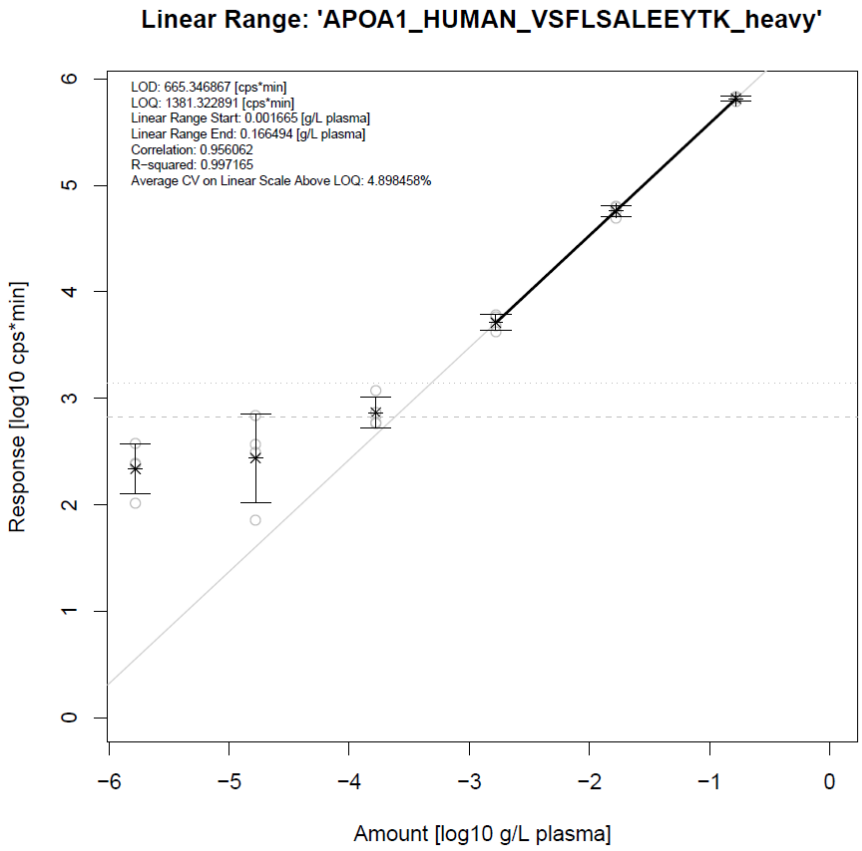

Supplemental Figure 1

Standard Curve for APOA2_HUMAN

Nano flow

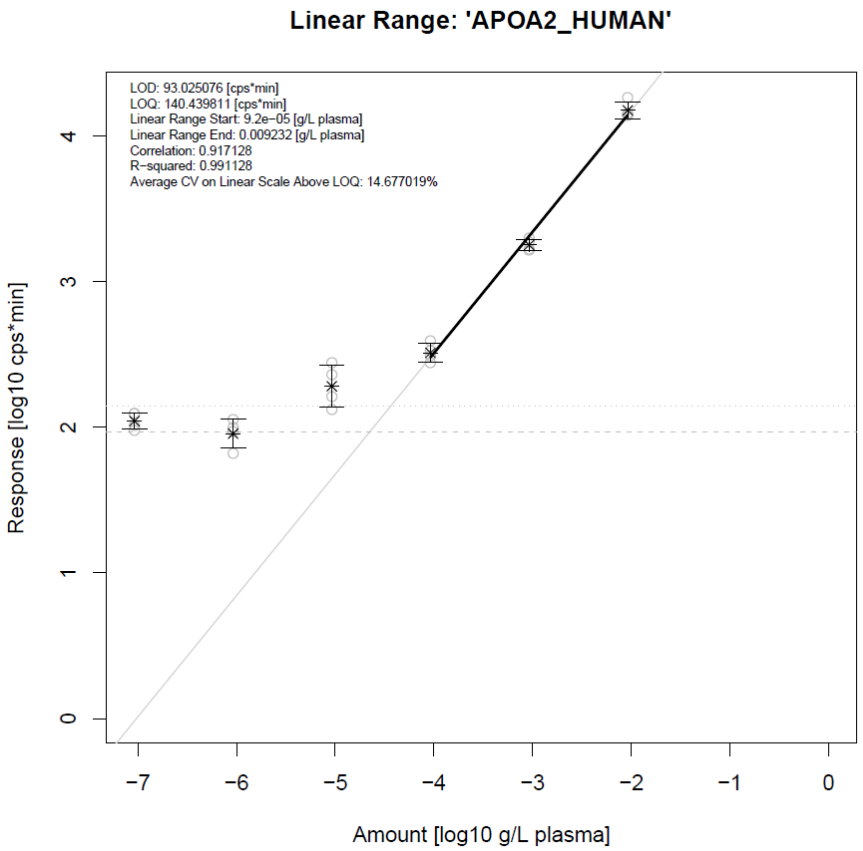

Standard flow

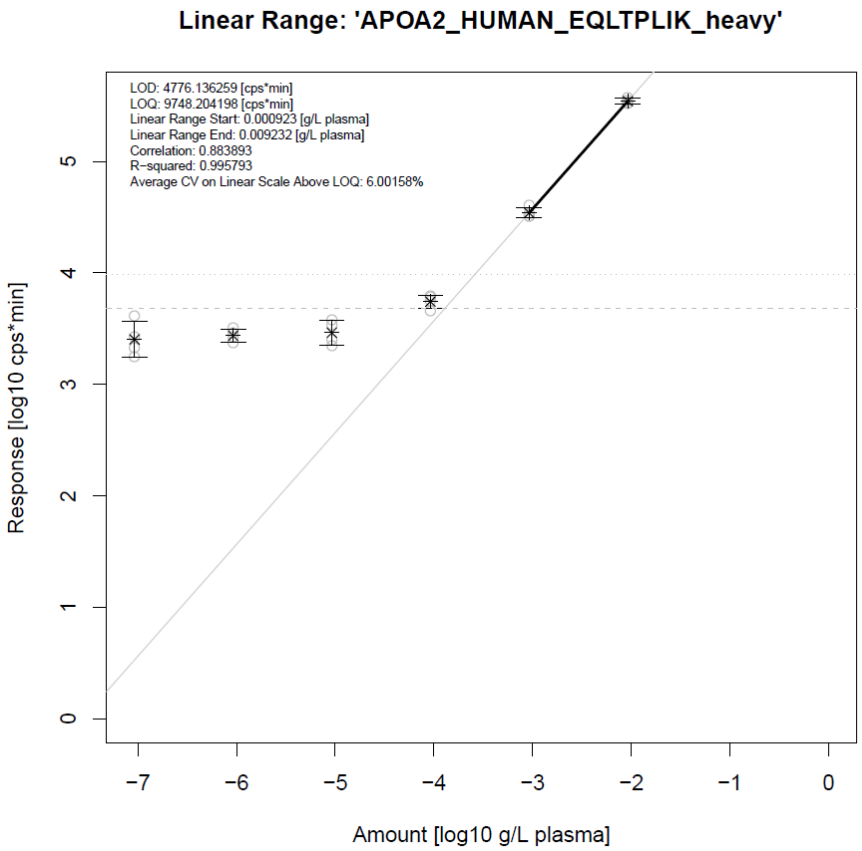

Supplemental Figure 1

Standard Curve for APOA4_HUMAN

Nano flow

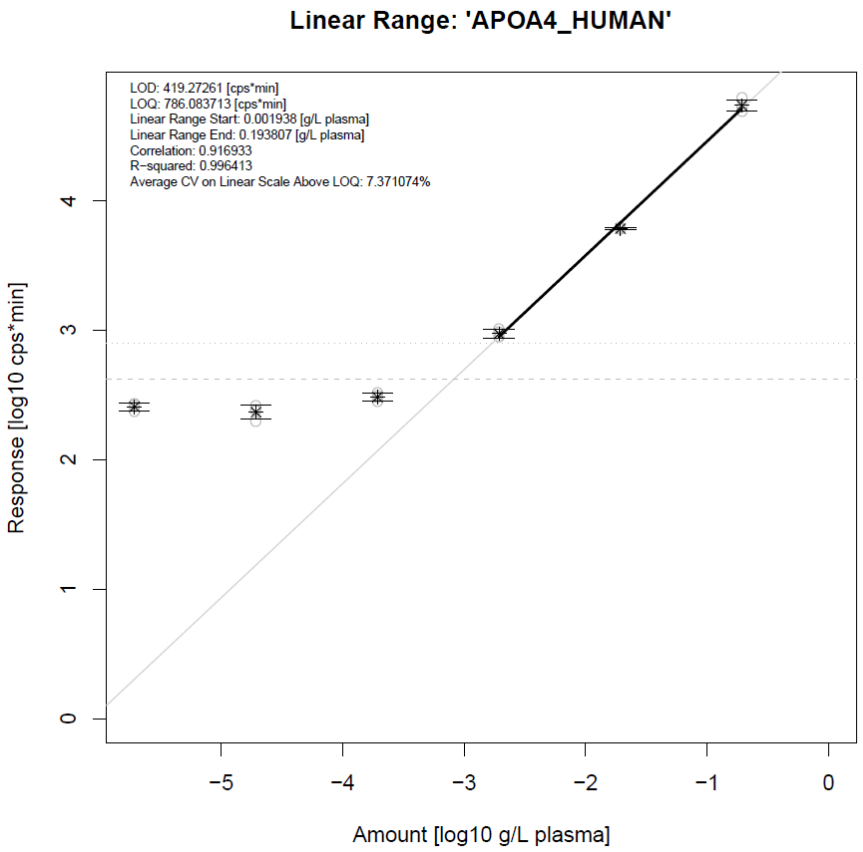

Standard flow

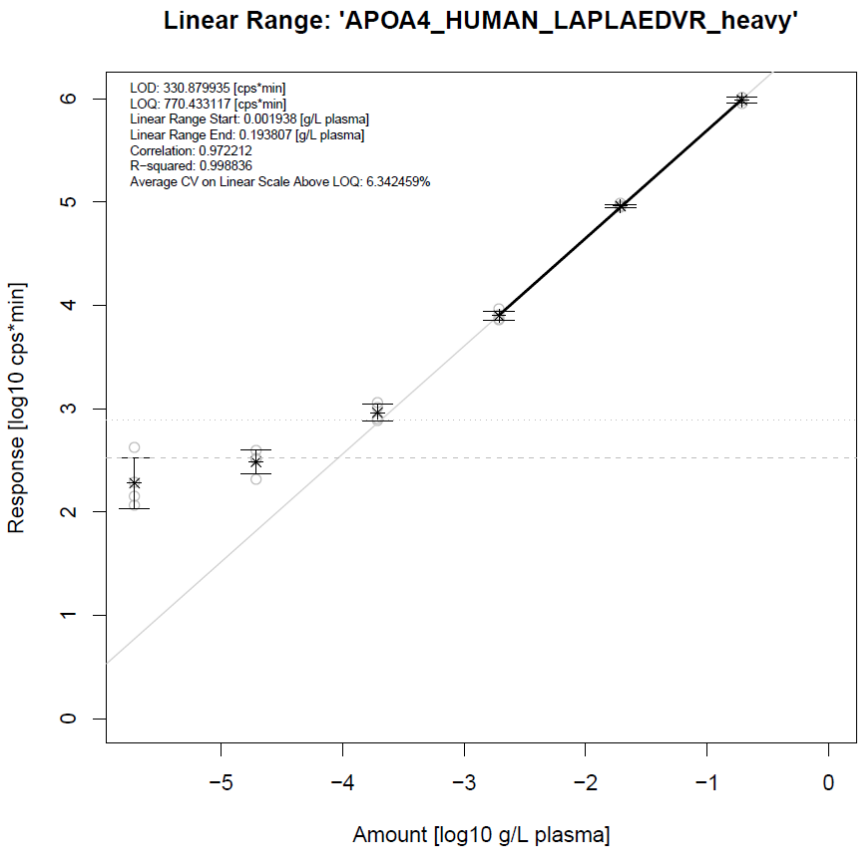

Supplemental Figure 1

Standard Curve for APOB_HUMAN

Nano flow

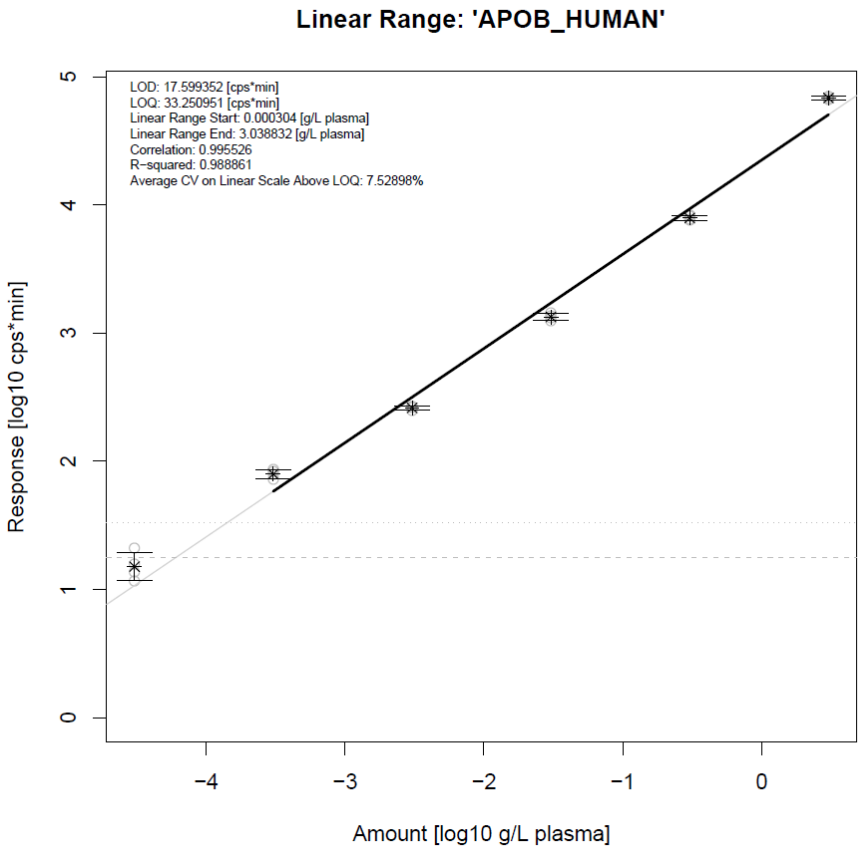

Standard flow

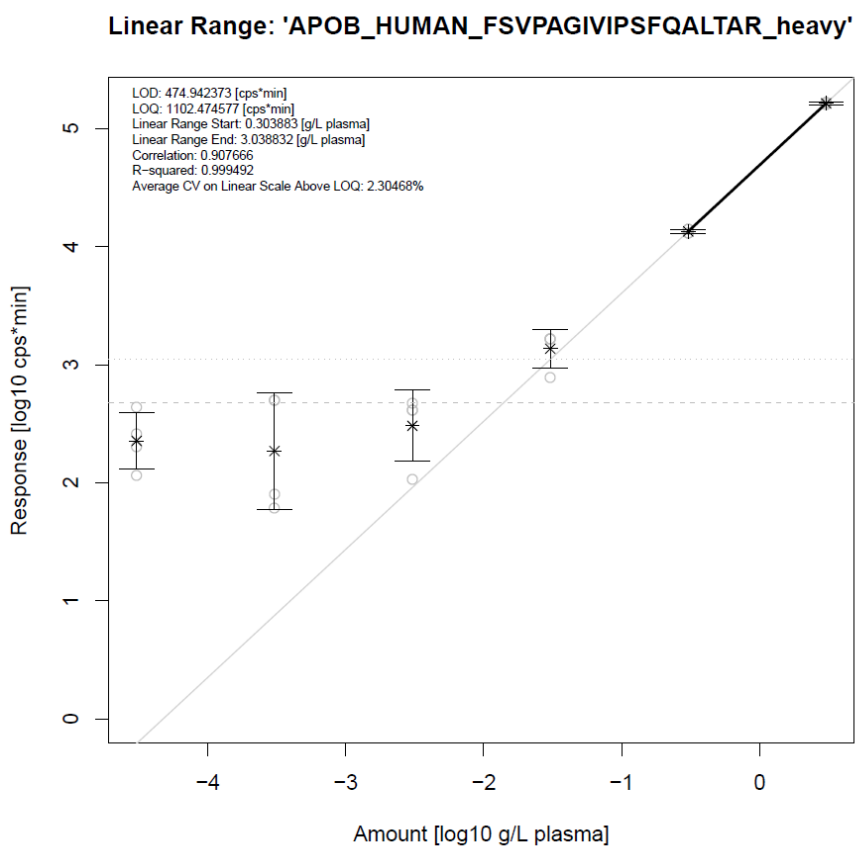

Supplemental Figure 1

Standard Curve for APOC1_HUMAN

Nano flow

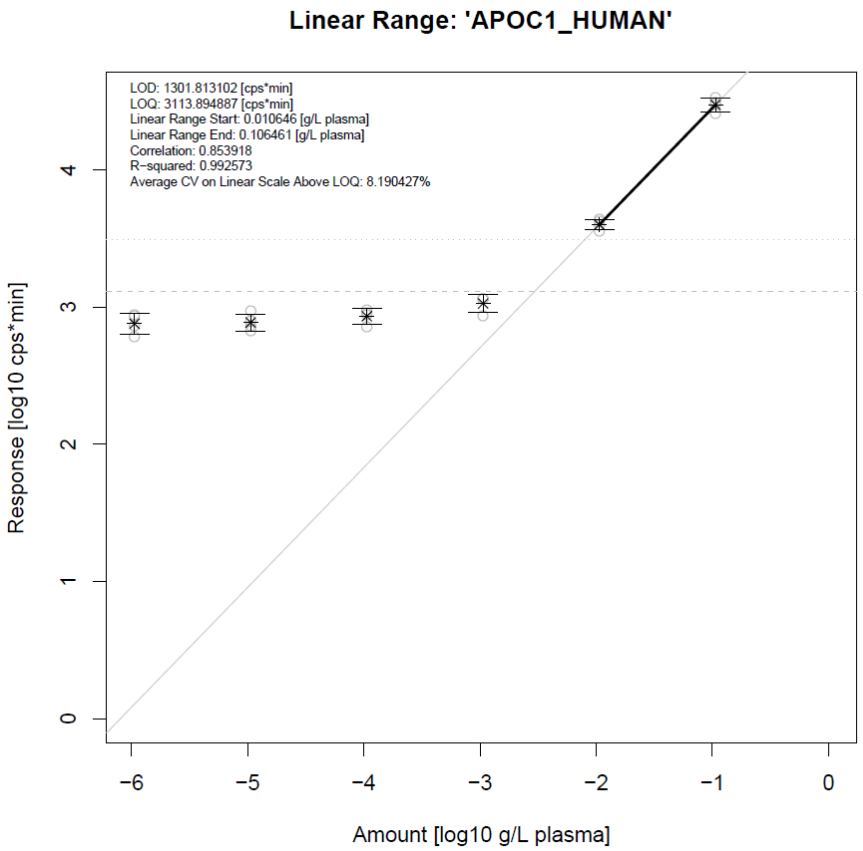

Standard flow

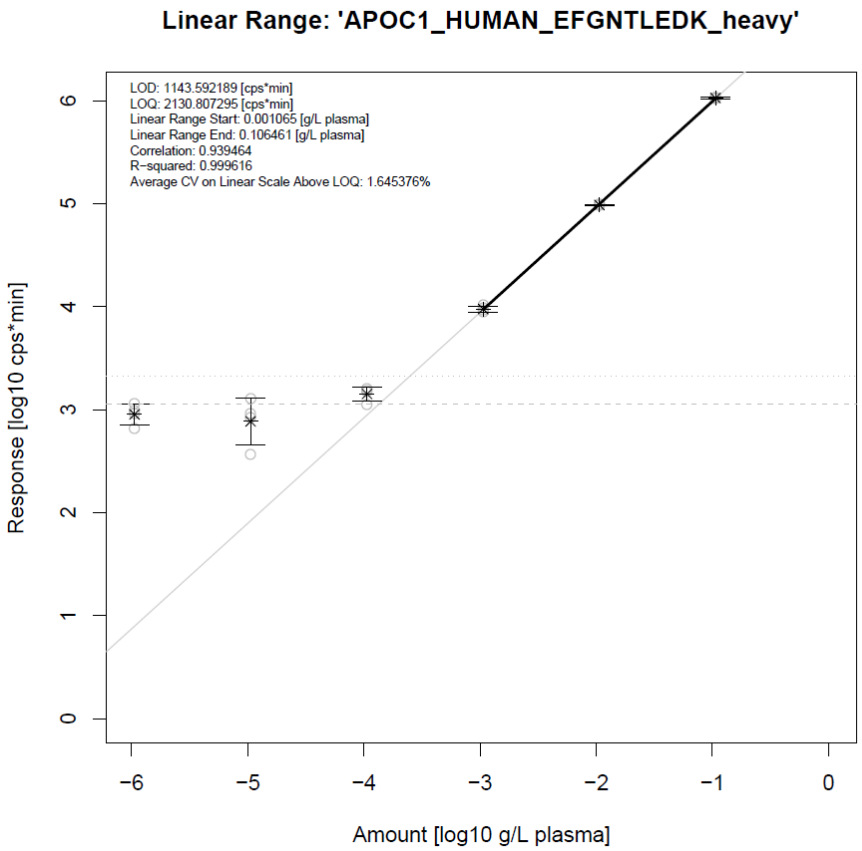

Supplemental Figure 1

Standard Curve for APOC2_HUMAN

Nano flow

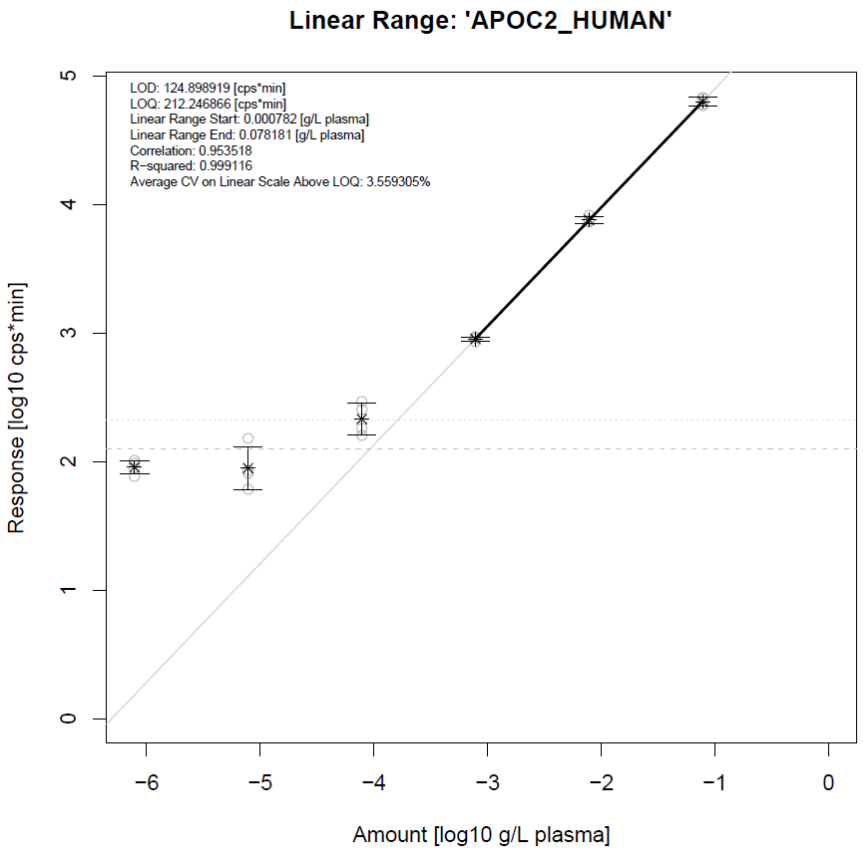

Standard flow

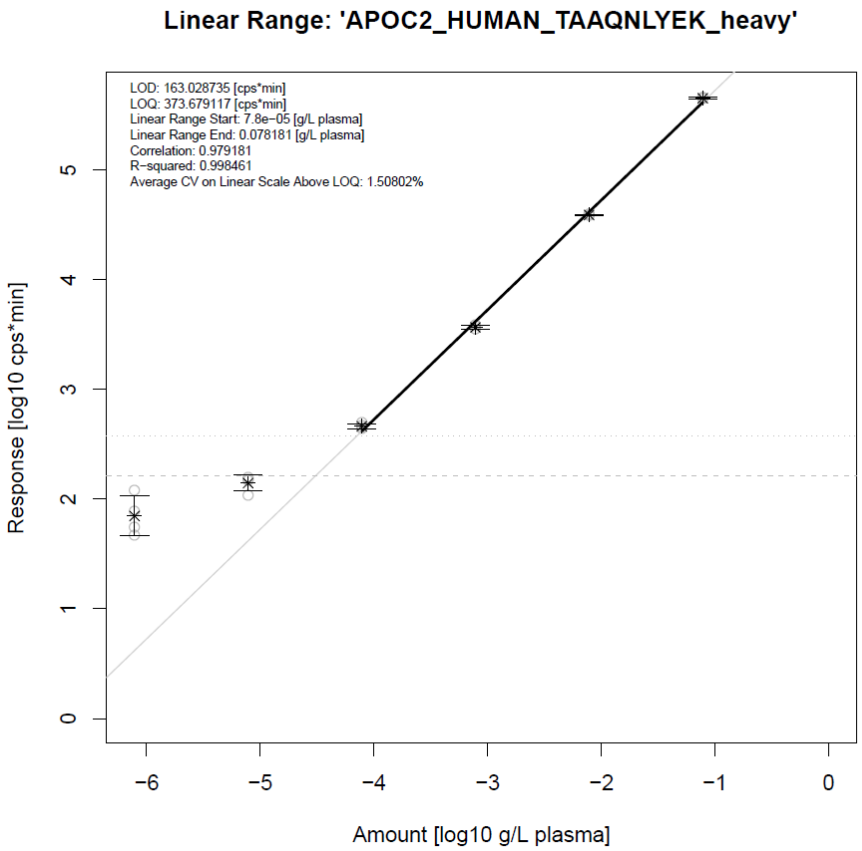

Supplemental Figure 1

Standard Curve for APOC3_HUMAN

Nano flow

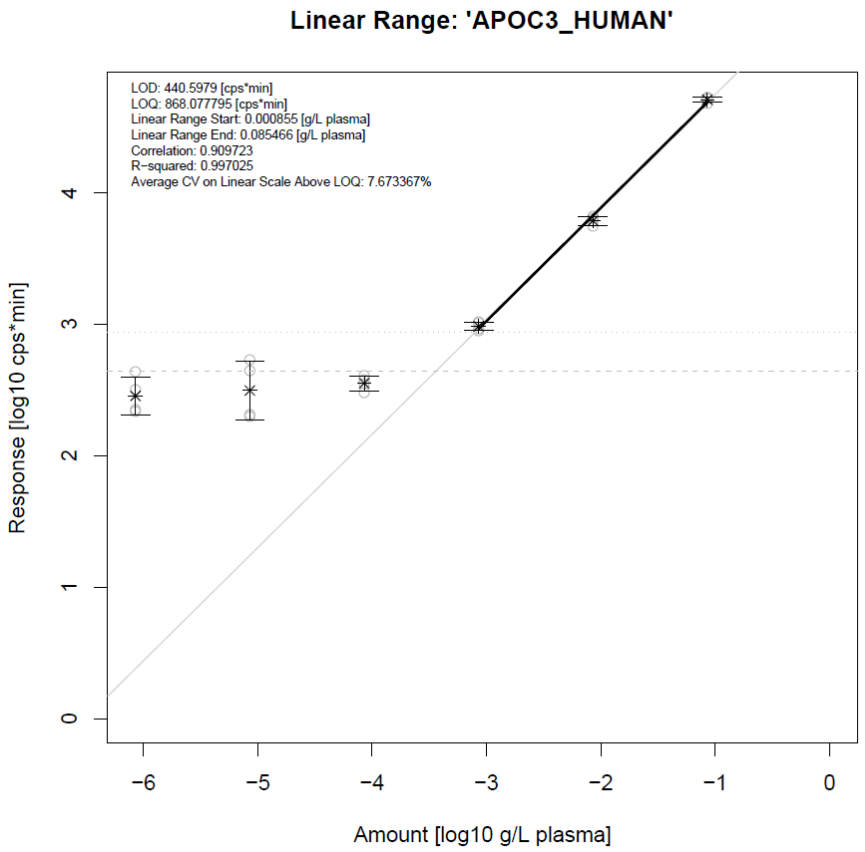

Standard flow

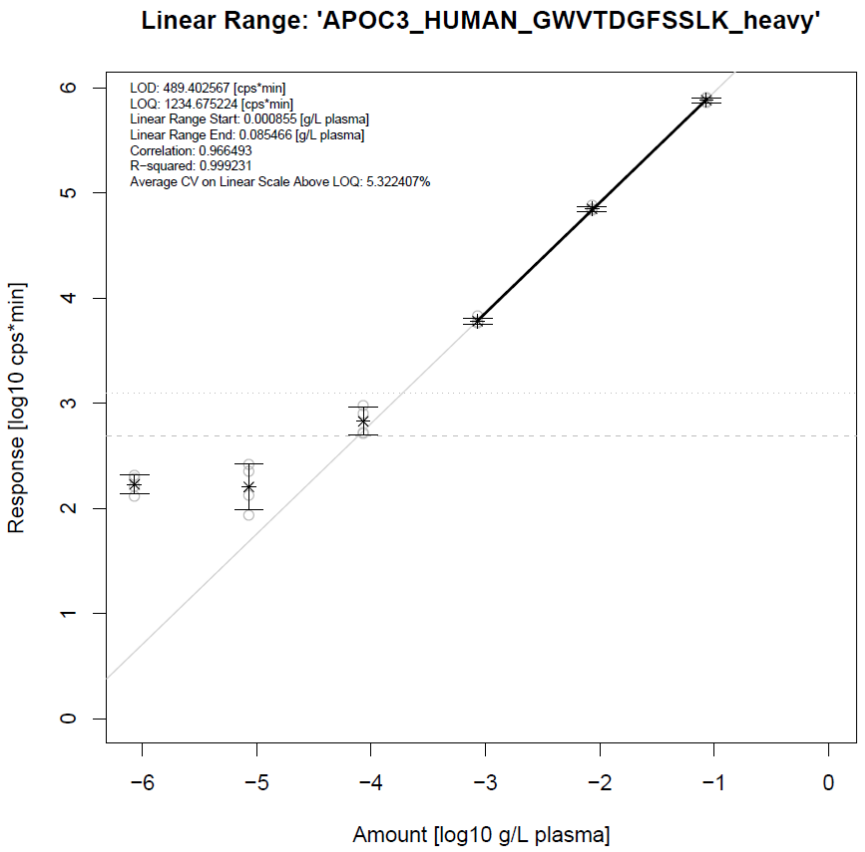

Supplemental Figure 1

Standard Curve for APOD_HUMAN

Nano flow

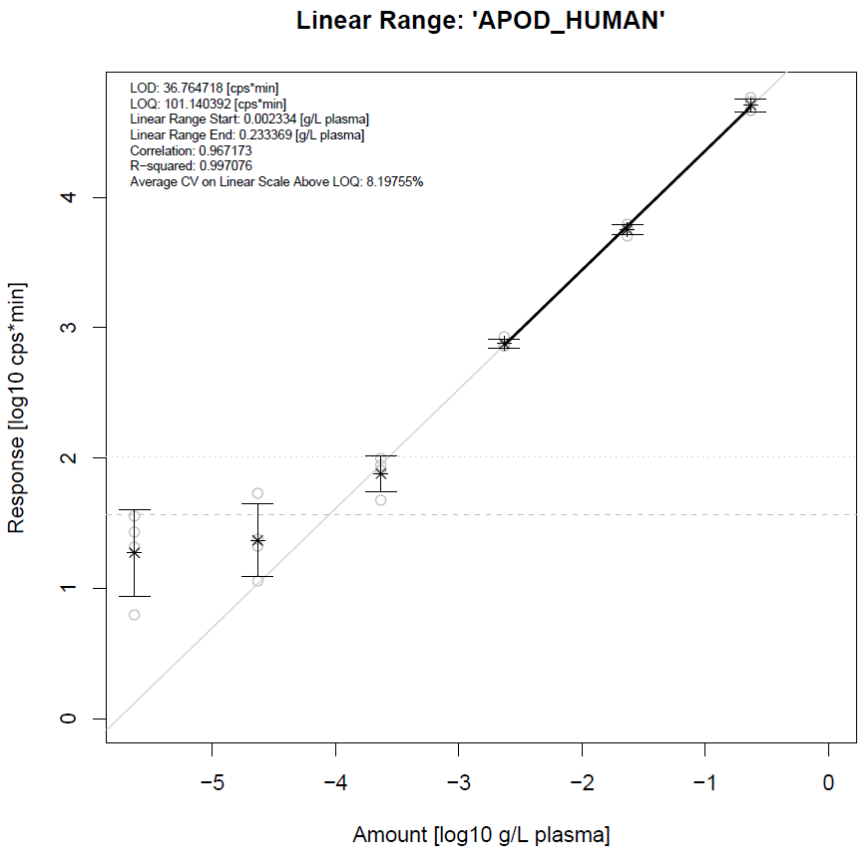

Standard flow

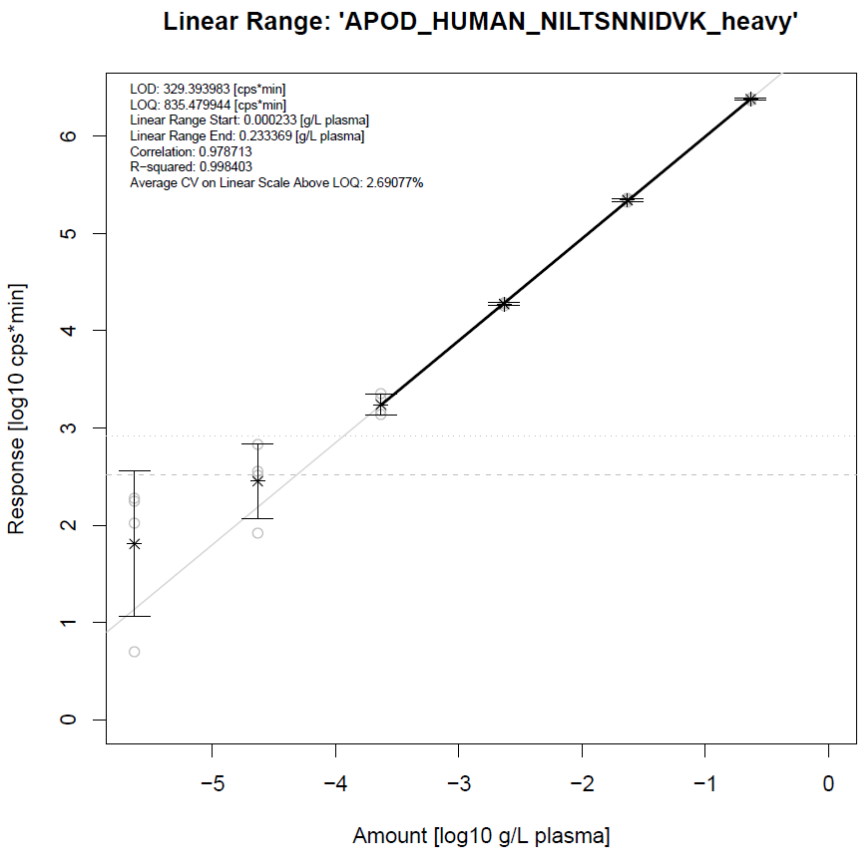

Supplemental Figure 1

Standard Curve for APOE_HUMAN

Nano flow

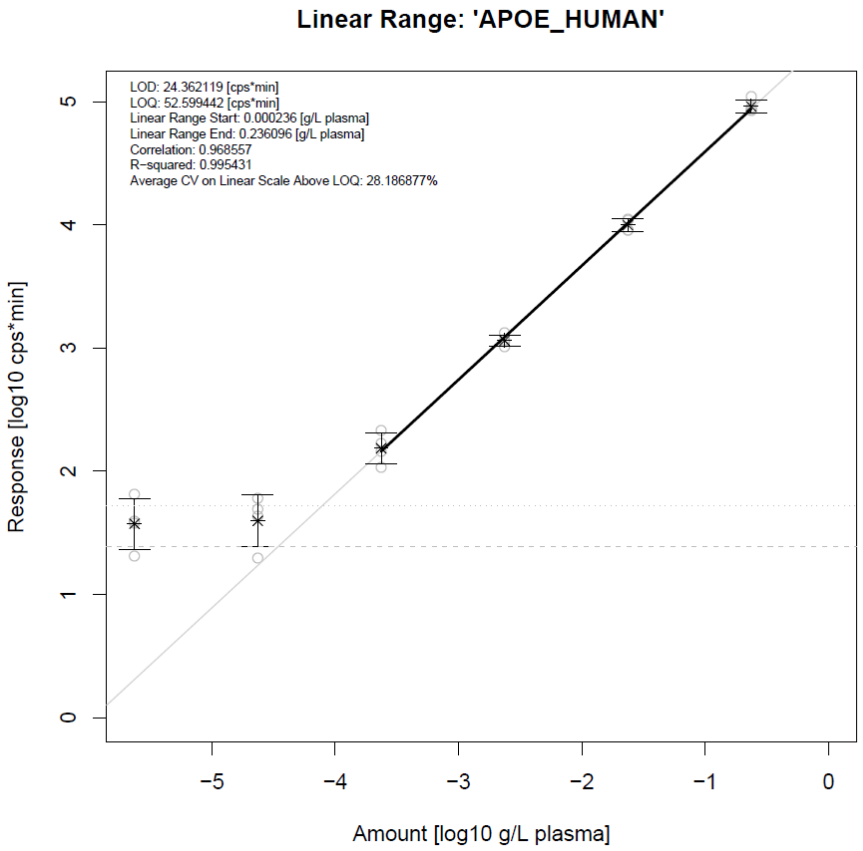

Standard flow

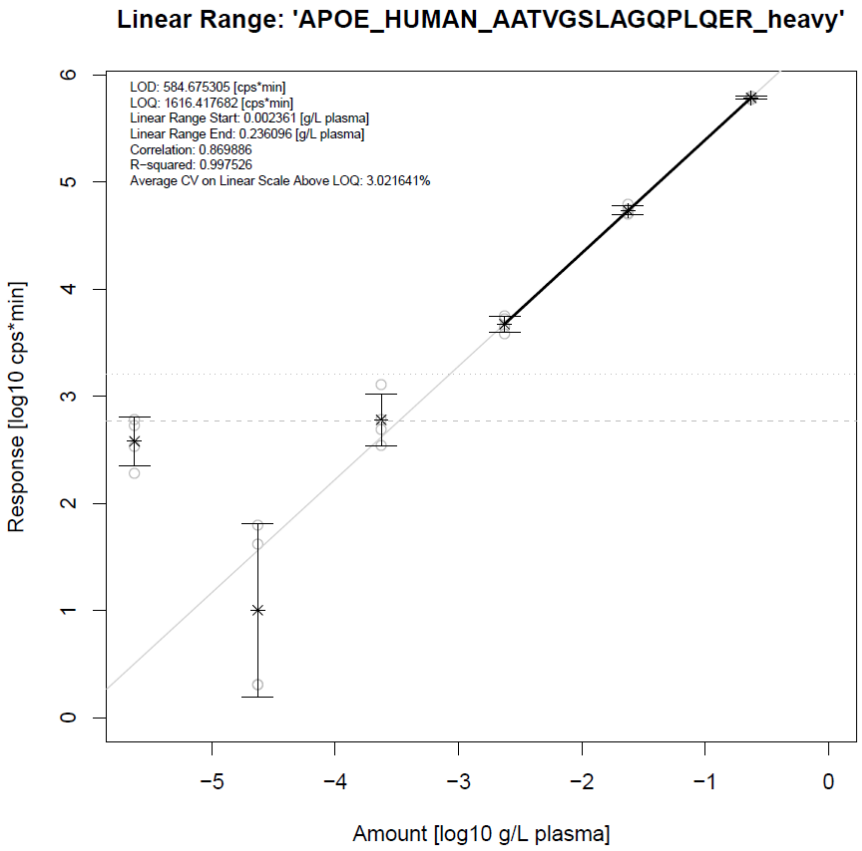

Supplemental Figure 1

Standard Curve for APOH_HUMAN

Nano flow

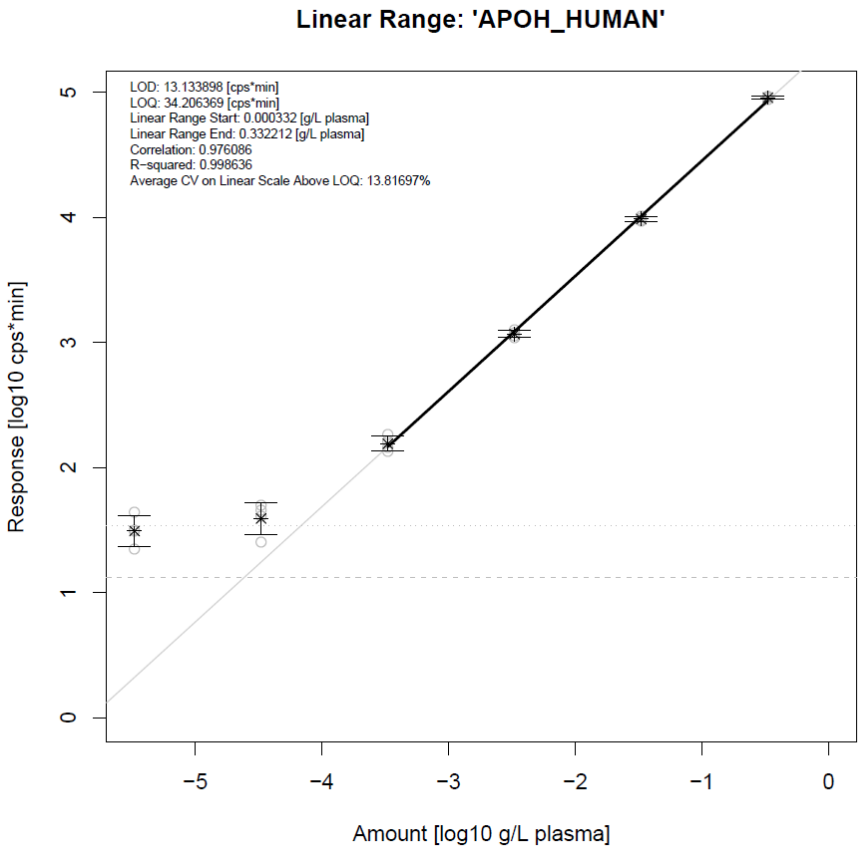

Standard flow

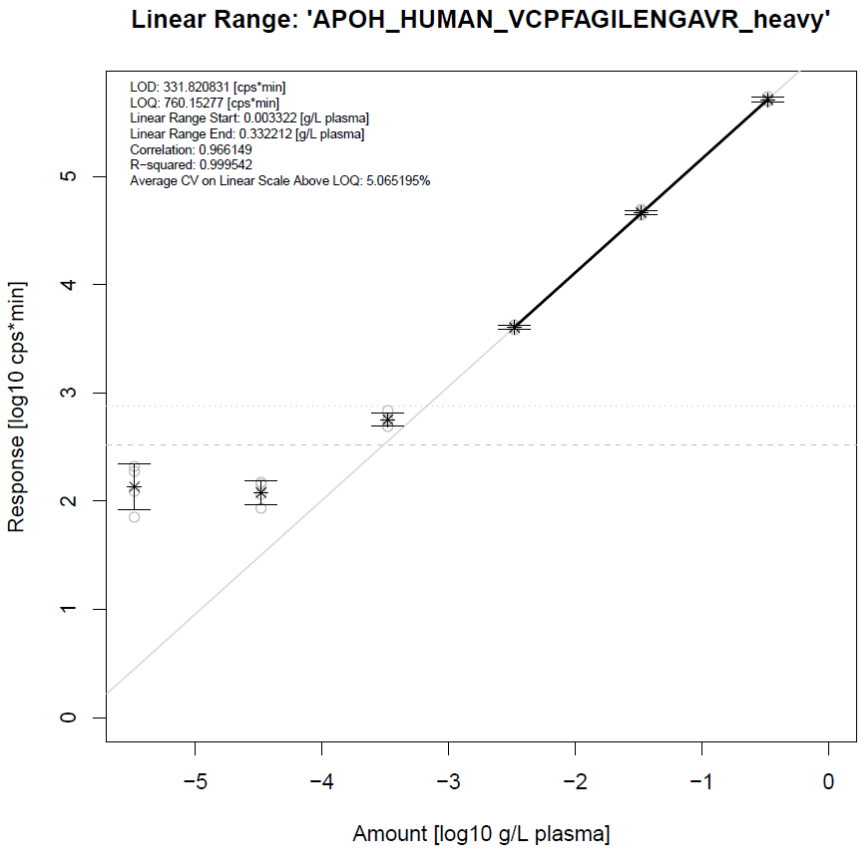

Supplemental Figure 1

Standard Curve for APOL1_HUMAN

Nano flow

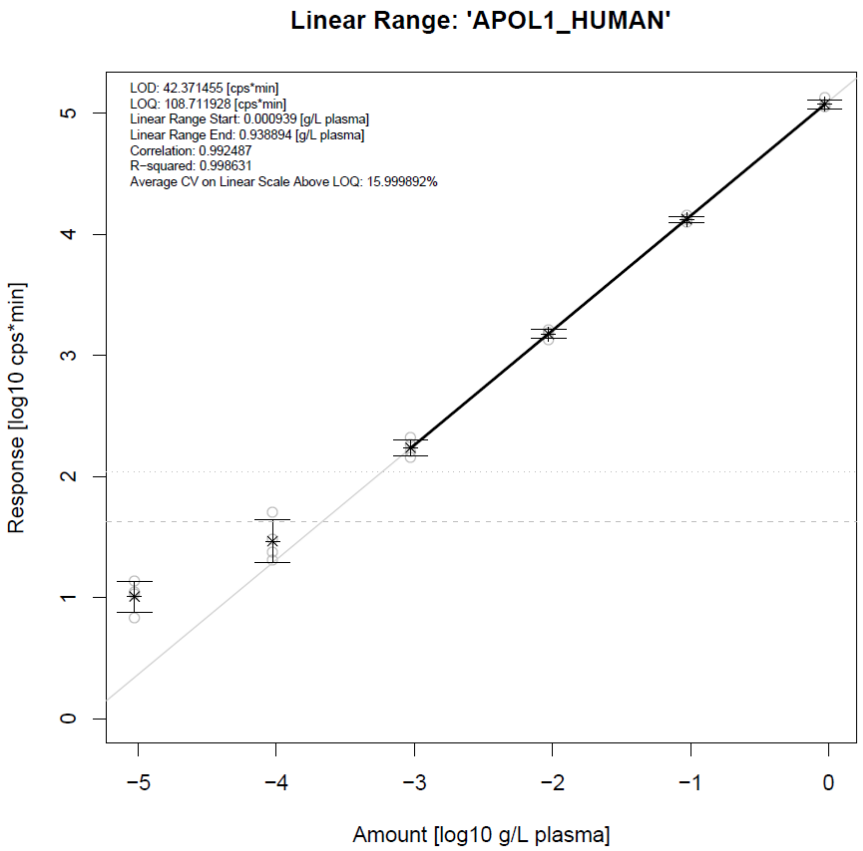

Standard flow

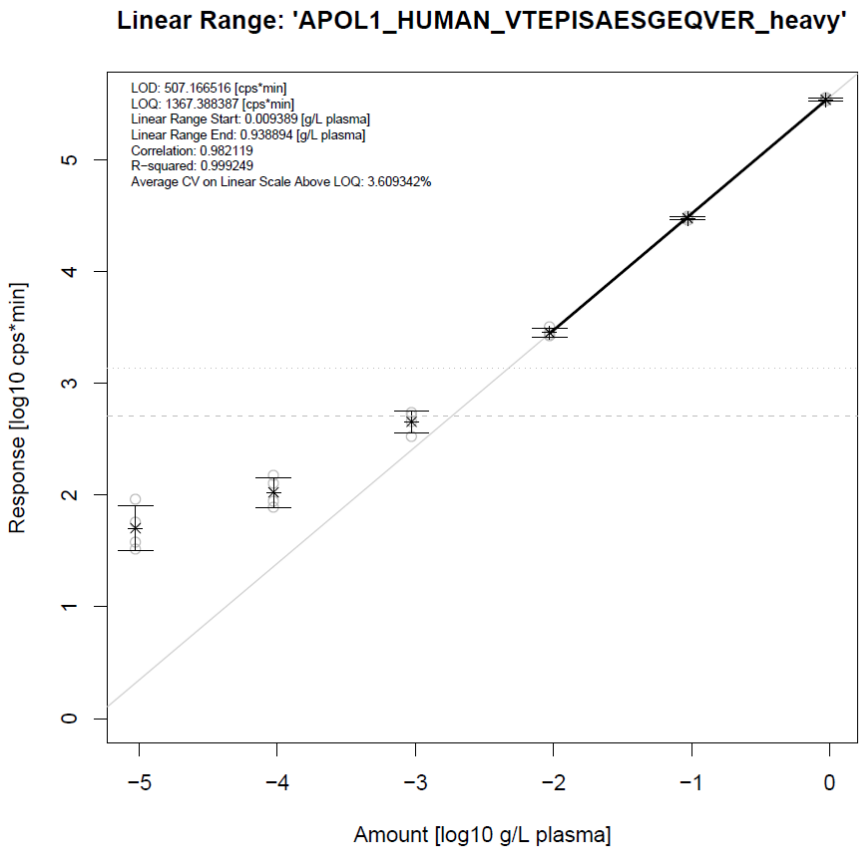

Supplemental Figure 1

Standard Curve for APOM_HUMAN

Nano flow

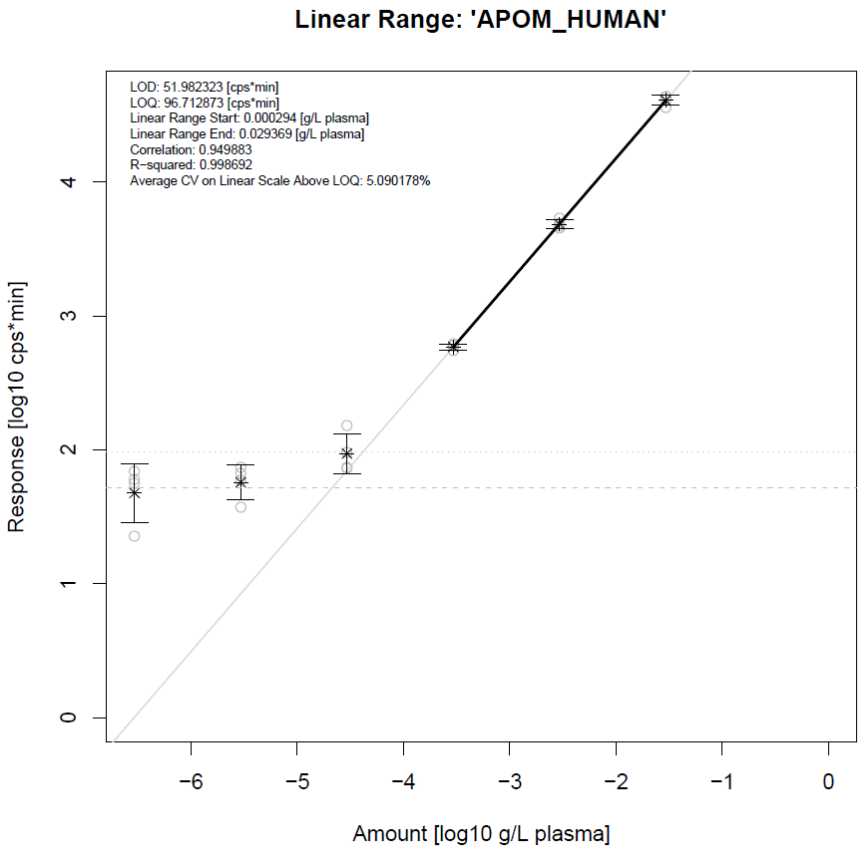

Standard flow

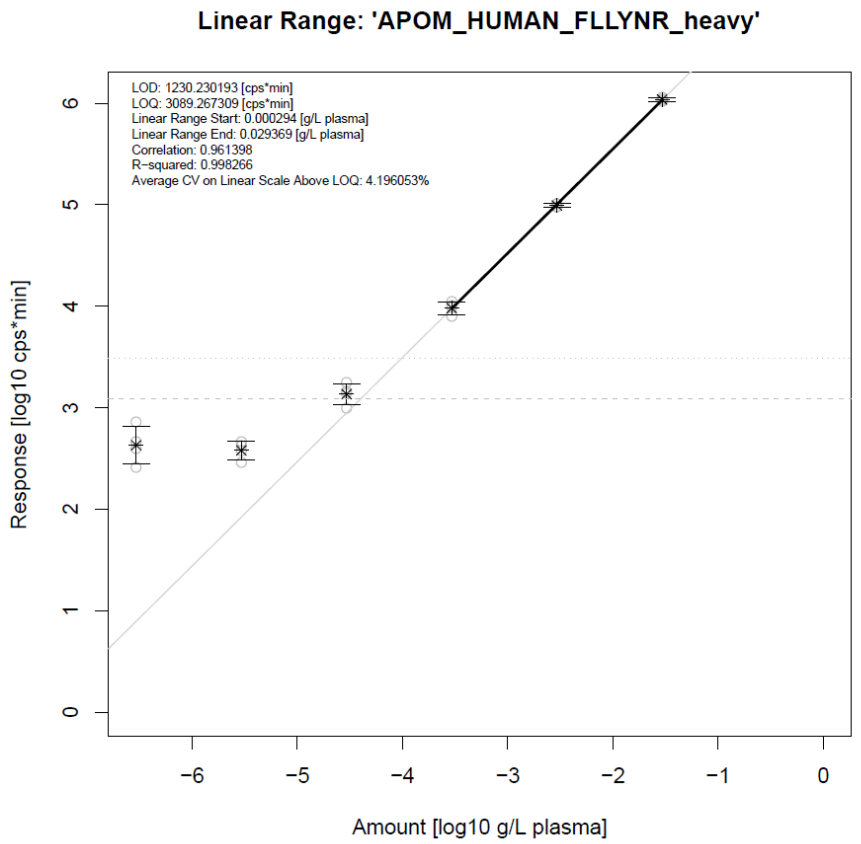

Supplemental Figure 2

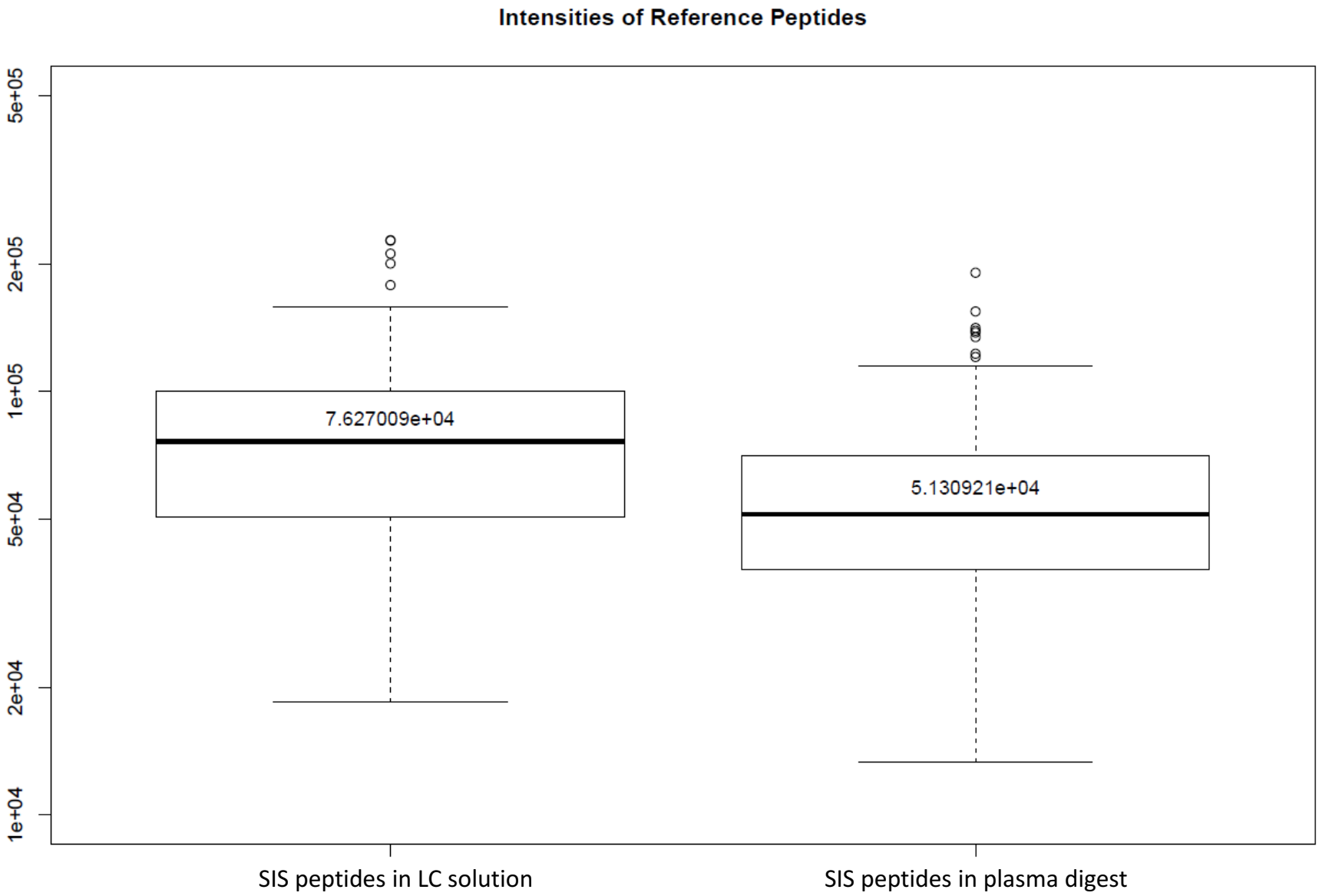

Supplemental Figure 3

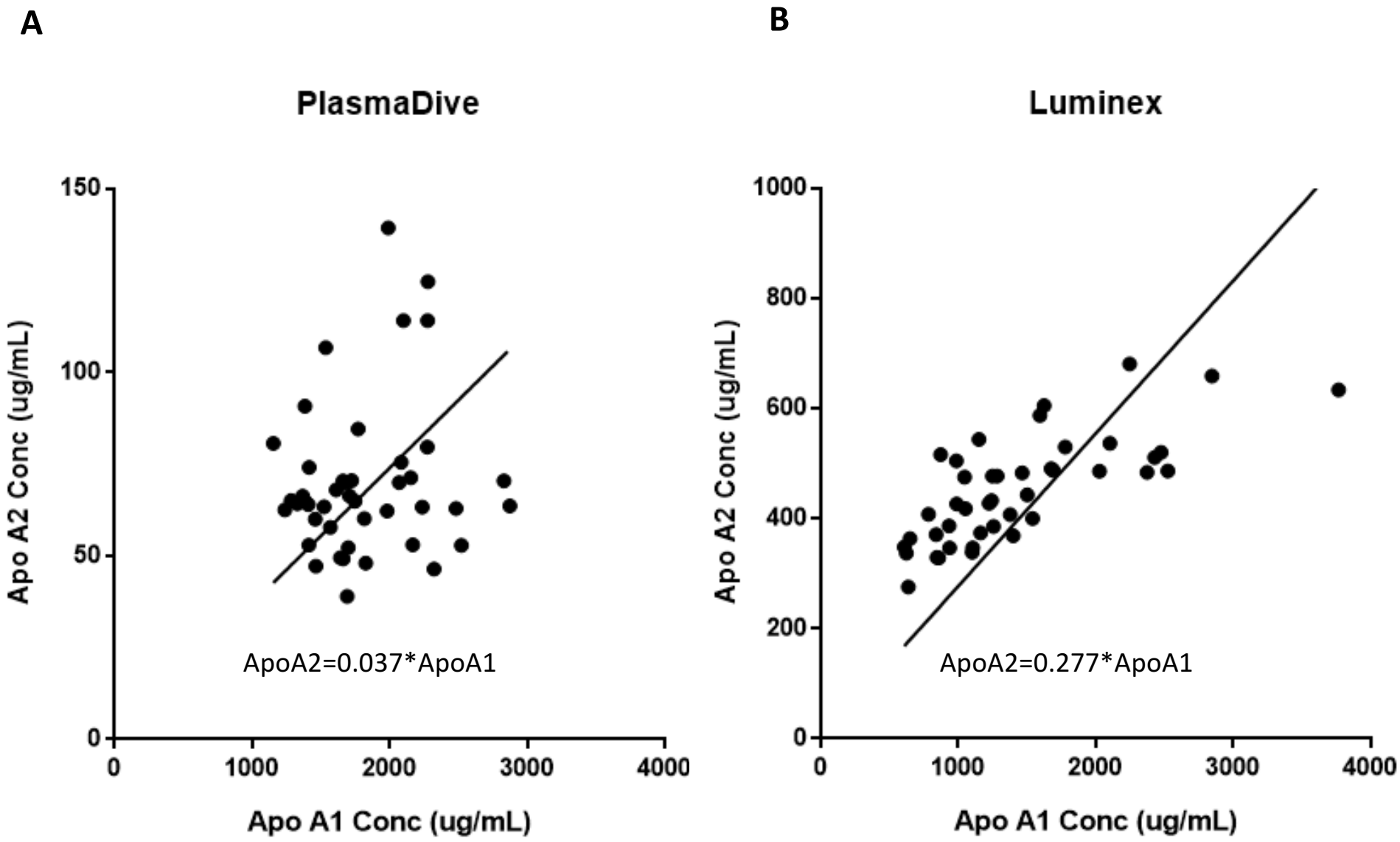

Supplemental Figure 4

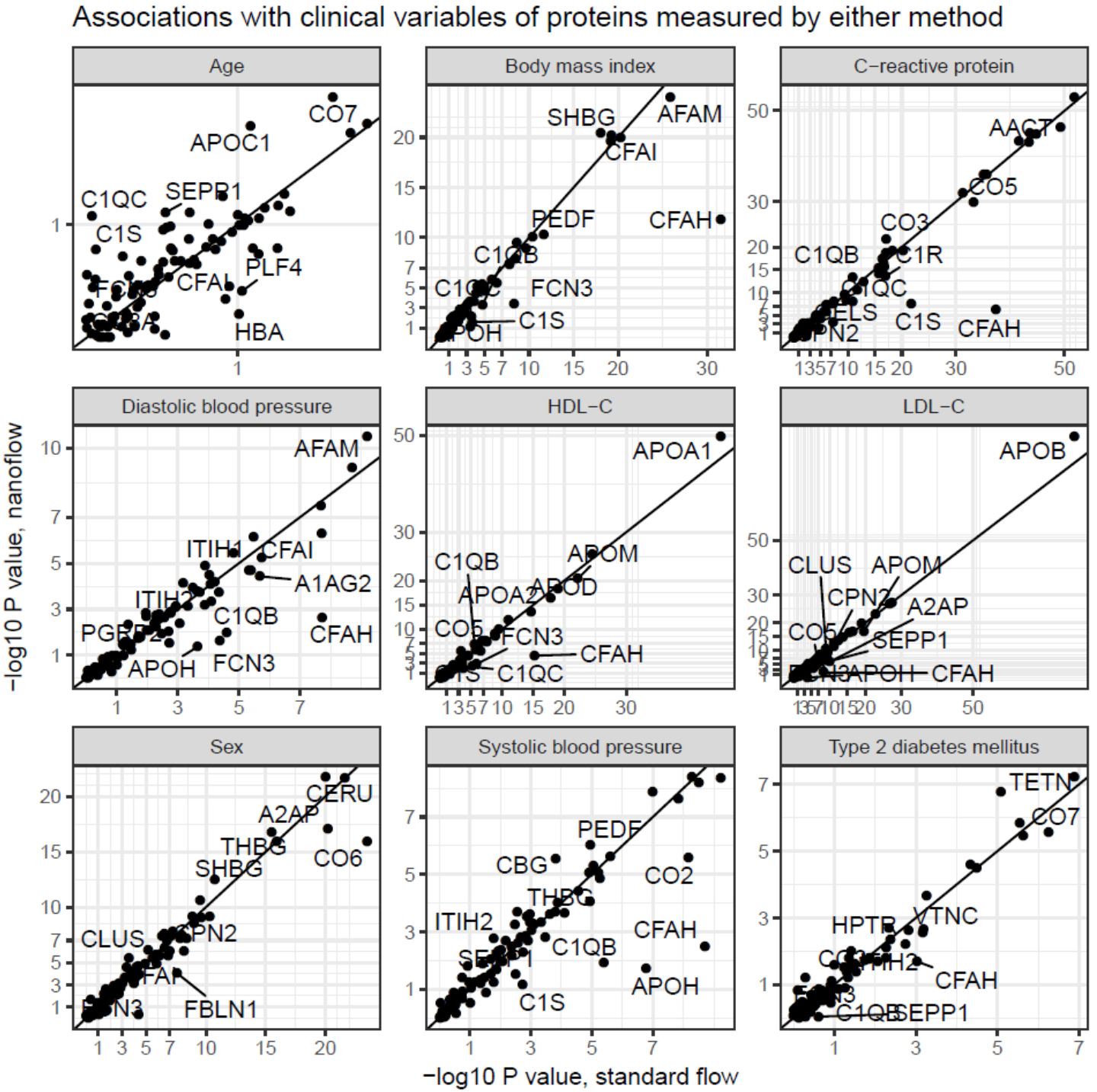

Supplemental Figure 5

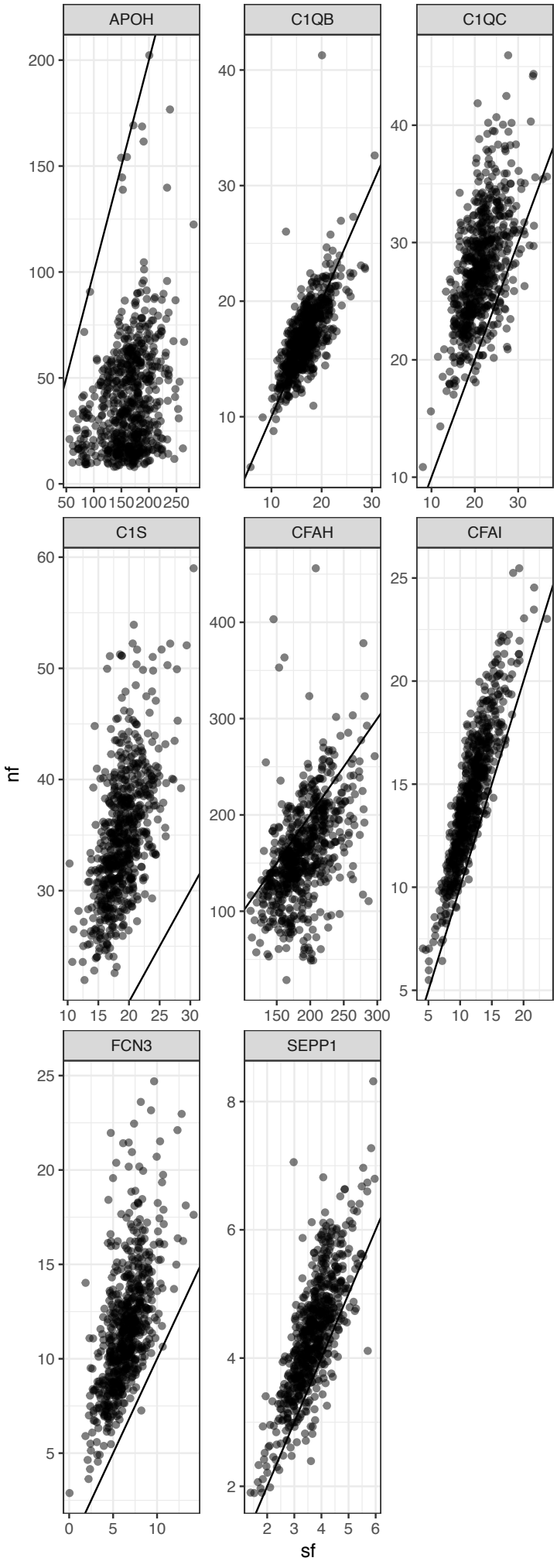

SUPPLEMENTAL TABLE 1:

Precursor m/z	Fragment m/z	CE	Start RT (min)	Stop RT (min)	Polarity	Comment
556.7666	302.1347	22.2	13.3	17.3	Positive	A1AG1_HUMAN.SDVVYTDWK.2
556.7666	712.3301	22.2	13.3	17.3	Positive	A1AG1_HUMAN.SDVVYTDWK.2
556.7666	910.4669	22.2	13.3	17.3	Positive	A1AG1_HUMAN.SDVVYTDWK.2
556.7666	811.3985	22.2	13.3	17.3	Positive	A1AG1_HUMAN.SDVVYTDWK.2
560.7737	720.3443	22.4	13.3	17.3	Positive	A1AG1_HUMAN.SDVVYTDWK.2
560.7737	819.4127	22.4	13.3	17.3	Positive	A1AG1_HUMAN.SDVVYTDWK.2
560.7737	918.4811	22.4	13.3	17.3	Positive	A1AG1_HUMAN.SDVVYTDWK.2
560.7737	302.1347	22.4	13.3	17.3	Positive	A1AG1_HUMAN.SDVVYTDWK.2
617.8564	869.5356	24.3	14.3	18.3	Positive	A1AG2_HUMAN.EHVAHLLFLR.2
617.8564	968.6040	24.3	14.3	18.3	Positive	A1AG2_HUMAN.EHVAHLLFLR.2
617.8564	548.3555	24.3	14.3	18.3	Positive	A1AG2_HUMAN.EHVAHLLFLR.2
617.8564	798.4985	24.3	14.3	18.3	Positive	A1AG2_HUMAN.EHVAHLLFLR.2
622.8610	879.5440	24.5	14.3	18.3	Positive	A1AG2_HUMAN.EHVAHLLFLR.2
622.8610	978.6130	24.5	14.3	18.3	Positive	A1AG2_HUMAN.EHVAHLLFLR.2
622.8610	808.5070	24.5	14.3	18.3	Positive	A1AG2_HUMAN.EHVAHLLFLR.2
622.8610	558.3640	24.5	14.3	18.3	Positive	A1AG2_HUMAN.EHVAHLLFLR.2
508.3109	415.2607	20.6	16.3	20.3	Positive	A1AT_HUMAN.SVLGQLGITK.2
508.3109	829.5142	20.6	16.3	20.3	Positive	A1AT_HUMAN.SVLGQLGITK.2
508.3109	716.4301	20.6	16.3	20.3	Positive	A1AT_HUMAN.SVLGQLGITK.2
508.3109	418.2660	20.6	16.3	20.3	Positive	A1AT_HUMAN.SVLGQLGITK.2
512.3180	426.2802	20.7	16.3	20.3	Positive	A1AT_HUMAN.SVLGQLGITK.2
512.3180	724.4443	20.7	16.3	20.3	Positive	A1AT_HUMAN.SVLGQLGITK.2
512.3180	419.2678	20.7	16.3	20.3	Positive	A1AT_HUMAN.SVLGQLGITK.2
512.3180	837.5284	20.7	16.3	20.3	Positive	A1AT_HUMAN.SVLGQLGITK.2
632.8302	762.4145	24.8	14.7	18.7	Positive	A1BG_HUMAN.SGLSTGWTQLSK.2
632.8302	819.4359	24.8	14.7	18.7	Positive	A1BG_HUMAN.SGLSTGWTQLSK.2
632.8302	920.4836	24.8	14.7	18.7	Positive	A1BG_HUMAN.SGLSTGWTQLSK.2
632.8302	1007.5156	24.8	14.7	18.7	Positive	A1BG_HUMAN.SGLSTGWTQLSK.2
636.8373	928.4978	25.0	14.7	18.7	Positive	A1BG_HUMAN.SGLSTGWTQLSK.2
636.8373	770.4287	25.0	14.7	18.7	Positive	A1BG_HUMAN.SGLSTGWTQLSK.2
636.8373	1015.5298	25.0	14.7	18.7	Positive	A1BG_HUMAN.SGLSTGWTQLSK.2
636.8373	827.4501	25.0	14.7	18.7	Positive	A1BG_HUMAN.SGLSTGWTQLSK.2
395.2289	529.2980	16.8	13.3	17.3	Positive	A2AP_HUMAN.LFGPDLK.2
395.2289	676.3665	16.8	13.3	17.3	Positive	A2AP_HUMAN.LFGPDLK.2
395.2289	375.2238	16.8	13.3	17.3	Positive	A2AP_HUMAN.LFGPDLK.2
395.2289	472.2766	16.8	13.3	17.3	Positive	A2AP_HUMAN.LFGPDLK.2
399.2360	537.3122	16.9	13.3	17.3	Positive	A2AP_HUMAN.LFGPDLK.2
399.2360	684.3807	16.9	13.3	17.3	Positive	A2AP_HUMAN.LFGPDLK.2
399.2360	383.2380	16.9	13.3	17.3	Positive	A2AP_HUMAN.LFGPDLK.2
399.2360	480.2908	16.9	13.3	17.3	Positive	A2AP_HUMAN.LFGPDLK.2
495.2800	890.4843	20.2	11.8	15.8	Positive	A2GL_HUMAN.VAAGAFQGLR.2
495.2800	620.3515	20.2	11.8	15.8	Positive	A2GL_HUMAN.VAAGAFQGLR.2
495.2800	748.4100	20.2	11.8	15.8	Positive	A2GL_HUMAN.VAAGAFQGLR.2
495.2800	819.4472	20.2	11.8	15.8	Positive	A2GL_HUMAN.VAAGAFQGLR.2
500.2841	630.3597	20.3	11.8	15.8	Positive	A2GL_HUMAN.VAAGAFQGLR.2
500.2841	829.4554	20.3	11.8	15.8	Positive	A2GL_HUMAN.VAAGAFQGLR.2
500.2841	758.4183	20.3	11.8	15.8	Positive	A2GL_HUMAN.VAAGAFQGLR.2
500.2841	900.4925	20.3	11.8	15.8	Positive	A2GL_HUMAN.VAAGAFQGLR.2
473.5372	560.2100	24.1	8.6	12.6	Positive	A2MG_HUMAN.HYDGSYSTFGER.3
473.5372	609.2991	24.1	8.6	12.6	Positive	A2MG_HUMAN.HYDGSYSTFGER.3
473.5372	361.1830	24.1	8.6	12.6	Positive	A2MG_HUMAN.HYDGSYSTFGER.3
473.5372	508.2514	24.1	8.6	12.6	Positive	A2MG_HUMAN.HYDGSYSTFGER.3
476.8733	560.2100	24.3	8.6	12.6	Positive	A2MG_HUMAN.HYDGSYSTFGER.3
476.8733	619.3074	24.3	8.6	12.6	Positive	A2MG_HUMAN.HYDGSYSTFGER.3
476.8733	371.1913	24.3	8.6	12.6	Positive	A2MG_HUMAN.HYDGSYSTFGER.3
476.8733	518.2597	24.3	8.6	12.6	Positive	A2MG_HUMAN.HYDGSYSTFGER.3
531.2975	300.1554	21.4	16.2	20.2	Positive	AACT_HUMAN.EIGELYLPK.2
531.2975	633.3970	21.4	16.2	20.2	Positive	AACT_HUMAN.EIGELYLPK.2
531.2975	357.2496	21.4	16.2	20.2	Positive	AACT_HUMAN.EIGELYLPK.2
531.2975	819.4611	21.4	16.2	20.2	Positive	AACT_HUMAN.EIGELYLPK.2
535.3046	827.4753	21.5	16.3	20.3	Positive	AACT_HUMAN.EIGELYLPK.2
535.3046	365.2638	21.5	16.3	20.3	Positive	AACT_HUMAN.EIGELYLPK.2
535.3046	641.4112	21.5	16.3	20.3	Positive	AACT_HUMAN.EIGELYLPK.2
535.3046	300.1554	21.5	16.3	20.3	Positive	AACT_HUMAN.EIGELYLPK.2
807.4072	779.4046	30.8	18.8	22.8	Positive	ABCF1_HUMAN.IGFFNQQYAEQLR.2
807.4072	907.4632	30.8	18.8	22.8	Positive	ABCF1_HUMAN.IGFFNQQYAEQLR.2
807.4072	1149.5647	30.8	18.8	22.8	Positive	ABCF1_HUMAN.IGFFNQQYAEQLR.2
807.4072	616.3413	30.8	18.8	22.8	Positive	ABCF1_HUMAN.IGFFNQQYAEQLR.2
812.4110	1159.5740	30.9	18.7	22.7	Positive	ABCF1_HUMAN.IGFFNQQYAEQLR.2
812.4110	917.4720	30.9	18.7	22.7	Positive	ABCF1_HUMAN.IGFFNQQYAEQLR.2
812.4110	626.3500	30.9	18.7	22.7	Positive	ABCF1_HUMAN.IGFFNQQYAEQLR.2
812.4110	789.4130	30.9	18.7	22.7	Positive	ABCF1_HUMAN.IGFFNQQYAEQLR.2
811.8538	1335.5885	30.9	11.8	15.8	Positive	AFAM_HUMAN.AESPEVC[CAM]FNEESPK.2
811.8538	1109.4932	30.9	11.8	15.8	Positive	AFAM_HUMAN.AESPEVC[CAM]FNEESPK.2
811.8538	1010.4248	30.9	11.8	15.8	Positive	AFAM_HUMAN.AESPEVC[CAM]FNEESPK.2
811.8538	850.3941	30.9	11.8	15.8	Positive	AFAM_HUMAN.AESPEVC[CAM]FNEESPK.2
815.8609	858.4083	31.1	11.8	15.8	Positive	AFAM_HUMAN.AESPEVC[CAM]FNEESPK.2
815.8609	1117.5074	31.1	11.8	15.8	Positive	AFAM_HUMAN.AESPEVC[CAM]FNEESPK.2

815.8609	1343.6027	31.1	11.8	15.8	Positive	AFAM_HUMAN.AESPEVC[CAM]FNEESPK.2
815.8609	1018.4390	31.1	11.8	15.8	Positive	AFAM_HUMAN.AESPEVC[CAM]FNEESPK.2
464.2504	651.3461	19.1	12.7	16.7	Positive	ALBU_HUMAN.YLYEIAR.2
464.2504	764.4301	19.1	12.7	16.7	Positive	ALBU_HUMAN.YLYEIAR.2
464.2504	359.2401	19.1	12.7	16.7	Positive	ALBU_HUMAN.YLYEIAR.2
464.2504	488.2827	19.1	12.7	16.7	Positive	ALBU_HUMAN.YLYEIAR.2
469.2545	661.3543	19.3	12.7	16.7	Positive	ALBU_HUMAN.YLYEIAR.2
469.2545	774.4384	19.3	12.7	16.7	Positive	ALBU_HUMAN.YLYEIAR.2
469.2545	369.2484	19.3	12.7	16.7	Positive	ALBU_HUMAN.YLYEIAR.2
469.2545	498.2910	19.3	12.7	16.7	Positive	ALBU_HUMAN.YLYEIAR.2
607.3397	1013.5561	24.0	13.7	17.7	Positive	AMBP_HUMAN.TVAAC[CAM]NLPIVR.2
607.3397	871.4818	24.0	13.7	17.7	Positive	AMBP_HUMAN.TVAAC[CAM]NLPIVR.2
607.3397	942.5189	24.0	13.7	17.7	Positive	AMBP_HUMAN.TVAAC[CAM]NLPIVR.2
607.3397	711.4512	24.0	13.7	17.7	Positive	AMBP_HUMAN.TVAAC[CAM]NLPIVR.2
612.3438	881.4901	24.1	13.7	17.7	Positive	AMBP_HUMAN.TVAAC[CAM]NLPIVR.2
612.3438	952.5272	24.1	13.7	17.7	Positive	AMBP_HUMAN.TVAAC[CAM]NLPIVR.2
612.3438	1023.5643	24.1	13.7	17.7	Positive	AMBP_HUMAN.TVAAC[CAM]NLPIVR.2
612.3438	721.4595	24.1	13.7	17.7	Positive	AMBP_HUMAN.TVAAC[CAM]NLPIVR.2
634.8823	600.4079	24.9	17.4	21.4	Positive	ANGT_HUMAN.ALQDQLVLVAAK.2
634.8823	1084.6361	24.9	17.4	21.4	Positive	ANGT_HUMAN.ALQDQLVLVAAK.2
634.8823	956.5775	24.9	17.4	21.4	Positive	ANGT_HUMAN.ALQDQLVLVAAK.2
634.8823	713.4920	24.9	17.4	21.4	Positive	ANGT_HUMAN.ALQDQLVLVAAK.2
638.8894	721.5062	25.0	17.4	21.4	Positive	ANGT_HUMAN.ALQDQLVLVAAK.2
638.8894	964.5917	25.0	17.4	21.4	Positive	ANGT_HUMAN.ALQDQLVLVAAK.2
638.8894	1092.6503	25.0	17.4	21.4	Positive	ANGT_HUMAN.ALQDQLVLVAAK.2
638.8894	608.4221	25.0	17.4	21.4	Positive	ANGT_HUMAN.ALQDQLVLVAAK.2
695.3816	623.3334	27.0	22.5	26.5	Positive	ANT3_HUMAN.EVPLNTIIFMGR.2
695.3816	951.5080	27.0	22.5	26.5	Positive	ANT3_HUMAN.EVPLNTIIFMGR.2
695.3816	837.4651	27.0	22.5	26.5	Positive	ANT3_HUMAN.EVPLNTIIFMGR.2
695.3816	736.4174	27.0	22.5	26.5	Positive	ANT3_HUMAN.EVPLNTIIFMGR.2
700.3857	633.3416	27.1	22.5	26.5	Positive	ANT3_HUMAN.EVPLNTIIFMGR.2
700.3857	847.4734	27.1	22.5	26.5	Positive	ANT3_HUMAN.EVPLNTIIFMGR.2
700.3857	746.4257	27.1	22.5	26.5	Positive	ANT3_HUMAN.EVPLNTIIFMGR.2
700.3857	961.5163	27.1	22.5	26.5	Positive	ANT3_HUMAN.EVPLNTIIFMGR.2
521.7618	533.3042	21.1	6.0	10.0	Positive	APOA_HUMAN.GTYSTTVTGR.2
521.7618	333.1881	21.1	6.0	10.0	Positive	APOA_HUMAN.GTYSTTVTGR.2
521.7618	634.3519	21.1	6.0	10.0	Positive	APOA_HUMAN.GTYSTTVTGR.2
521.7618	721.3839	21.1	6.0	10.0	Positive	APOA_HUMAN.GTYSTTVTGR.2
526.7613	543.3031	21.2	6.0	10.0	Positive	APOA_HUMAN.GTYSTTVTGR.2
526.7613	343.1870	21.2	6.0	10.0	Positive	APOA_HUMAN.GTYSTTVTGR.2
526.7613	644.3508	21.2	6.0	10.0	Positive	APOA_HUMAN.GTYSTTVTGR.2
526.7613	731.3828	21.2	6.0	10.0	Positive	APOA_HUMAN.GTYSTTVTGR.2
693.8612	940.4622	26.9	23.5	27.5	Positive	APOA1_HUMAN.VSFLSALEEYTK.2
693.8612	1053.5463	26.9	23.5	27.5	Positive	APOA1_HUMAN.VSFLSALEEYTK.2
693.8612	853.4302	26.9	23.5	27.5	Positive	APOA1_HUMAN.VSFLSALEEYTK.2
693.8612	782.3931	26.9	23.5	27.5	Positive	APOA1_HUMAN.VSFLSALEEYTK.2
697.8683	790.4073	27.0	23.6	27.6	Positive	APOA1_HUMAN.VSFLSALEEYTK.2
697.8683	861.4444	27.0	23.6	27.6	Positive	APOA1_HUMAN.VSFLSALEEYTK.2
697.8683	948.4764	27.0	23.6	27.6	Positive	APOA1_HUMAN.VSFLSALEEYTK.2
697.8683	1061.5605	27.0	23.6	27.6	Positive	APOA1_HUMAN.VSFLSALEEYTK.2
471.2869	571.3814	19.3	13.1	17.1	Positive	APOA2_HUMAN.EQLTPLIK.2
471.2869	684.4654	19.3	13.1	17.1	Positive	APOA2_HUMAN.EQLTPLIK.2
471.2869	373.2809	19.3	13.1	17.1	Positive	APOA2_HUMAN.EQLTPLIK.2
471.2869	470.3337	19.3	13.1	17.1	Positive	APOA2_HUMAN.EQLTPLIK.2
475.2940	579.3956	19.5	13.1	17.1	Positive	APOA2_HUMAN.EQLTPLIK.2
475.2940	692.4796	19.5	13.1	17.1	Positive	APOA2_HUMAN.EQLTPLIK.2
475.2940	381.2951	19.5	13.1	17.1	Positive	APOA2_HUMAN.EQLTPLIK.2
475.2940	478.3479	19.5	13.1	17.1	Positive	APOA2_HUMAN.EQLTPLIK.2
492.2796	589.2940	20.1	11.6	15.6	Positive	APOA4_HUMAN.LAPLAEDVR.2
492.2796	518.2569	20.1	11.6	15.6	Positive	APOA4_HUMAN.LAPLAEDVR.2
492.2796	799.4308	20.1	11.6	15.6	Positive	APOA4_HUMAN.LAPLAEDVR.2
492.2796	702.3781	20.1	11.6	15.6	Positive	APOA4_HUMAN.LAPLAEDVR.2
497.2838	599.3023	20.2	11.6	15.6	Positive	APOA4_HUMAN.LAPLAEDVR.2
497.2838	528.2652	20.2	11.6	15.6	Positive	APOA4_HUMAN.LAPLAEDVR.2
497.2838	809.4391	20.2	11.6	15.6	Positive	APOA4_HUMAN.LAPLAEDVR.2
497.2838	712.3863	20.2	11.6	15.6	Positive	APOA4_HUMAN.LAPLAEDVR.2
937.5304	1372.7947	35.2	26.2	30.2	Positive	APOB_HUMAN.FSVPAGIVIPSFQALTAR.2
937.5304	990.5367	35.2	26.2	30.2	Positive	APOB_HUMAN.FSVPAGIVIPSFQALTAR.2
937.5304	1103.6208	35.2	26.2	30.2	Positive	APOB_HUMAN.FSVPAGIVIPSFQALTAR.2
937.5304	1202.6892	35.2	26.2	30.2	Positive	APOB_HUMAN.FSVPAGIVIPSFQALTAR.2
942.5298	1212.6881	35.4	26.2	30.2	Positive	APOB_HUMAN.FSVPAGIVIPSFQALTAR.2
942.5298	1382.7936	35.4	26.2	30.2	Positive	APOB_HUMAN.FSVPAGIVIPSFQALTAR.2
942.5298	1000.5356	35.4	26.2	30.2	Positive	APOB_HUMAN.FSVPAGIVIPSFQALTAR.2
942.5298	1113.6197	35.4	26.2	30.2	Positive	APOB_HUMAN.FSVPAGIVIPSFQALTAR.2
526.7484	776.3785	21.2	9.2	13.2	Positive	APOC1_HUMAN.EFGNTLEDK.2
526.7484	391.1823	21.2	9.2	13.2	Positive	APOC1_HUMAN.EFGNTLEDK.2
526.7484	504.2664	21.2	9.2	13.2	Positive	APOC1_HUMAN.EFGNTLEDK.2
526.7484	605.3141	21.2	9.2	13.2	Positive	APOC1_HUMAN.EFGNTLEDK.2
530.7555	784.3927	21.4	9.2	13.2	Positive	APOC1_HUMAN.EFGNTLEDK.2
530.7555	399.1965	21.4	9.2	13.2	Positive	APOC1_HUMAN.EFGNTLEDK.2
530.7555	512.2806	21.4	9.2	13.2	Positive	APOC1_HUMAN.EFGNTLEDK.2

530.7555	613.3283	21.4	9.2	13.2	Positive	APOC1_HUMAN.EFGNTLEDK.2
519.2667	666.3457	21.0	6.2	10.2	Positive	APOC2_HUMAN.TAAQNLYEK.2
519.2667	439.2187	21.0	6.2	10.2	Positive	APOC2_HUMAN.TAAQNLYEK.2
519.2667	794.4043	21.0	6.2	10.2	Positive	APOC2_HUMAN.TAAQNLYEK.2
519.2667	865.4414	21.0	6.2	10.2	Positive	APOC2_HUMAN.TAAQNLYEK.2
523.2738	873.4556	21.1	6.2	10.2	Positive	APOC2_HUMAN.TAAQNLYEK.2
523.2738	447.2329	21.1	6.2	10.2	Positive	APOC2_HUMAN.TAAQNLYEK.2
523.2738	674.3599	21.1	6.2	10.2	Positive	APOC2_HUMAN.TAAQNLYEK.2
523.2738	802.4185	21.1	6.2	10.2	Positive	APOC2_HUMAN.TAAQNLYEK.2
598.8009	854.4254	23.7	18.2	22.2	Positive	APOC3_HUMAN.GWVTDGFSSLK.2
598.8009	953.4938	23.7	18.2	22.2	Positive	APOC3_HUMAN.GWVTDGFSSLK.2
598.8009	638.3508	23.7	18.2	22.2	Positive	APOC3_HUMAN.GWVTDGFSSLK.2
598.8009	753.3777	23.7	18.2	22.2	Positive	APOC3_HUMAN.GWVTDGFSSLK.2
602.8080	646.3650	23.8	18.2	22.2	Positive	APOC3_HUMAN.GWVTDGFSSLK.2
602.8080	961.5080	23.8	18.2	22.2	Positive	APOC3_HUMAN.GWVTDGFSSLK.2
602.8080	862.4396	23.8	18.2	22.2	Positive	APOC3_HUMAN.GWVTDGFSSLK.2
602.8080	761.3919	23.8	18.2	22.2	Positive	APOC3_HUMAN.GWVTDGFSSLK.2
615.8381	1003.5419	24.3	13.3	17.3	Positive	APOD_HUMAN.NILTSNNIDVK.2
615.8381	890.4578	24.3	13.3	17.3	Positive	APOD_HUMAN.NILTSNNIDVK.2
615.8381	789.4101	24.3	13.3	17.3	Positive	APOD_HUMAN.NILTSNNIDVK.2
615.8381	341.2183	24.3	13.3	17.3	Positive	APOD_HUMAN.NILTSNNIDVK.2
619.8452	341.2183	24.4	13.3	17.3	Positive	APOD_HUMAN.NILTSNNIDVK.2
619.8452	1011.5561	24.4	13.3	17.3	Positive	APOD_HUMAN.NILTSNNIDVK.2
619.8452	898.4720	24.4	13.3	17.3	Positive	APOD_HUMAN.NILTSNNIDVK.2
619.8452	797.4243	24.4	13.3	17.3	Positive	APOD_HUMAN.NILTSNNIDVK.2
749.4046	898.4741	28.8	12.6	16.6	Positive	APOE_HUMAN.AATVGSLAGQPLQER.2
749.4046	1155.6117	28.8	12.6	16.6	Positive	APOE_HUMAN.AATVGSLAGQPLQER.2
749.4046	827.4370	28.8	12.6	16.6	Positive	APOE_HUMAN.AATVGSLAGQPLQER.2
749.4046	642.3570	28.8	12.6	16.6	Positive	APOE_HUMAN.AATVGSLAGQPLQER.2
754.4088	837.4453	29.0	12.6	16.6	Positive	APOE_HUMAN.AATVGSLAGQPLQER.2
754.4088	908.4824	29.0	12.6	16.6	Positive	APOE_HUMAN.AATVGSLAGQPLQER.2
754.4088	1165.6199	29.0	12.6	16.6	Positive	APOE_HUMAN.AATVGSLAGQPLQER.2
754.4088	652.3652	29.0	12.6	16.6	Positive	APOE_HUMAN.AATVGSLAGQPLQER.2
751.8928	999.5582	28.9	19.8	23.8	Positive	APOH_HUMAN.VC[CAM]PFAGILENGAVR.2
751.8928	758.4155	28.9	19.8	23.8	Positive	APOH_HUMAN.VC[CAM]PFAGILENGAVR.2
751.8928	1243.6793	28.9	19.8	23.8	Positive	APOH_HUMAN.VC[CAM]PFAGILENGAVR.2
751.8928	928.5211	28.9	19.8	23.8	Positive	APOH_HUMAN.VC[CAM]PFAGILENGAVR.2
756.8970	938.5293	29.0	20.1	24.1	Positive	APOH_HUMAN.VC[CAM]PFAGILENGAVR.2
756.8970	1009.5664	29.0	20.1	24.1	Positive	APOH_HUMAN.VC[CAM]PFAGILENGAVR.2
756.8970	768.4238	29.0	20.1	24.1	Positive	APOH_HUMAN.VC[CAM]PFAGILENGAVR.2
756.8970	1253.6876	29.0	20.1	24.1	Positive	APOH_HUMAN.VC[CAM]PFAGILENGAVR.2
815.8996	804.3846	31.1	10.1	14.1	Positive	APOL1_HUMAN.VTEPISAESGEQVER.2
815.8996	933.4272	31.1	10.1	14.1	Positive	APOL1_HUMAN.VTEPISAESGEQVER.2
815.8996	1091.4964	31.1	10.1	14.1	Positive	APOL1_HUMAN.VTEPISAESGEQVER.2
815.8996	1301.6332	31.1	10.1	14.1	Positive	APOL1_HUMAN.VTEPISAESGEQVER.2
820.9037	1101.5046	31.2	10.1	14.1	Positive	APOL1_HUMAN.VTEPISAESGEQVER.2
820.9037	943.4355	31.2	10.1	14.1	Positive	APOL1_HUMAN.VTEPISAESGEQVER.2
820.9037	814.3929	31.2	10.1	14.1	Positive	APOL1_HUMAN.VTEPISAESGEQVER.2
820.9037	1311.6415	31.2	10.1	14.1	Positive	APOL1_HUMAN.VTEPISAESGEQVER.2
413.2345	678.3933	17.4	13.9	17.9	Positive	APOM_HUMAN.FLLYNR.2
413.2345	565.3093	17.4	13.9	17.9	Positive	APOM_HUMAN.FLLYNR.2
413.2345	452.2252	17.4	13.9	17.9	Positive	APOM_HUMAN.FLLYNR.2
418.2386	688.4016	17.5	13.9	17.9	Positive	APOM_HUMAN.FLLYNR.2
418.2386	575.3175	17.5	13.9	17.9	Positive	APOM_HUMAN.FLLYNR.2
418.2386	462.2335	17.5	13.9	17.9	Positive	APOM_HUMAN.FLLYNR.2
527.7529	300.1554	21.3	8.5	12.5	Positive	B3AT_HUMAN.IDAYMAQSR.2
527.7529	592.2872	21.3	8.5	12.5	Positive	B3AT_HUMAN.IDAYMAQSR.2
527.7529	755.3505	21.3	8.5	12.5	Positive	B3AT_HUMAN.IDAYMAQSR.2
527.7529	826.3876	21.3	8.5	12.5	Positive	B3AT_HUMAN.IDAYMAQSR.2
532.7570	300.1560	21.4	8.5	12.5	Positive	B3AT_HUMAN.IDAYMAQSR.2
532.7570	602.2960	21.4	8.5	12.5	Positive	B3AT_HUMAN.IDAYMAQSR.2
532.7570	765.3590	21.4	8.5	12.5	Positive	B3AT_HUMAN.IDAYMAQSR.2
532.7570	836.3960	21.4	8.5	12.5	Positive	B3AT_HUMAN.IDAYMAQSR.2
538.7706	632.3548	21.6	13.8	17.8	Positive	C1QB_HUMAN.GNLC[CAM]VNLMR.2
538.7706	533.2864	21.6	13.8	17.8	Positive	C1QB_HUMAN.GNLC[CAM]VNLMR.2
538.7706	792.3855	21.6	13.8	17.8	Positive	C1QB_HUMAN.GNLC[CAM]VNLMR.2
538.7706	905.4696	21.6	13.8	17.8	Positive	C1QB_HUMAN.GNLC[CAM]VNLMR.2
543.7701	543.2853	21.8	13.8	17.8	Positive	C1QB_HUMAN.GNLC[CAM]VNLMR.2
543.7701	915.4684	21.8	13.8	17.8	Positive	C1QB_HUMAN.GNLC[CAM]VNLMR.2
543.7701	802.3844	21.8	13.8	17.8	Positive	C1QB_HUMAN.GNLC[CAM]VNLMR.2
543.7701	642.3537	21.8	13.8	17.8	Positive	C1QB_HUMAN.GNLC[CAM]VNLMR.2
542.7929	623.3511	21.8	15.1	19.1	Positive	C1QC_HUMAN.FQSVFTVTR.2
542.7929	363.1663	21.8	15.1	19.1	Positive	C1QC_HUMAN.FQSVFTVTR.2
542.7929	722.4196	21.8	15.1	19.1	Positive	C1QC_HUMAN.FQSVFTVTR.2
542.7929	809.4516	21.8	15.1	19.1	Positive	C1QC_HUMAN.FQSVFTVTR.2
547.7971	633.3594	21.9	15.1	19.1	Positive	C1QC_HUMAN.FQSVFTVTR.2
547.7971	363.1663	21.9	15.1	19.1	Positive	C1QC_HUMAN.FQSVFTVTR.2
547.7971	819.4598	21.9	15.1	19.1	Positive	C1QC_HUMAN.FQSVFTVTR.2
547.7971	732.4278	21.9	15.1	19.1	Positive	C1QC_HUMAN.FQSVFTVTR.2
639.8054	812.3971	25.1	10.1	14.1	Positive	C1R_HUMAN.YTTTMGVNTYK.2
639.8054	913.4448	25.1	10.1	14.1	Positive	C1R_HUMAN.YTTTMGVNTYK.2

639.8054	681.3566	25.1	10.1	14.1	Positive	C1R_HUMAN.YTTTMGVNTYK.2
639.8054	1014.4925	25.1	10.1	14.1	Positive	C1R_HUMAN.YTTTMGVNTYK.2
643.8125	689.3708	25.2	10.1	14.1	Positive	C1R_HUMAN.YTTTMGVNTYK.2
643.8125	1022.5067	25.2	10.1	14.1	Positive	C1R_HUMAN.YTTTMGVNTYK.2
643.8125	820.4113	25.2	10.1	14.1	Positive	C1R_HUMAN.YTTTMGVNTYK.2
643.8125	921.4590	25.2	10.1	14.1	Positive	C1R_HUMAN.YTTTMGVNTYK.2
639.3279	571.3926	25.1	16.1	20.1	Positive	C1S_HUMAN.TNFDNDIALVR.2
639.3279	800.4625	25.1	16.1	20.1	Positive	C1S_HUMAN.TNFDNDIALVR.2
639.3279	915.4894	25.1	16.1	20.1	Positive	C1S_HUMAN.TNFDNDIALVR.2
639.3279	1062.5578	25.1	16.1	20.1	Positive	C1S_HUMAN.TNFDNDIALVR.2
644.3320	581.4009	25.2	15.9	19.9	Positive	C1S_HUMAN.TNFDNDIALVR.2
644.3320	810.4707	25.2	15.9	19.9	Positive	C1S_HUMAN.TNFDNDIALVR.2
644.3320	1072.5661	25.2	15.9	19.9	Positive	C1S_HUMAN.TNFDNDIALVR.2
644.3320	925.4977	25.2	15.9	19.9	Positive	C1S_HUMAN.TNFDNDIALVR.2
625.3430	743.4774	24.6	17.4	21.4	Positive	C4BPA_HUMAN.EDVYVVGTVLR.2
625.3430	644.4090	24.6	17.4	21.4	Positive	C4BPA_HUMAN.EDVYVVGTVLR.2
625.3430	545.3406	24.6	17.4	21.4	Positive	C4BPA_HUMAN.EDVYVVGTVLR.2
625.3430	344.1452	24.6	17.4	21.4	Positive	C4BPA_HUMAN.EDVYVVGTVLR.2
630.3471	753.4857	24.7	17.4	21.4	Positive	C4BPA_HUMAN.EDVYVVGTVLR.2
630.3471	654.4173	24.7	17.4	21.4	Positive	C4BPA_HUMAN.EDVYVVGTVLR.2
630.3471	555.3488	24.7	17.4	21.4	Positive	C4BPA_HUMAN.EDVYVVGTVLR.2
630.3471	344.1452	24.7	17.4	21.4	Positive	C4BPA_HUMAN.EDVYVVGTVLR.2
740.3650	547.3200	28.5	18.7	22.7	Positive	CBG_HUMAN.GTWTQPFDLASTR.2
740.3650	906.4690	28.5	18.7	22.7	Positive	CBG_HUMAN.GTWTQPFDLASTR.2
740.3650	363.1990	28.5	18.7	22.7	Positive	CBG_HUMAN.GTWTQPFDLASTR.2
740.3650	434.2360	28.5	18.7	22.7	Positive	CBG_HUMAN.GTWTQPFDLASTR.2
745.3690	557.3290	28.7	18.6	22.6	Positive	CBG_HUMAN.GTWTQPFDLASTR.2
745.3690	373.2070	28.7	18.6	22.6	Positive	CBG_HUMAN.GTWTQPFDLASTR.2
745.3690	916.4770	28.7	18.6	22.6	Positive	CBG_HUMAN.GTWTQPFDLASTR.2
745.3690	444.2450	28.7	18.6	22.6	Positive	CBG_HUMAN.GTWTQPFDLASTR.2
458.2560	616.3413	18.9	14.8	18.8	Positive	CD5L_HUMAN.IWLDNVR.2
458.2560	802.4206	18.9	14.8	18.8	Positive	CD5L_HUMAN.IWLDNVR.2
458.2560	388.2303	18.9	14.8	18.8	Positive	CD5L_HUMAN.IWLDNVR.2
458.2560	503.2572	18.9	14.8	18.8	Positive	CD5L_HUMAN.IWLDNVR.2
463.2601	626.3496	19.1	14.8	18.8	Positive	CD5L_HUMAN.IWLDNVR.2
463.2601	812.4289	19.1	14.8	18.8	Positive	CD5L_HUMAN.IWLDNVR.2
463.2601	398.2386	19.1	14.8	18.8	Positive	CD5L_HUMAN.IWLDNVR.2
463.2601	513.2655	19.1	14.8	18.8	Positive	CD5L_HUMAN.IWLDNVR.2
735.4234	420.2275	28.3	24.7	28.7	Positive	CERU_HUMAN.DIASGLIGPLIIC[CAM]K.2
735.4234	743.4484	28.3	24.7	28.7	Positive	CERU_HUMAN.DIASGLIGPLIIC[CAM]K.2
735.4234	913.5539	28.3	24.7	28.7	Positive	CERU_HUMAN.DIASGLIGPLIIC[CAM]K.2
735.4234	800.4699	28.3	24.7	28.7	Positive	CERU_HUMAN.DIASGLIGPLIIC[CAM]K.2
739.4210	808.4649	28.5	24.7	28.7	Positive	CERU_HUMAN.DIASGLIGPLIIC[CAM]K.2
739.4210	921.5490	28.5	24.7	28.7	Positive	CERU_HUMAN.DIASGLIGPLIIC[CAM]K.2
739.4210	428.2226	28.5	24.7	28.7	Positive	CERU_HUMAN.DIASGLIGPLIIC[CAM]K.2
739.4210	751.4434	28.5	24.7	28.7	Positive	CERU_HUMAN.DIASGLIGPLIIC[CAM]K.2
638.3346	843.4247	25.0	15.1	19.1	Positive	CFAB_HUMAN.YGLVTYATYPK.2
638.3346	742.3770	25.0	15.1	19.1	Positive	CFAB_HUMAN.YGLVTYATYPK.2
638.3346	334.1761	25.0	15.1	19.1	Positive	CFAB_HUMAN.YGLVTYATYPK.2
638.3346	942.4931	25.0	15.1	19.1	Positive	CFAB_HUMAN.YGLVTYATYPK.2
642.3417	334.1761	25.2	15.1	19.1	Positive	CFAB_HUMAN.YGLVTYATYPK.2
642.3417	851.4389	25.2	15.1	19.1	Positive	CFAB_HUMAN.YGLVTYATYPK.2
642.3417	950.5073	25.2	15.1	19.1	Positive	CFAB_HUMAN.YGLVTYATYPK.2
642.3417	750.3912	25.2	15.1	19.1	Positive	CFAB_HUMAN.YGLVTYATYPK.2
355.2013	486.2671	18.9	12.2	16.2	Positive	CFAH_HUMAN.IDVHLVPDR.3
355.2013	599.3511	18.9	12.2	16.2	Positive	CFAH_HUMAN.IDVHLVPDR.3
355.2013	387.1987	18.9	12.2	16.2	Positive	CFAH_HUMAN.IDVHLVPDR.3
355.2013	465.2456	18.9	12.2	16.2	Positive	CFAH_HUMAN.IDVHLVPDR.3
358.5374	496.2753	19.1	12.2	16.2	Positive	CFAH_HUMAN.IDVHLVPDR.3
358.5374	609.3594	19.1	12.2	16.2	Positive	CFAH_HUMAN.IDVHLVPDR.3
358.5374	397.2069	19.1	12.2	16.2	Positive	CFAH_HUMAN.IDVHLVPDR.3
358.5374	465.2456	19.1	12.2	16.2	Positive	CFAH_HUMAN.IDVHLVPDR.3
503.7820	893.4727	20.4	13.6	17.6	Positive	CFAI_HUMAN.IVIEYVDR.2
503.7820	681.3202	20.4	13.6	17.6	Positive	CFAI_HUMAN.IVIEYVDR.2
503.7820	794.4043	20.4	13.6	17.6	Positive	CFAI_HUMAN.IVIEYVDR.2
503.7820	552.2776	20.4	13.6	17.6	Positive	CFAI_HUMAN.IVIEYVDR.2
508.7862	903.4810	20.6	13.6	17.6	Positive	CFAI_HUMAN.IVIEYVDR.2
508.7862	562.2859	20.6	13.6	17.6	Positive	CFAI_HUMAN.IVIEYVDR.2
508.7862	691.3285	20.6	13.6	17.6	Positive	CFAI_HUMAN.IVIEYVDR.2
508.7862	804.4126	20.6	13.6	17.6	Positive	CFAI_HUMAN.IVIEYVDR.2
697.3515	678.3570	27.0	23.1	27.1	Positive	CLUS_HUMAN.ASSIIDELFQDR.2
697.3515	922.4265	27.0	23.1	27.1	Positive	CLUS_HUMAN.ASSIIDELFQDR.2
697.3515	1035.5106	27.0	23.1	27.1	Positive	CLUS_HUMAN.ASSIIDELFQDR.2
697.3515	565.2729	27.0	23.1	27.1	Positive	CLUS_HUMAN.ASSIIDELFQDR.2
702.3557	575.2812	27.2	23.0	27.0	Positive	CLUS_HUMAN.ASSIIDELFQDR.2
702.3557	688.3652	27.2	23.0	27.0	Positive	CLUS_HUMAN.ASSIIDELFQDR.2
702.3557	932.4348	27.2	23.0	27.0	Positive	CLUS_HUMAN.ASSIIDELFQDR.2
702.3557	1045.5188	27.2	23.0	27.0	Positive	CLUS_HUMAN.ASSIIDELFQDR.2
625.8426	783.4036	24.6	19.6	23.6	Positive	CO2_HUMAN.AVISPGFDVFAK.2
625.8426	880.4563	24.6	19.6	23.6	Positive	CO2_HUMAN.AVISPGFDVFAK.2
625.8426	967.4884	24.6	19.6	23.6	Positive	CO2_HUMAN.AVISPGFDVFAK.2

625.8426	371.2289	24.6	19.6	23.6	Positive	CO2_HUMAN.AVISPGFDVFAK.2
629.8497	888.4705	24.7	19.6	23.6	Positive	CO2_HUMAN.AVISPGFDVFAK.2
629.8497	371.2289	24.7	19.6	23.6	Positive	CO2_HUMAN.AVISPGFDVFAK.2
629.8497	791.4178	24.7	19.6	23.6	Positive	CO2_HUMAN.AVISPGFDVFAK.2
629.8497	975.5026	24.7	19.6	23.6	Positive	CO2_HUMAN.AVISPGFDVFAK.2
606.3302	775.4308	23.9	14.5	18.5	Positive	CO3_HUMAN.IHWESASLLR.2
606.3302	646.3883	23.9	14.5	18.5	Positive	CO3_HUMAN.IHWESASLLR.2
606.3302	961.5102	23.9	14.5	18.5	Positive	CO3_HUMAN.IHWESASLLR.2
606.3302	437.2296	23.9	14.5	18.5	Positive	CO3_HUMAN.IHWESASLLR.2
611.3343	437.2296	24.1	14.5	18.5	Positive	CO3_HUMAN.IHWESASLLR.2
611.3343	656.3965	24.1	14.5	18.5	Positive	CO3_HUMAN.IHWESASLLR.2
611.3343	971.5184	24.1	14.5	18.5	Positive	CO3_HUMAN.IHWESASLLR.2
611.3343	785.4391	24.1	14.5	18.5	Positive	CO3_HUMAN.IHWESASLLR.2
728.3392	956.4796	28.1	9.8	13.8	Positive	CO5_HUMAN.TDAPDLPEENQAR.2
728.3392	843.3955	28.1	9.8	13.8	Positive	CO5_HUMAN.TDAPDLPEENQAR.2
728.3392	1168.5593	28.1	9.8	13.8	Positive	CO5_HUMAN.TDAPDLPEENQAR.2
733.3433	966.4879	28.2	9.8	13.8	Positive	CO5_HUMAN.TDAPDLPEENQAR.2
733.3433	853.4038	28.2	9.8	13.8	Positive	CO5_HUMAN.TDAPDLPEENQAR.2
733.3433	1178.5676	28.2	9.8	13.8	Positive	CO5_HUMAN.TDAPDLPEENQAR.2
623.8210	747.3706	24.5	13.2	17.2	Positive	CO6_HUMAN.IGESIELTC[CAM]PK.2
623.8210	947.4866	24.5	13.2	17.2	Positive	CO6_HUMAN.IGESIELTC[CAM]PK.2
623.8210	618.3280	24.5	13.2	17.2	Positive	CO6_HUMAN.IGESIELTC[CAM]PK.2
623.8210	404.1962	24.5	13.2	17.2	Positive	CO6_HUMAN.IGESIELTC[CAM]PK.2
627.8185	412.1913	24.7	13.1	17.1	Positive	CO6_HUMAN.IGESIELTC[CAM]PK.2
627.8185	955.4817	24.7	13.1	17.1	Positive	CO6_HUMAN.IGESIELTC[CAM]PK.2
627.8185	755.3656	24.7	13.1	17.1	Positive	CO6_HUMAN.IGESIELTC[CAM]PK.2
627.8185	626.3230	24.7	13.1	17.1	Positive	CO6_HUMAN.IGESIELTC[CAM]PK.2
550.2871	577.2828	22.0	14.9	18.9	Positive	CO7_HUMAN.VLFYVDSEK.2
550.2871	887.4145	22.0	14.9	18.9	Positive	CO7_HUMAN.VLFYVDSEK.2
550.2871	740.3461	22.0	14.9	18.9	Positive	CO7_HUMAN.VLFYVDSEK.2
550.2871	363.1874	22.0	14.9	18.9	Positive	CO7_HUMAN.VLFYVDSEK.2
554.2942	585.2970	22.2	14.9	18.9	Positive	CO7_HUMAN.VLFYVDSEK.2
554.2942	371.2016	22.2	14.9	18.9	Positive	CO7_HUMAN.VLFYVDSEK.2
554.2942	895.4287	22.2	14.9	18.9	Positive	CO7_HUMAN.VLFYVDSEK.2
554.2942	748.3603	22.2	14.9	18.9	Positive	CO7_HUMAN.VLFYVDSEK.2
526.7904	915.5146	21.2	8.0	12.0	Positive	CO8A_HUMAN.HTSLGPLEAK.2
526.7904	814.4669	21.2	8.0	12.0	Positive	CO8A_HUMAN.HTSLGPLEAK.2
526.7904	614.3508	21.2	8.0	12.0	Positive	CO8A_HUMAN.HTSLGPLEAK.2
526.7904	835.4308	21.2	8.0	12.0	Positive	CO8A_HUMAN.HTSLGPLEAK.2
530.7975	822.4811	21.4	8.0	12.0	Positive	CO8A_HUMAN.HTSLGPLEAK.2
530.7975	923.5288	21.4	8.0	12.0	Positive	CO8A_HUMAN.HTSLGPLEAK.2
530.7975	835.4308	21.4	8.0	12.0	Positive	CO8A_HUMAN.HTSLGPLEAK.2
530.7975	622.3650	21.4	8.0	12.0	Positive	CO8A_HUMAN.HTSLGPLEAK.2
621.8765	1042.6295	24.5	19.4	23.4	Positive	CO9_HUMAN.LSPIYNLVPVK.2
621.8765	343.2340	24.5	19.4	23.4	Positive	CO9_HUMAN.LSPIYNLVPVK.2
621.8765	669.4294	24.5	19.4	23.4	Positive	CO9_HUMAN.LSPIYNLVPVK.2
621.8765	832.4927	24.5	19.4	23.4	Positive	CO9_HUMAN.LSPIYNLVPVK.2
625.8836	840.5069	24.6	19.4	23.4	Positive	CO9_HUMAN.LSPIYNLVPVK.2
625.8836	677.4436	24.6	19.4	23.4	Positive	CO9_HUMAN.LSPIYNLVPVK.2
625.8836	351.2482	24.6	19.4	23.4	Positive	CO9_HUMAN.LSPIYNLVPVK.2
625.8836	1050.6437	24.6	19.4	23.4	Positive	CO9_HUMAN.LSPIYNLVPVK.2
801.4359	732.4039	30.6	19.0	23.0	Positive	CPN2_HUMAN.LSNNALSGLPQGVFGK.2
801.4359	989.5415	30.6	19.0	23.0	Positive	CPN2_HUMAN.LSNNALSGLPQGVFGK.2
801.4359	1102.6255	30.6	19.0	23.0	Positive	CPN2_HUMAN.LSNNALSGLPQGVFGK.2
801.4359	351.2027	30.6	19.0	23.0	Positive	CPN2_HUMAN.LSNNALSGLPQGVFGK.2
805.4430	740.4181	30.7	18.9	22.9	Positive	CPN2_HUMAN.LSNNALSGLPQGVFGK.2
805.4430	997.5557	30.7	18.9	22.9	Positive	CPN2_HUMAN.LSNNALSGLPQGVFGK.2
805.4430	1110.6397	30.7	18.9	22.9	Positive	CPN2_HUMAN.LSNNALSGLPQGVFGK.2
805.4430	359.2169	30.7	18.9	22.9	Positive	CPN2_HUMAN.LSNNALSGLPQGVFGK.2
464.2822	763.4723	19.1	12.0	18.0	Positive	DECOY1
464.2822	562.3562	19.1	12.0	18.0	Positive	DECOY1
464.2822	444.2722	19.1	12.0	18.0	Positive	DECOY1
493.2766	657.3563	20.1	11.0	15.0	Positive	DECOY2
493.2766	381.1667	20.1	11.0	15.0	Positive	DECOY2
493.2766	728.3934	20.1	11.0	15.0	Positive	DECOY2
496.2766	731.3934	20.2	15.5	19.5	Positive	DECOY3
496.2766	660.3563	20.2	15.5	19.5	Positive	DECOY3
496.2766	332.1969	20.2	15.5	19.5	Positive	DECOY3
570.8144	589.3257	22.7	13.2	17.2	Positive	DECOY4
570.8144	855.4996	22.7	13.2	17.2	Positive	DECOY4
570.8144	704.4097	22.7	13.2	17.2	Positive	DECOY4
575.8088	765.4141	22.9	14.5	18.5	Positive	DECOY5
575.8088	618.3457	22.9	14.5	18.5	Positive	DECOY5
575.8088	992.5411	22.9	14.5	18.5	Positive	DECOY5
617.8666	660.4090	24.3	14.0	35.0	Positive	DECOY6
617.8666	723.4461	24.3	14.0	35.0	Positive	DECOY6
617.8666	882.5152	24.3	14.0	35.0	Positive	DECOY6
658.8508	846.4567	25.7	14.9	18.9	Positive	DECOY7
658.8508	658.3770	25.7	14.9	18.9	Positive	DECOY7
658.8508	745.4090	25.7	14.9	18.9	Positive	DECOY7
708.3621	875.4472	27.4	14.0	35.0	Positive	DECOY8

708.3621	974.4949	27.4	14.0	35.0	Positive	DECOY8
708.3621	646.2998	27.4	14.0	35.0	Positive	DECOY8
716.3308	891.4108	27.7	18.0	24.0	Positive	DECOY9
716.3308	801.3424	27.7	18.0	24.0	Positive	DECOY9
716.3308	1243.5590	27.7	18.0	24.0	Positive	DECOY9
663.9158	373.2809	25.9	22.5	26.5	Positive	F13A_HUMAN.STVLTIPEIIIK.2
663.9158	825.5444	25.9	22.5	26.5	Positive	F13A_HUMAN.STVLTIPEIIIK.2
663.9158	712.4604	25.9	22.5	26.5	Positive	F13A_HUMAN.STVLTIPEIIIK.2
663.9158	926.5921	25.9	22.5	26.5	Positive	F13A_HUMAN.STVLTIPEIIIK.2
667.9133	833.5395	26.0	22.5	26.5	Positive	F13A_HUMAN.STVLTIPEIIIK.2
667.9133	934.5871	26.0	22.5	26.5	Positive	F13A_HUMAN.STVLTIPEIIIK.2
667.9133	381.2760	26.0	22.5	26.5	Positive	F13A_HUMAN.STVLTIPEIIIK.2
667.9133	720.4554	26.0	22.5	26.5	Positive	F13A_HUMAN.STVLTIPEIIIK.2
589.7775	322.1397	23.4	14.9	18.9	Positive	FBLN1_HUMAN.TGYYFDGISR.2
589.7775	432.2565	23.4	14.9	18.9	Positive	FBLN1_HUMAN.TGYYFDGISR.2
589.7775	857.4152	23.4	14.9	18.9	Positive	FBLN1_HUMAN.TGYYFDGISR.2
589.7775	694.3519	23.4	14.9	18.9	Positive	FBLN1_HUMAN.TGYYFDGISR.2
594.7816	442.2648	23.5	14.9	18.9	Positive	FBLN1_HUMAN.TGYYFDGISR.2
594.7816	867.4235	23.5	14.9	18.9	Positive	FBLN1_HUMAN.TGYYFDGISR.2
594.7816	704.3601	23.5	14.9	18.9	Positive	FBLN1_HUMAN.TGYYFDGISR.2
594.7816	322.1397	23.5	14.9	18.9	Positive	FBLN1_HUMAN.TGYYFDGISR.2
512.7460	576.2889	20.7	14.4	18.4	Positive	FCN3_HUMAN.YGIDWASGR.2
512.7460	861.4213	20.7	14.4	18.4	Positive	FCN3_HUMAN.YGIDWASGR.2
512.7460	691.3158	20.7	14.4	18.4	Positive	FCN3_HUMAN.YGIDWASGR.2
512.7460	390.2096	20.7	14.4	18.4	Positive	FCN3_HUMAN.YGIDWASGR.2
517.7501	871.4296	20.9	14.4	18.4	Positive	FCN3_HUMAN.YGIDWASGR.2
517.7501	400.2178	20.9	14.4	18.4	Positive	FCN3_HUMAN.YGIDWASGR.2
517.7501	586.2971	20.9	14.4	18.4	Positive	FCN3_HUMAN.YGIDWASGR.2
517.7501	701.3241	20.9	14.4	18.4	Positive	FCN3_HUMAN.YGIDWASGR.2
407.2289	579.3501	17.2	10.9	14.9	Positive	FETUA_HUMAN.FSVVYAK.2
407.2289	666.3821	17.2	10.9	14.9	Positive	FETUA_HUMAN.FSVVYAK.2
407.2289	381.2132	17.2	10.9	14.9	Positive	FETUA_HUMAN.FSVVYAK.2
407.2289	480.2817	17.2	10.9	14.9	Positive	FETUA_HUMAN.FSVVYAK.2
411.2360	587.3643	17.3	10.9	14.9	Positive	FETUA_HUMAN.FSVVYAK.2
411.2360	674.3963	17.3	10.9	14.9	Positive	FETUA_HUMAN.FSVVYAK.2
411.2360	389.2274	17.3	10.9	14.9	Positive	FETUA_HUMAN.FSVVYAK.2
411.2360	488.2959	17.3	10.9	14.9	Positive	FETUA_HUMAN.FSVVYAK.2
570.7802	723.4036	22.7	9.1	13.1	Positive	FIBA_HUMAN.GSESGIFTNTK.2
570.7802	610.3195	22.7	9.1	13.1	Positive	FIBA_HUMAN.GSESGIFTNTK.2
570.7802	867.4571	22.7	9.1	13.1	Positive	FIBA_HUMAN.GSESGIFTNTK.2
570.7802	780.4250	22.7	9.1	13.1	Positive	FIBA_HUMAN.GSESGIFTNTK.2
574.7873	618.3337	22.9	9.1	13.1	Positive	FIBA_HUMAN.GSESGIFTNTK.2
574.7873	731.4178	22.9	9.1	13.1	Positive	FIBA_HUMAN.GSESGIFTNTK.2
574.7873	788.4392	22.9	9.1	13.1	Positive	FIBA_HUMAN.GSESGIFTNTK.2
574.7873	875.4713	22.9	9.1	13.1	Positive	FIBA_HUMAN.GSESGIFTNTK.2
654.8126	706.3366	25.6	8.4	12.4	Positive	FIBB_HUMAN.QGFGNVATNTDGK.2
654.8126	805.4050	25.6	8.4	12.4	Positive	FIBB_HUMAN.QGFGNVATNTDGK.2
654.8126	333.1557	25.6	8.4	12.4	Positive	FIBB_HUMAN.QGFGNVATNTDGK.2
654.8126	635.2995	25.6	8.4	12.4	Positive	FIBB_HUMAN.QGFGNVATNTDGK.2
658.8197	813.4192	25.7	8.4	12.4	Positive	FIBB_HUMAN.QGFGNVATNTDGK.2
658.8197	333.1557	25.7	8.4	12.4	Positive	FIBB_HUMAN.QGFGNVATNTDGK.2
658.8197	643.3137	25.7	8.4	12.4	Positive	FIBB_HUMAN.QGFGNVATNTDGK.2
658.8197	714.3508	25.7	8.4	12.4	Positive	FIBB_HUMAN.QGFGNVATNTDGK.2
597.7475	645.3566	23.6	11.3	15.3	Positive	FIBG_HUMAN.DNC[CAM]C[CAM]ILDER.2
597.7475	532.2726	23.6	11.3	15.3	Positive	FIBG_HUMAN.DNC[CAM]C[CAM]ILDER.2
597.7475	419.1885	23.6	11.3	15.3	Positive	FIBG_HUMAN.DNC[CAM]C[CAM]ILDER.2
597.7475	805.3873	23.6	11.3	15.3	Positive	FIBG_HUMAN.DNC[CAM]C[CAM]ILDER.2
602.7517	655.3649	23.8	11.3	15.3	Positive	FIBG_HUMAN.DNC[CAM]C[CAM]ILDER.2
602.7517	815.3955	23.8	11.3	15.3	Positive	FIBG_HUMAN.DNC[CAM]C[CAM]ILDER.2
602.7517	542.2808	23.8	11.3	15.3	Positive	FIBG_HUMAN.DNC[CAM]C[CAM]ILDER.2
602.7517	429.1968	23.8	11.3	15.3	Positive	FIBG_HUMAN.DNC[CAM]C[CAM]ILDER.2
772.3856	978.4891	29.6	14.8	18.8	Positive	FINC_HUMAN.SYTITGLQPGTDYK.2
772.3856	680.3250	29.6	14.8	18.8	Positive	FINC_HUMAN.SYTITGLQPGTDYK.2
772.3856	1079.5368	29.6	14.8	18.8	Positive	FINC_HUMAN.SYTITGLQPGTDYK.2
772.3856	352.1503	29.6	14.8	18.8	Positive	FINC_HUMAN.SYTITGLQPGTDYK.2
776.3927	986.5033	29.7	14.8	18.8	Positive	FINC_HUMAN.SYTITGLQPGTDYK.2
776.3927	688.3392	29.7	14.8	18.8	Positive	FINC_HUMAN.SYTITGLQPGTDYK.2
776.3927	1087.5510	29.7	14.8	18.8	Positive	FINC_HUMAN.SYTITGLQPGTDYK.2
776.3927	352.1503	29.7	14.8	18.8	Positive	FINC_HUMAN.SYTITGLQPGTDYK.2
660.3513	893.4727	25.8	15.2	19.2	Positive	GELS_HUMAN.AGALNSNDAFVLK.2
660.3513	359.2653	25.8	15.2	19.2	Positive	GELS_HUMAN.AGALNSNDAFVLK.2
660.3513	806.4407	25.8	15.2	19.2	Positive	GELS_HUMAN.AGALNSNDAFVLK.2
660.3513	1007.5156	25.8	15.2	19.2	Positive	GELS_HUMAN.AGALNSNDAFVLK.2
664.3584	367.2795	25.9	15.2	19.2	Positive	GELS_HUMAN.AGALNSNDAFVLK.2
664.3584	814.4549	25.9	15.2	19.2	Positive	GELS_HUMAN.AGALNSNDAFVLK.2
664.3584	901.4869	25.9	15.2	19.2	Positive	GELS_HUMAN.AGALNSNDAFVLK.2
664.3584	1015.5298	25.9	15.2	19.2	Positive	GELS_HUMAN.AGALNSNDAFVLK.2
657.8656	516.2963	25.7	21.1	25.1	Positive	GPX3_HUMAN.FLVGPDGIPIMR.2
657.8656	898.4815	25.7	21.1	25.1	Positive	GPX3_HUMAN.FLVGPDGIPIMR.2
657.8656	955.5030	25.7	21.1	25.1	Positive	GPX3_HUMAN.FLVGPDGIPIMR.2
657.8656	686.4018	25.7	21.1	25.1	Positive	GPX3_HUMAN.FLVGPDGIPIMR.2

662.8697	526.3045	25.9	21.1	25.1	Positive	GPX3_HUMAN.FLVGPDGIPIMR.2
662.8697	908.4898	25.9	21.1	25.1	Positive	GPX3_HUMAN.FLVGPDGIPIMR.2
662.8697	696.4101	25.9	21.1	25.1	Positive	GPX3_HUMAN.FLVGPDGIPIMR.2
662.8697	965.5112	25.9	21.1	25.1	Positive	GPX3_HUMAN.FLVGPDGIPIMR.2
765.3708	365.1932	29.3	9.3	13.3	Positive	HBA_HUMAN.VGAHAGEYGAEALER.2
765.3708	436.2303	29.3	9.3	13.3	Positive	HBA_HUMAN.VGAHAGEYGAEALER.2
765.3708	1094.5113	29.3	9.3	13.3	Positive	HBA_HUMAN.VGAHAGEYGAEALER.2
765.3708	1165.5484	29.3	9.3	13.3	Positive	HBA_HUMAN.VGAHAGEYGAEALER.2
770.3749	1175.5567	29.5	9.2	13.2	Positive	HBA_HUMAN.VGAHAGEYGAEALER.2
770.3749	1104.5195	29.5	9.2	13.2	Positive	HBA_HUMAN.VGAHAGEYGAEALER.2
770.3749	365.1932	29.5	9.2	13.2	Positive	HBA_HUMAN.VGAHAGEYGAEALER.2
770.3749	436.2303	29.5	9.2	13.2	Positive	HBA_HUMAN.VGAHAGEYGAEALER.2
663.8999	717.4076	25.9	23.3	27.3	Positive	HBD_HUMAN.LLGNVLVC[CAM]VLAR.2
663.8999	1100.6245	25.9	23.3	27.3	Positive	HBD_HUMAN.LLGNVLVC[CAM]VLAR.2
663.8999	618.3392	25.9	23.3	27.3	Positive	HBD_HUMAN.LLGNVLVC[CAM]VLAR.2
663.8999	830.4917	25.9	23.3	27.3	Positive	HBD_HUMAN.LLGNVLVC[CAM]VLAR.2
668.8994	727.4065	26.1	23.3	27.3	Positive	HBD_HUMAN.LLGNVLVC[CAM]VLAR.2
668.8994	840.4906	26.1	23.3	27.3	Positive	HBD_HUMAN.LLGNVLVC[CAM]VLAR.2
668.8994	1110.6234	26.1	23.3	27.3	Positive	HBD_HUMAN.LLGNVLVC[CAM]VLAR.2
668.8994	628.3381	26.1	23.3	27.3	Positive	HBD_HUMAN.LLGNVLVC[CAM]VLAR.2
501.2397	422.1704	20.4	2.5	6.5	Positive	HBE_HUMAN.LSELHC[CAM]DK.2
501.2397	559.2293	20.4	2.5	6.5	Positive	HBE_HUMAN.LSELHC[CAM]DK.2
501.2397	672.3134	20.4	2.5	6.5	Positive	HBE_HUMAN.LSELHC[CAM]DK.2
501.2397	888.3880	20.4	2.5	6.5	Positive	HBE_HUMAN.LSELHC[CAM]DK.2
505.3140	567.3780	20.5	2.6	6.6	Positive	HBE_HUMAN.LSELHC[CAM]DK.2
505.3140	896.5360	20.5	2.6	6.6	Positive	HBE_HUMAN.LSELHC[CAM]DK.2
505.3140	430.3190	20.5	2.6	6.6	Positive	HBE_HUMAN.LSELHC[CAM]DK.2
505.3140	680.4620	20.5	2.6	6.6	Positive	HBE_HUMAN.LSELHC[CAM]DK.2
610.8066	775.4097	24.1	17.2	21.2	Positive	HEMO_HUMAN.NFPSPVDAAFR.2
610.8066	579.2885	24.1	17.2	21.2	Positive	HEMO_HUMAN.NFPSPVDAAFR.2
610.8066	862.4417	24.1	17.2	21.2	Positive	HEMO_HUMAN.NFPSPVDAAFR.2
610.8066	959.4945	24.1	17.2	21.2	Positive	HEMO_HUMAN.NFPSPVDAAFR.2
615.8107	785.4180	24.3	17.2	21.2	Positive	HEMO_HUMAN.NFPSPVDAAFR.2
615.8107	589.2968	24.3	17.2	21.2	Positive	HEMO_HUMAN.NFPSPVDAAFR.2
615.8107	969.5028	24.3	17.2	21.2	Positive	HEMO_HUMAN.NFPSPVDAAFR.2
615.8107	872.4500	24.3	17.2	21.2	Positive	HEMO_HUMAN.NFPSPVDAAFR.2
514.7904	814.4417	20.8	11.0	15.0	Positive	HEP2_HUMAN.TLEAQLTPR.2
514.7904	373.2194	20.8	11.0	15.0	Positive	HEP2_HUMAN.TLEAQLTPR.2
514.7904	614.3620	20.8	11.0	15.0	Positive	HEP2_HUMAN.TLEAQLTPR.2
514.7904	685.3991	20.8	11.0	15.0	Positive	HEP2_HUMAN.TLEAQLTPR.2
519.7945	824.4500	21.0	11.0	15.0	Positive	HEP2_HUMAN.TLEAQLTPR.2
519.7945	624.3703	21.0	11.0	15.0	Positive	HEP2_HUMAN.TLEAQLTPR.2
519.7945	695.4074	21.0	11.0	15.0	Positive	HEP2_HUMAN.TLEAQLTPR.2
519.7945	383.2277	21.0	11.0	15.0	Positive	HEP2_HUMAN.TLEAQLTPR.2
602.3220	374.2398	23.8	14.9	18.9	Positive	HPT_HUMAN.VTSIQDWVQK.2
602.3220	675.3461	23.8	14.9	18.9	Positive	HPT_HUMAN.VTSIQDWVQK.2
602.3220	803.4046	23.8	14.9	18.9	Positive	HPT_HUMAN.VTSIQDWVQK.2
602.3220	1003.5207	23.8	14.9	18.9	Positive	HPT_HUMAN.VTSIQDWVQK.2
606.3291	382.2540	23.9	14.9	18.9	Positive	HPT_HUMAN.VTSIQDWVQK.2
606.3291	811.4188	23.9	14.9	18.9	Positive	HPT_HUMAN.VTSIQDWVQK.2
606.3291	683.3603	23.9	14.9	18.9	Positive	HPT_HUMAN.VTSIQDWVQK.2
606.3291	1011.5349	23.9	14.9	18.9	Positive	HPT_HUMAN.VTSIQDWVQK.2
772.3624	795.3632	29.6	15.3	19.3	Positive	HPTR_HUMAN.VGYVSGWGQSDNFK.2
772.3624	320.1605	29.6	15.3	19.3	Positive	HPTR_HUMAN.VGYVSGWGQSDNFK.2
772.3624	1038.4639	29.6	15.3	19.3	Positive	HPTR_HUMAN.VGYVSGWGQSDNFK.2
772.3624	1125.4960	29.6	15.3	19.3	Positive	HPTR_HUMAN.VGYVSGWGQSDNFK.2
776.3695	803.3774	29.7	15.3	19.3	Positive	HPTR_HUMAN.VGYVSGWGQSDNFK.2
776.3695	320.1605	29.7	15.3	19.3	Positive	HPTR_HUMAN.VGYVSGWGQSDNFK.2
776.3695	1046.4781	29.7	15.3	19.3	Positive	HPTR_HUMAN.VGYVSGWGQSDNFK.2
776.3695	1133.5102	29.7	15.3	19.3	Positive	HPTR_HUMAN.VGYVSGWGQSDNFK.2
745.8492	722.3832	28.7	19.1	23.1	Positive	HRG_HUMAN.GGEGTGYFVDFSVR.2
745.8492	869.4516	28.7	19.1	23.1	Positive	HRG_HUMAN.GGEGTGYFVDFSVR.2
745.8492	1089.5364	28.7	19.1	23.1	Positive	HRG_HUMAN.GGEGTGYFVDFSVR.2
745.8492	623.3148	28.7	19.1	23.1	Positive	HRG_HUMAN.GGEGTGYFVDFSVR.2
750.8486	633.3136	28.8	19.1	23.1	Positive	HRG_HUMAN.GGEGTGYFVDFSVR.2
750.8486	732.3821	28.8	19.1	23.1	Positive	HRG_HUMAN.GGEGTGYFVDFSVR.2
750.8486	879.4505	28.8	19.1	23.1	Positive	HRG_HUMAN.GGEGTGYFVDFSVR.2
750.8486	1099.5353	28.8	19.1	23.1	Positive	HRG_HUMAN.GGEGTGYFVDFSVR.2
609.6635	908.4948	30.1	18.8	22.8	Positive	IC1_HUMAN.GVTSVSQIFHSPDLAIR.3
609.6635	771.4359	30.1	18.8	22.8	Positive	IC1_HUMAN.GVTSVSQIFHSPDLAIR.3
609.6635	1055.5633	30.1	18.8	22.8	Positive	IC1_HUMAN.GVTSVSQIFHSPDLAIR.3
612.9996	1065.5715	30.3	18.8	22.8	Positive	IC1_HUMAN.GVTSVSQIFHSPDLAIR.3
612.9996	781.4442	30.3	18.8	22.8	Positive	IC1_HUMAN.GVTSVSQIFHSPDLAIR.3
612.9996	918.5031	30.3	18.8	22.8	Positive	IC1_HUMAN.GVTSVSQIFHSPDLAIR.3
770.8675	576.2988	29.5	17.6	21.6	Positive	IGHA1_HUMAN.DASGVTFTWTPSSGK.2
770.8675	331.1248	29.5	17.6	21.6	Positive	IGHA1_HUMAN.DASGVTFTWTPSSGK.2
770.8675	331.1248	29.5	17.6	21.6	Positive	IGHA1_HUMAN.DASGVTFTWTPSSGK.2
770.8675	475.2511	29.5	17.6	21.6	Positive	IGHA1_HUMAN.DASGVTFTWTPSSGK.2
774.8651	313.1143	29.7	17.6	21.6	Positive	IGHA1_HUMAN.DASGVTFTWTPSSGK.2
774.8651	331.1248	29.7	17.6	21.6	Positive	IGHA1_HUMAN.DASGVTFTWTPSSGK.2
774.8651	483.2461	29.7	17.6	21.6	Positive	IGHA1_HUMAN.DASGVTFTWTPSSGK.2

774.8651	584.2938	29.7	17.6	21.6	Positive	IGHA1_HUMAN.DASGVTFTWTPSSGK.2
756.8519	576.2988	29.0	15.6	19.6	Positive	IGHA2_HUMAN.DASGATFTWTPSSGK.2
756.8519	863.4258	29.0	15.6	19.6	Positive	IGHA2_HUMAN.DASGATFTWTPSSGK.2
756.8519	1111.5419	29.0	15.6	19.6	Positive	IGHA2_HUMAN.DASGATFTWTPSSGK.2
756.8519	475.2511	29.0	15.6	19.6	Positive	IGHA2_HUMAN.DASGATFTWTPSSGK.2
760.8590	584.3140	29.2	15.6	19.6	Positive	IGHA2_HUMAN.DASGATFTWTPSSGK.2
760.8590	871.4410	29.2	15.6	19.6	Positive	IGHA2_HUMAN.DASGATFTWTPSSGK.2
760.8590	1119.5570	29.2	15.6	19.6	Positive	IGHA2_HUMAN.DASGATFTWTPSSGK.2
760.8590	483.2660	29.2	15.6	19.6	Positive	IGHA2_HUMAN.DASGATFTWTPSSGK.2
593.8270	418.2296	23.5	15.4	19.4	Positive	IGHG1_HUMAN.GPSVFPLAPSSK.2
593.8270	846.4720	23.5	15.4	19.4	Positive	IGHG1_HUMAN.GPSVFPLAPSSK.2
593.8270	699.4036	23.5	15.4	19.4	Positive	IGHG1_HUMAN.GPSVFPLAPSSK.2
597.8341	426.2438	23.6	15.4	19.4	Positive	IGHG1_HUMAN.GPSVFPLAPSSK.2
597.8341	707.4178	23.6	15.4	19.4	Positive	IGHG1_HUMAN.GPSVFPLAPSSK.2
597.8341	854.4862	23.6	15.4	19.4	Positive	IGHG1_HUMAN.GPSVFPLAPSSK.2
412.7475	557.3293	17.3	9.8	13.8	Positive	IGHG2_HUMAN.GLPAPIEK.2
412.7475	654.3821	17.3	9.8	13.8	Positive	IGHG2_HUMAN.GLPAPIEK.2
412.7475	389.2395	17.3	9.8	13.8	Positive	IGHG2_HUMAN.GLPAPIEK.2
412.7475	486.2922	17.3	9.8	13.8	Positive	IGHG2_HUMAN.GLPAPIEK.2
416.7550	565.3440	17.5	9.8	13.8	Positive	IGHG2_HUMAN.GLPAPIEK.2
416.7550	662.3970	17.5	9.8	13.8	Positive	IGHG2_HUMAN.GLPAPIEK.2
416.7550	397.2540	17.5	9.8	13.8	Positive	IGHG2_HUMAN.GLPAPIEK.2
416.7550	494.3070	17.5	9.8	13.8	Positive	IGHG2_HUMAN.GLPAPIEK.2
708.8490	853.4526	27.4	12.2	16.2	Positive	IGHG3_HUMAN.WYVDGVEVHNAK.2
708.8490	968.4796	27.4	12.2	16.2	Positive	IGHG3_HUMAN.WYVDGVEVHNAK.2
708.8490	1067.5480	27.4	12.2	16.2	Positive	IGHG3_HUMAN.WYVDGVEVHNAK.2
708.8490	1230.6113	27.4	12.2	16.2	Positive	IGHG3_HUMAN.WYVDGVEVHNAK.2
712.8561	861.4668	27.6	12.2	16.2	Positive	IGHG3_HUMAN.WYVDGVEVHNAK.2
712.8561	976.4938	27.6	12.2	16.2	Positive	IGHG3_HUMAN.WYVDGVEVHNAK.2
712.8561	1075.5622	27.6	12.2	16.2	Positive	IGHG3_HUMAN.WYVDGVEVHNAK.2
712.8561	1238.6255	27.6	12.2	16.2	Positive	IGHG3_HUMAN.WYVDGVEVHNAK.2
951.4676	1406.6587	35.7	21.9	25.9	Positive	IGHG4_HUMAN.TTPPVLDSDGSFFLYSR.2
951.4676	976.4887	35.7	21.9	25.9	Positive	IGHG4_HUMAN.TTPPVLDSDGSFFLYSR.2
951.4676	1178.5477	35.7	21.9	25.9	Positive	IGHG4_HUMAN.TTPPVLDSDGSFFLYSR.2
951.4676	1293.5746	35.7	21.9	25.9	Positive	IGHG4_HUMAN.TTPPVLDSDGSFFLYSR.2
956.4718	1303.5829	35.8	21.9	25.9	Positive	IGHG4_HUMAN.TTPPVLDSDGSFFLYSR.2
956.4718	1416.6669	35.8	21.9	25.9	Positive	IGHG4_HUMAN.TTPPVLDSDGSFFLYSR.2
956.4718	986.4970	35.8	21.9	25.9	Positive	IGHG4_HUMAN.TTPPVLDSDGSFFLYSR.2
956.4718	1188.5559	35.8	21.9	25.9	Positive	IGHG4_HUMAN.TTPPVLDSDGSFFLYSR.2
809.4076	546.2882	30.8	8.9	12.9	Positive	IGHM_HUMAN.QVGSGVTTDQVQAEAK.2
809.4076	989.4898	30.8	8.9	12.9	Positive	IGHM_HUMAN.QVGSGVTTDQVQAEAK.2
809.4076	1090.5375	30.8	8.9	12.9	Positive	IGHM_HUMAN.QVGSGVTTDQVQAEAK.2
809.4076	1390.6809	30.8	8.9	12.9	Positive	IGHM_HUMAN.QVGSGVTTDQVQAEAK.2
813.4147	554.3024	31.0	8.9	12.9	Positive	IGHM_HUMAN.QVGSGVTTDQVQAEAK.2
813.4147	997.5040	31.0	8.9	12.9	Positive	IGHM_HUMAN.QVGSGVTTDQVQAEAK.2
813.4147	1098.5517	31.0	8.9	12.9	Positive	IGHM_HUMAN.QVGSGVTTDQVQAEAK.2
813.4147	1398.6951	31.0	8.9	12.9	Positive	IGHM_HUMAN.QVGSGVTTDQVQAEAK.2
695.3101	631.3410	27.0	8.8	12.8	Positive	IGJ_HUMAN.SSEDPNEDIVER.2
695.3101	971.4793	27.0	8.8	12.8	Positive	IGJ_HUMAN.SSEDPNEDIVER.2
695.3101	1086.5062	27.0	8.8	12.8	Positive	IGJ_HUMAN.SSEDPNEDIVER.2
695.3101	486.2433	27.0	8.8	12.8	Positive	IGJ_HUMAN.SSEDPNEDIVER.2
700.3142	641.3492	27.1	8.8	12.8	Positive	IGJ_HUMAN.SSEDPNEDIVER.2
700.3142	491.2474	27.1	8.8	12.8	Positive	IGJ_HUMAN.SSEDPNEDIVER.2
700.3142	981.4875	27.1	8.8	12.8	Positive	IGJ_HUMAN.SSEDPNEDIVER.2
700.3142	1096.5145	27.1	8.8	12.8	Positive	IGJ_HUMAN.SSEDPNEDIVER.2
644.8220	604.3310	25.2	8.7	12.7	Positive	iRT-pep.AGGSSEPVTGLADK.2
644.8220	1016.5300	25.2	8.7	12.7	Positive	iRT-pep.AGGSSEPVTGLADK.2
644.8220	800.4520	25.2	8.7	12.7	Positive	iRT-pep.AGGSSEPVTGLADK.2
726.8350	584.2700	28.0	17.3	21.3	Positive	iRT-pep.DAVTPADFSEWSK.2
726.8350	1066.4800	28.0	17.3	21.3	Positive	iRT-pep.DAVTPADFSEWSK.2
726.8350	533.7460	28.0	17.3	21.3	Positive	iRT-pep.DAVTPADFSEWSK.2
776.9290	1051.5600	29.7	23.1	27.1	Positive	iRT-pep.FLLQFGAQGSPLFK.2
776.9290	504.3190	29.7	23.1	27.1	Positive	iRT-pep.FLLQFGAQGSPLFK.2
776.9290	904.4890	29.7	23.1	27.1	Positive	iRT-pep.FLLQFGAQGSPLFK.2
699.3380	855.4360	27.1	16.4	20.4	Positive	iRT-pep.GDLDAASYYAPVR.2
699.3380	605.3410	27.1	16.4	20.4	Positive	iRT-pep.GDLDAASYYAPVR.2
699.3380	926.4740	27.1	16.4	20.4	Positive	iRT-pep.GDLDAASYYAPVR.2
636.8690	626.3990	25.0	21.6	25.6	Positive	iRT-pep.GTFIIDPAAIVR.2
636.8690	741.4260	25.0	21.6	25.6	Positive	iRT-pep.GTFIIDPAAIVR.2
636.8690	854.5100	25.0	21.6	25.6	Positive	iRT-pep.GTFIIDPAAIVR.2
487.2570	503.2940	19.9	3.9	7.9	Positive	iRT-pep.LGGNETQVR.2
487.2570	860.4230	19.9	3.9	7.9	Positive	iRT-pep.LGGNETQVR.2
487.2570	803.4010	19.9	3.9	7.9	Positive	iRT-pep.LGGNETQVR.2
622.8530	598.3680	24.5	19.6	23.6	Positive	iRT-pep.TGFIIDPGGVIR.2
622.8530	713.3950	24.5	19.6	23.6	Positive	iRT-pep.TGFIIDPGGVIR.2
622.8530	826.4790	24.5	19.6	23.6	Positive	iRT-pep.TGFIIDPGGVIR.2
669.8380	1041.5000	26.1	13.0	17.0	Positive	iRT-pep.TPVISGGPYYER.2
669.8380	841.3840	26.1	13.0	17.0	Positive	iRT-pep.TPVISGGPYYER.2
669.8380	928.4160	26.1	13.0	17.0	Positive	iRT-pep.TPVISGGPYYER.2
683.8530	1069.5300	26.6	13.9	17.9	Positive	iRT-pep.TPVITGAPYYER.2
683.8530	956.4480	26.6	13.9	17.9	Positive	iRT-pep.TPVITGAPYYER.2

683.8530	855.4000	26.6	13.9	17.9	Positive	iRT-pep.TPVITGAPYYER.2
683.8270	819.3890	26.6	10.8	14.8	Positive	iRT-pep.VEATFGVDESANK.2
683.8270	663.2950	26.6	10.8	14.8	Positive	iRT-pep.VEATFGVDESANK.2
683.8270	966.4530	26.6	10.8	14.8	Positive	iRT-pep.VEATFGVDESANK.2
547.2970	704.3580	21.9	11.9	15.9	Positive	iRT-pep.YILAGVESNK.2
547.2970	817.4420	21.9	11.9	15.9	Positive	iRT-pep.YILAGVESNK.2
547.2970	633.3210	21.9	11.9	15.9	Positive	iRT-pep.YILAGVESNK.2
579.3173	444.2929	23.0	9.7	13.7	Positive	ITIH1_HUMAN.AAISGENAGLVR.2
579.3173	629.3729	23.0	9.7	13.7	Positive	ITIH1_HUMAN.AAISGENAGLVR.2
579.3173	815.4370	23.0	9.7	13.7	Positive	ITIH1_HUMAN.AAISGENAGLVR.2
579.3173	902.4690	23.0	9.7	13.7	Positive	ITIH1_HUMAN.AAISGENAGLVR.2
584.3214	454.3012	23.2	9.7	13.7	Positive	ITIH1_HUMAN.AAISGENAGLVR.2
584.3214	639.3812	23.2	9.7	13.7	Positive	ITIH1_HUMAN.AAISGENAGLVR.2
584.3214	825.4453	23.2	9.7	13.7	Positive	ITIH1_HUMAN.AAISGENAGLVR.2
584.3214	912.4773	23.2	9.7	13.7	Positive	ITIH1_HUMAN.AAISGENAGLVR.2
791.9310	942.5367	30.2	14.7	18.7	Positive	ITIH2_HUMAN.IQPSGGTNINEALLR.2
791.9310	1341.7121	30.2	14.7	18.7	Positive	ITIH2_HUMAN.IQPSGGTNINEALLR.2
791.9310	715.4097	30.2	14.7	18.7	Positive	ITIH2_HUMAN.IQPSGGTNINEALLR.2
791.9310	1244.6593	30.2	14.7	18.7	Positive	ITIH2_HUMAN.IQPSGGTNINEALLR.2
796.9351	952.5450	30.4	14.7	18.7	Positive	ITIH2_HUMAN.IQPSGGTNINEALLR.2
796.9351	725.4180	30.4	14.7	18.7	Positive	ITIH2_HUMAN.IQPSGGTNINEALLR.2
796.9351	1351.7204	30.4	14.7	18.7	Positive	ITIH2_HUMAN.IQPSGGTNINEALLR.2
796.9351	1254.6676	30.4	14.7	18.7	Positive	ITIH2_HUMAN.IQPSGGTNINEALLR.2
524.3261	615.4076	21.1	21.2	25.2	Positive	ITIH4_HUMAN.LGVYELLLK.2
524.3261	934.5608	21.1	21.2	25.2	Positive	ITIH4_HUMAN.LGVYELLLK.2
524.3261	877.5393	21.1	21.2	25.2	Positive	ITIH4_HUMAN.LGVYELLLK.2
524.3261	778.4709	21.1	21.2	25.2	Positive	ITIH4_HUMAN.LGVYELLLK.2
528.3332	942.5750	21.3	21.2	25.2	Positive	ITIH4_HUMAN.LGVYELLLK.2
528.3332	885.5535	21.3	21.2	25.2	Positive	ITIH4_HUMAN.LGVYELLLK.2
528.3332	786.4851	21.3	21.2	25.2	Positive	ITIH4_HUMAN.LGVYELLLK.2
528.3332	623.4218	21.3	21.2	25.2	Positive	ITIH4_HUMAN.LGVYELLLK.2
730.3624	1112.5331	28.1	11.6	15.6	Positive	KLKB1_HUMAN.IAYGTQGSSGYSLR.2
730.3624	954.4639	28.1	11.6	15.6	Positive	KLKB1_HUMAN.IAYGTQGSSGYSLR.2
730.3624	826.4054	28.1	11.6	15.6	Positive	KLKB1_HUMAN.IAYGTQGSSGYSLR.2
730.3624	769.3839	28.1	11.6	15.6	Positive	KLKB1_HUMAN.IAYGTQGSSGYSLR.2
735.3666	779.3922	28.3	11.6	15.6	Positive	KLKB1_HUMAN.IAYGTQGSSGYSLR.2
735.3666	836.4136	28.3	11.6	15.6	Positive	KLKB1_HUMAN.IAYGTQGSSGYSLR.2
735.3666	964.4722	28.3	11.6	15.6	Positive	KLKB1_HUMAN.IAYGTQGSSGYSLR.2
735.3666	1122.5413	28.3	11.6	15.6	Positive	KLKB1_HUMAN.IAYGTQGSSGYSLR.2
515.7715	607.3198	20.9	19.4	23.4	Positive	KNG1_HUMAN.YFIDFVAR.2
515.7715	492.2929	20.9	19.4	23.4	Positive	KNG1_HUMAN.YFIDFVAR.2
515.7715	720.4039	20.9	19.4	23.4	Positive	KNG1_HUMAN.YFIDFVAR.2
515.7715	867.4723	20.9	19.4	23.4	Positive	KNG1_HUMAN.YFIDFVAR.2
520.7756	617.3281	21.0	19.4	23.4	Positive	KNG1_HUMAN.YFIDFVAR.2
520.7756	877.4806	21.0	19.4	23.4	Positive	KNG1_HUMAN.YFIDFVAR.2
520.7756	730.4122	21.0	19.4	23.4	Positive	KNG1_HUMAN.YFIDFVAR.2
520.7756	502.3012	21.0	19.4	23.4	Positive	KNG1_HUMAN.YFIDFVAR.2
488.7642	347.1714	19.9	8.6	12.6	Positive	MBL2_HUMAN.FQASVATPR.2
488.7642	444.2565	19.9	8.6	12.6	Positive	MBL2_HUMAN.FQASVATPR.2
488.7642	630.3570	19.9	8.6	12.6	Positive	MBL2_HUMAN.FQASVATPR.2
488.7642	701.3941	19.9	8.6	12.6	Positive	MBL2_HUMAN.FQASVATPR.2
493.7683	640.3652	20.1	8.6	12.6	Positive	MBL2_HUMAN.FQASVATPR.2
493.7683	347.1714	20.1	8.6	12.6	Positive	MBL2_HUMAN.FQASVATPR.2
493.7683	454.2648	20.1	8.6	12.6	Positive	MBL2_HUMAN.FQASVATPR.2
493.7683	711.4023	20.1	8.6	12.6	Positive	MBL2_HUMAN.FQASVATPR.2
607.8350	372.2241	24.0	13.1	17.1	Positive	PEDF_HUMAN.ELLDTVTAPQK.2
607.8350	544.3089	24.0	13.1	17.1	Positive	PEDF_HUMAN.ELLDTVTAPQK.2
607.8350	744.4250	24.0	13.1	17.1	Positive	PEDF_HUMAN.ELLDTVTAPQK.2
607.8350	859.4520	24.0	13.1	17.1	Positive	PEDF_HUMAN.ELLDTVTAPQK.2
611.8421	867.4662	24.1	13.1	17.1	Positive	PEDF_HUMAN.ELLDTVTAPQK.2
611.8421	752.4392	24.1	13.1	17.1	Positive	PEDF_HUMAN.ELLDTVTAPQK.2
611.8421	552.3231	24.1	13.1	17.1	Positive	PEDF_HUMAN.ELLDTVTAPQK.2
611.8421	380.2383	24.1	13.1	17.1	Positive	PEDF_HUMAN.ELLDTVTAPQK.2
517.9633	312.1779	26.1	14.8	18.8	Positive	PGRP2_HUMAN.AGLLRPDYALLGHR.3
517.9633	369.1993	26.1	14.8	18.8	Positive	PGRP2_HUMAN.AGLLRPDYALLGHR.3
517.9633	482.2834	26.1	14.8	18.8	Positive	PGRP2_HUMAN.AGLLRPDYALLGHR.3
517.9633	595.3675	26.1	14.8	18.8	Positive	PGRP2_HUMAN.AGLLRPDYALLGHR.3
521.6050	605.3760	26.3	14.8	18.8	Positive	PGRP2_HUMAN.AGLLRPDYALLGHR.3
521.6050	322.1870	26.3	14.8	18.8	Positive	PGRP2_HUMAN.AGLLRPDYALLGHR.3
521.6050	379.2080	26.3	14.8	18.8	Positive	PGRP2_HUMAN.AGLLRPDYALLGHR.3
521.6050	492.2920	26.3	14.8	18.8	Positive	PGRP2_HUMAN.AGLLRPDYALLGHR.3
667.3629	591.3501	26.0	19.2	23.2	Positive	PLF4_HUMAN.IC[CAM]LDLQAPLYK.2
667.3629	947.5197	26.0	19.2	23.2	Positive	PLF4_HUMAN.IC[CAM]LDLQAPLYK.2
667.3629	1060.6037	26.0	19.2	23.2	Positive	PLF4_HUMAN.IC[CAM]LDLQAPLYK.2
667.3629	520.3130	26.0	19.2	23.2	Positive	PLF4_HUMAN.IC[CAM]LDLQAPLYK.2
671.3604	599.3451	26.1	19.1	23.1	Positive	PLF4_HUMAN.IC[CAM]LDLQAPLYK.2
671.3604	955.5147	26.1	19.1	23.1	Positive	PLF4_HUMAN.IC[CAM]LDLQAPLYK.2
671.3604	1068.5988	26.1	19.1	23.1	Positive	PLF4_HUMAN.IC[CAM]LDLQAPLYK.2
671.3604	528.3080	26.1	19.1	23.1	Positive	PLF4_HUMAN.IC[CAM]LDLQAPLYK.2
649.8280	961.4738	25.4	9.0	13.0	Positive	PLMN_HUMAN.HSIFTPETNPR.2
649.8280	713.3577	25.4	9.0	13.0	Positive	PLMN_HUMAN.HSIFTPETNPR.2

649.8280	1161.5899	25.4	9.0	13.0	Positive	PLMN_HUMAN.HSIFTPETNPR.2
649.8280	1074.5578	25.4	9.0	13.0	Positive	PLMN_HUMAN.HSIFTPETNPR.2
654.8322	723.3659	25.6	9.0	13.0	Positive	PLMN_HUMAN.HSIFTPETNPR.2
654.8322	1171.5981	25.6	9.0	13.0	Positive	PLMN_HUMAN.HSIFTPETNPR.2
654.8322	1084.5661	25.6	9.0	13.0	Positive	PLMN_HUMAN.HSIFTPETNPR.2
654.8322	971.4820	25.6	9.0	13.0	Positive	PLMN_HUMAN.HSIFTPETNPR.2
514.3186	431.2401	20.8	14.8	18.8	Positive	PON1_HUMAN.LLIGTVFHK.2
514.3186	801.4618	20.8	14.8	18.8	Positive	PON1_HUMAN.LLIGTVFHK.2
514.3186	688.3777	20.8	14.8	18.8	Positive	PON1_HUMAN.LLIGTVFHK.2
514.3186	631.3562	20.8	14.8	18.8	Positive	PON1_HUMAN.LLIGTVFHK.2
518.3257	439.2543	20.9	14.8	18.8	Positive	PON1_HUMAN.LLIGTVFHK.2
518.3257	639.3704	20.9	14.8	18.8	Positive	PON1_HUMAN.LLIGTVFHK.2
518.3257	696.3919	20.9	14.8	18.8	Positive	PON1_HUMAN.LLIGTVFHK.2
518.3257	809.4759	20.9	14.8	18.8	Positive	PON1_HUMAN.LLIGTVFHK.2
581.2735	927.4393	23.1	15.6	19.6	Positive	RET4_HUMAN.FSGTWYAMAK.2
581.2735	583.2908	23.1	15.6	19.6	Positive	RET4_HUMAN.FSGTWYAMAK.2
581.2735	420.2275	23.1	15.6	19.6	Positive	RET4_HUMAN.FSGTWYAMAK.2
581.2735	1014.4713	23.1	15.6	19.6	Positive	RET4_HUMAN.FSGTWYAMAK.2
585.2806	591.3050	23.2	15.5	19.5	Positive	RET4_HUMAN.FSGTWYAMAK.2
585.2806	935.4535	23.2	15.5	19.5	Positive	RET4_HUMAN.FSGTWYAMAK.2
585.2806	1022.4855	23.2	15.5	19.5	Positive	RET4_HUMAN.FSGTWYAMAK.2
585.2806	428.2417	23.2	15.5	19.5	Positive	RET4_HUMAN.FSGTWYAMAK.2
566.7744	819.3778	22.6	10.9	14.9	Positive	SAA4_HUMAN.EALQGVGDMGR.2
566.7744	535.2293	22.6	10.9	14.9	Positive	SAA4_HUMAN.EALQGVGDMGR.2
566.7744	363.1809	22.6	10.9	14.9	Positive	SAA4_HUMAN.EALQGVGDMGR.2
566.7744	691.3192	22.6	10.9	14.9	Positive	SAA4_HUMAN.EALQGVGDMGR.2
571.7785	701.3275	22.8	10.9	14.9	Positive	SAA4_HUMAN.EALQGVGDMGR.2
571.7785	373.1892	22.8	10.9	14.9	Positive	SAA4_HUMAN.EALQGVGDMGR.2
571.7785	829.3860	22.8	10.9	14.9	Positive	SAA4_HUMAN.EALQGVGDMGR.2
571.7785	545.2376	22.8	10.9	14.9	Positive	SAA4_HUMAN.EALQGVGDMGR.2
549.7931	985.4949	22.0	11.0	15.0	Positive	SEPP1_HUMAN.LPTDSELAPR.2
549.7931	787.3945	22.0	11.0	15.0	Positive	SEPP1_HUMAN.LPTDSELAPR.2
549.7931	888.4421	22.0	11.0	15.0	Positive	SEPP1_HUMAN.LPTDSELAPR.2
549.7931	672.3675	22.0	11.0	15.0	Positive	SEPP1_HUMAN.LPTDSELAPR.2
554.7973	682.3758	22.2	11.0	15.0	Positive	SEPP1_HUMAN.LPTDSELAPR.2
554.7973	797.4027	22.2	11.0	15.0	Positive	SEPP1_HUMAN.LPTDSELAPR.2
554.7973	995.5032	22.2	11.0	15.0	Positive	SEPP1_HUMAN.LPTDSELAPR.2
554.7973	898.4504	22.2	11.0	15.0	Positive	SEPP1_HUMAN.LPTDSELAPR.2
721.4299	804.4363	27.8	23.8	27.8	Positive	SHBG_HUMAN.IALGGLLFPASNLR.2
721.4299	657.3678	27.8	23.8	27.8	Positive	SHBG_HUMAN.IALGGLLFPASNLR.2
721.4299	1144.6473	27.8	23.8	27.8	Positive	SHBG_HUMAN.IALGGLLFPASNLR.2
721.4299	917.5203	27.8	23.8	27.8	Positive	SHBG_HUMAN.IALGGLLFPASNLR.2
726.4341	927.5286	28.0	23.8	27.8	Positive	SHBG_HUMAN.IALGGLLFPASNLR.2
726.4341	1154.6556	28.0	23.8	27.8	Positive	SHBG_HUMAN.IALGGLLFPASNLR.2
726.4341	814.4445	28.0	23.8	27.8	Positive	SHBG_HUMAN.IALGGLLFPASNLR.2
726.4341	667.3761	28.0	23.8	27.8	Positive	SHBG_HUMAN.IALGGLLFPASNLR.2
676.3770	846.4931	26.3	15.5	19.5	Positive	STOM_HUMAN.YLQTLTTIAAEK.2
676.3770	733.4090	26.3	15.5	19.5	Positive	STOM_HUMAN.YLQTLTTIAAEK.2
676.3770	418.2296	26.3	15.5	19.5	Positive	STOM_HUMAN.YLQTLTTIAAEK.2
676.3770	947.5408	26.3	15.5	19.5	Positive	STOM_HUMAN.YLQTLTTIAAEK.2
680.3840	854.5080	26.4	15.4	19.4	Positive	STOM_HUMAN.YLQTLTTIAAEK.2
680.3840	955.5560	26.4	15.4	19.4	Positive	STOM_HUMAN.YLQTLTTIAAEK.2
680.3840	426.2440	26.4	15.4	19.4	Positive	STOM_HUMAN.YLQTLTTIAAEK.2
680.3840	741.4240	26.4	15.4	19.4	Positive	STOM_HUMAN.YLQTLTTIAAEK.2
657.3874	672.4291	25.7	20.6	24.6	Positive	TETN_HUMAN.LDTLAQEVALLK.2
657.3874	871.5247	25.7	20.6	24.6	Positive	TETN_HUMAN.LDTLAQEVALLK.2
657.3874	800.4876	25.7	20.6	24.6	Positive	TETN_HUMAN.LDTLAQEVALLK.2
657.3874	330.1660	25.7	20.6	24.6	Positive	TETN_HUMAN.LDTLAQEVALLK.2
661.3945	330.1660	25.8	20.6	24.6	Positive	TETN_HUMAN.LDTLAQEVALLK.2
661.3945	680.4433	25.8	20.6	24.6	Positive	TETN_HUMAN.LDTLAQEVALLK.2
661.3945	879.5389	25.8	20.6	24.6	Positive	TETN_HUMAN.LDTLAQEVALLK.2
661.3945	808.5018	25.8	20.6	24.6	Positive	TETN_HUMAN.LDTLAQEVALLK.2
543.3395	900.5917	21.8	21.8	25.8	Positive	THBG_HUMAN.NALALFVLPK.2
543.3395	603.3865	21.8	21.8	25.8	Positive	THBG_HUMAN.NALALFVLPK.2
543.3395	787.5076	21.8	21.8	25.8	Positive	THBG_HUMAN.NALALFVLPK.2
543.3395	716.4705	21.8	21.8	25.8	Positive	THBG_HUMAN.NALALFVLPK.2
547.3466	795.5218	21.9	21.7	25.7	Positive	THBG_HUMAN.NALALFVLPK.2
547.3466	724.4847	21.9	21.7	25.7	Positive	THBG_HUMAN.NALALFVLPK.2
547.3466	908.6059	21.9	21.7	25.7	Positive	THBG_HUMAN.NALALFVLPK.2
547.3466	611.4007	21.9	21.7	25.7	Positive	THBG_HUMAN.NALALFVLPK.2
781.3677	909.4577	29.9	16.3	20.3	Positive	THRB_HUMAN.TATSEYQTFFNPR.2
781.3677	680.3515	29.9	16.3	20.3	Positive	THRB_HUMAN.TATSEYQTFFNPR.2
781.3677	1072.5211	29.9	16.3	20.3	Positive	THRB_HUMAN.TATSEYQTFFNPR.2
786.3718	919.4660	30.1	16.3	20.3	Positive	THRB_HUMAN.TATSEYQTFFNPR.2
786.3718	690.3597	30.1	16.3	20.3	Positive	THRB_HUMAN.TATSEYQTFFNPR.2
786.3718	1082.5293	30.1	16.3	20.3	Positive	THRB_HUMAN.TATSEYQTFFNPR.2
418.2207	506.2755	17.5	11.0	15.0	Positive	TotalIGHG.DTLMISR.2
418.2207	619.3596	17.5	11.0	15.0	Positive	TotalIGHG.DTLMISR.2
418.2207	330.1660	17.5	11.0	15.0	Positive	TotalIGHG.DTLMISR.2
418.2207	375.2350	17.5	11.0	15.0	Positive	TotalIGHG.DTLMISR.2
423.2249	516.2838	17.7	11.0	15.0	Positive	TotalIGHG.DTLMISR.2

423.2249	629.3679	17.7	11.0	15.0	Positive	TotallGHG.DTLMISR.2
423.2249	330.1660	17.7	11.0	15.0	Positive	TotallGHG.DTLMISR.2
423.2249	385.2433	17.7	11.0	15.0	Positive	TotallGHG.DTLMISR.2
642.2882	771.3784	25.2	14.6	18.6	Positive	TRFE_HUMAN.EGYYGYTGAFR.2
642.2882	934.4417	25.2	14.6	18.6	Positive	TRFE_HUMAN.EGYYGYTGAFR.2
642.2882	551.2936	25.2	14.6	18.6	Positive	TRFE_HUMAN.EGYYGYTGAFR.2
642.2882	714.3570	25.2	14.6	18.6	Positive	TRFE_HUMAN.EGYYGYTGAFR.2
647.2923	781.3867	25.3	14.6	18.6	Positive	TRFE_HUMAN.EGYYGYTGAFR.2
647.2923	944.4500	25.3	14.6	18.6	Positive	TRFE_HUMAN.EGYYGYTGAFR.2
647.2923	561.3019	25.3	14.6	18.6	Positive	TRFE_HUMAN.EGYYGYTGAFR.2
647.2923	724.3652	25.3	14.6	18.6	Positive	TRFE_HUMAN.EGYYGYTGAFR.2
683.8831	941.5316	26.6	15.5	19.5	Positive	TTHY_HUMAN.GSPAINVAVHVFR.2
683.8831	728.4202	26.6	15.5	19.5	Positive	TTHY_HUMAN.GSPAINVAVHVFR.2
683.8831	1054.6156	26.6	15.5	19.5	Positive	TTHY_HUMAN.GSPAINVAVHVFR.2
683.8831	313.1506	26.6	15.5	19.5	Positive	TTHY_HUMAN.GSPAINVAVHVFR.2
688.8873	951.5398	26.7	15.5	19.5	Positive	TTHY_HUMAN.GSPAINVAVHVFR.2
688.8873	738.4285	26.7	15.5	19.5	Positive	TTHY_HUMAN.GSPAINVAVHVFR.2
688.8873	313.1506	26.7	15.5	19.5	Positive	TTHY_HUMAN.GSPAINVAVHVFR.2
688.8873	1064.6239	26.7	15.5	19.5	Positive	TTHY_HUMAN.GSPAINVAVHVFR.2
627.8619	691.3733	24.7	15.2	19.2	Positive	VTDB_HUMAN.HLSLLTTLSNR.2
627.8619	804.4574	24.7	15.2	19.2	Positive	VTDB_HUMAN.HLSLLTTLSNR.2
627.8619	1117.6575	24.7	15.2	19.2	Positive	VTDB_HUMAN.HLSLLTTLSNR.2
627.8619	1004.5735	24.7	15.2	19.2	Positive	VTDB_HUMAN.HLSLLTTLSNR.2
632.8660	1014.5818	24.8	15.2	19.2	Positive	VTDB_HUMAN.HLSLLTTLSNR.2
632.8660	1127.6658	24.8	15.2	19.2	Positive	VTDB_HUMAN.HLSLLTTLSNR.2
632.8660	814.4657	24.8	15.2	19.2	Positive	VTDB_HUMAN.HLSLLTTLSNR.2
632.8660	701.3816	24.8	15.2	19.2	Positive	VTDB_HUMAN.HLSLLTTLSNR.2
711.8304	762.3417	27.5	16.2	20.2	Positive	VTNC_HUMAN.FEDGVLDPDYPR.2
711.8304	875.4258	27.5	16.2	20.2	Positive	VTNC_HUMAN.FEDGVLDPDYPR.2
711.8304	435.2350	27.5	16.2	20.2	Positive	VTNC_HUMAN.FEDGVLDPDYPR.2
711.8304	647.3148	27.5	16.2	20.2	Positive	VTNC_HUMAN.FEDGVLDPDYPR.2
716.8346	772.3500	27.7	16.2	20.2	Positive	VTNC_HUMAN.FEDGVLDPDYPR.2
716.8346	885.4340	27.7	16.2	20.2	Positive	VTNC_HUMAN.FEDGVLDPDYPR.2
716.8346	445.2433	27.7	16.2	20.2	Positive	VTNC_HUMAN.FEDGVLDPDYPR.2
716.8346	657.3230	27.7	16.2	20.2	Positive	VTNC_HUMAN.FEDGVLDPDYPR.2
726.3454	717.3712	28.0	13.0	17.0	Positive	ZA2G_HUMAN.AYLEEEC[CAM]PATLR.2
726.3454	975.4564	28.0	13.0	17.0	Positive	ZA2G_HUMAN.AYLEEEC[CAM]PATLR.2
726.3454	1104.4990	28.0	13.0	17.0	Positive	ZA2G_HUMAN.AYLEEEC[CAM]PATLR.2
726.3454	557.3406	28.0	13.0	17.0	Positive	ZA2G_HUMAN.AYLEEEC[CAM]PATLR.2
731.3448	727.3701	28.2	12.9	16.9	Positive	ZA2G_HUMAN.AYLEEEC[CAM]PATLR.2
731.3448	985.4553	28.2	12.9	16.9	Positive	ZA2G_HUMAN.AYLEEEC[CAM]PATLR.2
731.3448	1114.4979	28.2	12.9	16.9	Positive	ZA2G_HUMAN.AYLEEEC[CAM]PATLR.2
731.3448	567.3395	28.2	12.9	16.9	Positive	ZA2G_HUMAN.AYLEEEC[CAM]PATLR.2

SUPPLEMENTAL TABLE 2:

Compound Group	Compound Name	ISTD?	Precursor Ion	MS1 Res	Product Ion	MS2 Res	Primary	Ret Time (min)	Delta Ret Time	Collision Energy
A1AG1_HUMAN	SDVVYTDWK.heavy	TRUE	560.773671	Unit	819.41268	Unit	TRUE	10.58	0.8	18.3
A1AG1_HUMAN	SDVVYTDWK.heavy	TRUE	560.773671	Unit	720.344266	Unit	TRUE	10.58	0.8	18.3
A1AG1_HUMAN	SDVVYTDWK.heavy	TRUE	560.773671	Unit	302.134661	Unit	TRUE	10.58	0.8	18.3
A1AG1_HUMAN	SDVVYTDWK.light	FALSE	556.766571	Unit	811.398481	Unit	TRUE	10.58	0.8	18.3
A1AG1_HUMAN	SDVVYTDWK.light	FALSE	556.766571	Unit	712.330067	Unit	TRUE	10.58	0.8	18.3
A1AG1_HUMAN	SDVVYTDWK.light	FALSE	556.766571	Unit	302.134661	Unit	TRUE	10.58	0.8	18.3
A1AG2_HUMAN	EHVAHLLFLR.heavy	TRUE	622.860524	Unit	978.612266	Unit	TRUE	13.16	0.8	20.2
A1AG2_HUMAN	EHVAHLLFLR.heavy	TRUE	622.860524	Unit	879.543852	Unit	TRUE	13.16	0.8	20.2
A1AG2_HUMAN	EHVAHLLFLR.heavy	TRUE	622.860524	Unit	808.506739	Unit	TRUE	13.16	0.8	20.2
A1AG2_HUMAN	EHVAHLLFLR.light	FALSE	617.856389	Unit	968.603997	Unit	TRUE	13.16	0.8	20.2
A1AG2_HUMAN	EHVAHLLFLR.light	FALSE	617.856389	Unit	869.535583	Unit	TRUE	13.16	0.8	20.2
A1AG2_HUMAN	EHVAHLLFLR.light	FALSE	617.856389	Unit	798.49847	Unit	TRUE	13.16	0.8	20.2
A1AT_HUMAN	SVLGQLGITK.heavy	TRUE	512.318048	Unit	837.528378	Unit	TRUE	13.95	0.8	16.8
A1AT_HUMAN	SVLGQLGITK.heavy	TRUE	512.318048	Unit	724.444314	Unit	TRUE	13.95	0.8	16.8
A1AT_HUMAN	SVLGQLGITK.heavy	TRUE	512.318048	Unit	419.267827	Unit	TRUE	13.95	0.8	16.8
A1AT_HUMAN	SVLGQLGITK.light	FALSE	508.310949	Unit	829.514179	Unit	TRUE	13.95	0.8	16.8
A1AT_HUMAN	SVLGQLGITK.light	FALSE	508.310949	Unit	716.430115	Unit	TRUE	13.95	0.8	16.8
A1AT_HUMAN	SVLGQLGITK.light	FALSE	508.310949	Unit	415.260728	Unit	TRUE	13.95	0.8	16.8
A1BG_HUMAN	SGLSTGWTQLSK.heavy	TRUE	636.837334	Unit	1015.529835	Unit	TRUE	12.29	0.8	20.6
A1BG_HUMAN	SGLSTGWTQLSK.heavy	TRUE	636.837334	Unit	928.497806	Unit	TRUE	12.29	0.8	20.6
A1BG_HUMAN	SGLSTGWTQLSK.heavy	TRUE	636.837334	Unit	827.450128	Unit	TRUE	12.29	0.8	20.6
A1BG_HUMAN	SGLSTGWTQLSK.light	FALSE	632.830234	Unit	1007.515636	Unit	TRUE	12.29	0.8	20.6
A1BG_HUMAN	SGLSTGWTQLSK.light	FALSE	632.830234	Unit	920.483607	Unit	TRUE	12.29	0.8	20.6
A1BG_HUMAN	SGLSTGWTQLSK.light	FALSE	632.830234	Unit	819.435929	Unit	TRUE	12.29	0.8	20.6
A2AP_HUMAN	LFGPDLK.heavy	TRUE	399.235996	Unit	684.380651	Unit	TRUE	11.66	0.8	13.3
A2AP_HUMAN	LFGPDLK.heavy	TRUE	399.235996	Unit	537.312237	Unit	TRUE	11.66	0.8	13.3
A2AP_HUMAN	LFGPDLK.heavy	TRUE	399.235996	Unit	268.2111	Unit	TRUE	11.66	0.8	13.3
A2AP_HUMAN	LFGPDLK.heavy	TRUE	399.235996	Unit	155.127	Unit	TRUE	11.66	0.8	13.3
A2AP_HUMAN	LFGPDLK.light	FALSE	395.228896	Unit	676.366452	Unit	TRUE	11.66	0.8	13.3
A2AP_HUMAN	LFGPDLK.light	FALSE	395.228896	Unit	529.298038	Unit	TRUE	11.66	0.8	13.3
A2AP_HUMAN	LFGPDLK.light	FALSE	395.228896	Unit	260.1969	Unit	TRUE	11.66	0.8	13.3
A2AP_HUMAN	LFGPDLK.light	FALSE	395.228896	Unit	147.1128	Unit	TRUE	11.66	0.8	13.3
A2GL_HUMAN	VAAGAFQGLR.heavy	TRUE	500.284118	Unit	829.455431	Unit	TRUE	10.07	0.8	16.4
A2GL_HUMAN	VAAGAFQGLR.heavy	TRUE	500.284118	Unit	758.418318	Unit	TRUE	10.07	0.8	16.4
A2GL_HUMAN	VAAGAFQGLR.heavy	TRUE	500.284118	Unit	630.35974	Unit	TRUE	10.07	0.8	16.4
A2GL_HUMAN	VAAGAFQGLR.light	FALSE	495.279983	Unit	819.447162	Unit	TRUE	10.07	0.8	16.4
A2GL_HUMAN	VAAGAFQGLR.light	FALSE	495.279983	Unit	748.410049	Unit	TRUE	10.07	0.8	16.4
A2GL_HUMAN	VAAGAFQGLR.light	FALSE	495.279983	Unit	620.351471	Unit	TRUE	10.07	0.8	16.4
A2MG_HUMAN	HYDGSYSTFGER.heavy	TRUE	476.873318	Unit	560.209952	Unit	TRUE	6.61	0.8	15.8
A2MG_HUMAN	HYDGSYSTFGER.heavy	TRUE	476.873318	Unit	518.259692	Unit	TRUE	6.61	0.8	15.8
A2MG_HUMAN	HYDGSYSTFGER.heavy	TRUE	476.873318	Unit	371.191278	Unit	TRUE	6.61	0.8	15.8
A2MG_HUMAN	HYDGSYSTFGER.light	FALSE	473.537229	Unit	560.209952	Unit	TRUE	6.61	0.8	12.2
A2MG_HUMAN	HYDGSYSTFGER.light	FALSE	473.537229	Unit	508.251423	Unit	TRUE	6.61	0.8	12.2
A2MG_HUMAN	HYDGSYSTFGER.light	FALSE	473.537229	Unit	361.183009	Unit	TRUE	6.61	0.8	12.2
AACT_HUMAN	EIGELYLPK.heavy	TRUE	535.304607	Unit	827.47528	Unit	TRUE	13.93	0.8	17.5
AACT_HUMAN	EIGELYLPK.heavy	TRUE	535.304607	Unit	641.411223	Unit	TRUE	13.93	0.8	17.5
AACT_HUMAN	EIGELYLPK.heavy	TRUE	535.304607	Unit	365.263831	Unit	TRUE	13.93	0.8	17.5
AACT_HUMAN	EIGELYLPK.light	FALSE	531.297507	Unit	819.461081	Unit	TRUE	13.93	0.8	17.5
AACT_HUMAN	EIGELYLPK.light	FALSE	531.297507	Unit	633.397024	Unit	TRUE	13.93	0.8	17.5
AACT_HUMAN	EIGELYLPK.light	FALSE	531.297507	Unit	357.249632	Unit	TRUE	13.93	0.8	17.5
ABCF1_HUMAN	IGFFNQQYAEQLR.heavy	TRUE	812.411306	Unit	917.471475	Unit	TRUE	16.06	0.8	26
ABCF1_HUMAN	IGFFNQQYAEQLR.heavy	TRUE	812.411306	Unit	789.412898	Unit	TRUE	16.06	0.8	26
ABCF1_HUMAN	IGFFNQQYAEQLR.heavy	TRUE	812.411306	Unit	626.349569	Unit	TRUE	16.06	0.8	26
ABCF1_HUMAN	IGFFNQQYAEQLR.light	FALSE	807.407172	Unit	907.463206	Unit	TRUE	16.06	0.8	26
ABCF1_HUMAN	IGFFNQQYAEQLR.light	FALSE	807.407172	Unit	779.404629	Unit	TRUE	16.06	0.8	26
ABCF1_HUMAN	IGFFNQQYAEQLR.light	FALSE	807.407172	Unit	616.3413	Unit	TRUE	16.06	0.8	26
AFAM_HUMAN	AESPEVC[+57.0]FNEESPK.heavy	TRUE	815.860877	Unit	1018.438971	Unit	TRUE	9.11	0.8	26.2
AFAM_HUMAN	AESPEVC[+57.0]FNEESPK.heavy	TRUE	815.860877	Unit	715.821023	Unit	TRUE	9.11	0.8	26.2
AFAM_HUMAN	AESPEVC[+57.0]FNEESPK.heavy	TRUE	815.860877	Unit	672.305009	Unit	TRUE	9.11	0.8	26.2
AFAM_HUMAN	AESPEVC[+57.0]FNEESPK.light	FALSE	811.853777	Unit	1010.424772	Unit	TRUE	9.11	0.8	26.2
AFAM_HUMAN	AESPEVC[+57.0]FNEESPK.light	FALSE	811.853777	Unit	711.813924	Unit	TRUE	9.11	0.8	26.2
AFAM_HUMAN	AESPEVC[+57.0]FNEESPK.light	FALSE	811.853777	Unit	668.29791	Unit	TRUE	9.11	0.8	26.2
ALBU_HUMAN	YLYEIAR.heavy	TRUE	469.254494	Unit	774.438384	Unit	TRUE	10.57	0.8	15.4
ALBU_HUMAN	YLYEIAR.heavy	TRUE	469.254494	Unit	498.290992	Unit	TRUE	10.57	0.8	15.4
ALBU_HUMAN	YLYEIAR.heavy	TRUE	469.254494	Unit	369.248399	Unit	TRUE	10.57	0.8	15.4
ALBU_HUMAN	YLYEIAR.light	FALSE	464.25036	Unit	764.430115	Unit	TRUE	10.57	0.8	15.4
ALBU_HUMAN	YLYEIAR.light	FALSE	464.25036	Unit	488.282723	Unit	TRUE	10.57	0.8	15.4
ALBU_HUMAN	YLYEIAR.light	FALSE	464.25036	Unit	359.24013	Unit	TRUE	10.57	0.8	15.4
AMBP_HUMAN	TVAAC[+57.0]NLPIVR.heavy	TRUE	612.343849	Unit	1023.56433	Unit	TRUE	12.09	0.8	19.8
AMBP_HUMAN	TVAAC[+57.0]NLPIVR.heavy	TRUE	612.343849	Unit	952.527216	Unit	TRUE	12.09	0.8	19.8
AMBP_HUMAN	TVAAC[+57.0]NLPIVR.heavy	TRUE	612.343849	Unit	881.490103	Unit	TRUE	12.09	0.8	19.8
AMBP_HUMAN	TVAAC[+57.0]NLPIVR.light	FALSE	607.339715	Unit	1013.556061	Unit	TRUE	12.09	0.8	19.8
AMBP_HUMAN	TVAAC[+57.0]NLPIVR.light	FALSE	607.339715	Unit	942.518947	Unit	TRUE	12.09	0.8	19.8
AMBP_HUMAN	TVAAC[+57.0]NLPIVR.light	FALSE	607.339715	Unit	871.481834	Unit	TRUE	12.09	0.8	19.8
ANGT_HUMAN	ALQDQLVLVAAK.heavy	TRUE	638.889369	Unit	1092.650284	Unit	TRUE	14.74	0.8	25
ANGT_HUMAN	ALQDQLVLVAAK.heavy	TRUE	638.889369	Unit	964.591707	Unit	TRUE	14.74	0.8	25
ANGT_HUMAN	ALQDQLVLVAAK.heavy	TRUE	638.889369	Unit	608.422122	Unit	TRUE	14.74	0.8	25
ANGT_HUMAN	ALQDQLVLVAAK.light	FALSE	634.88227	Unit	1084.636085	Unit	TRUE	14.74	0.8	25

ANGT_HUMAN	ALQDQLVLVAAK.light	FALSE	634.88227	Unit	956.577508	Unit	TRUE	14.74	0.8	25
ANGT_HUMAN	ALQDQLVLVAAK.light	FALSE	634.88227	Unit	600.407923	Unit	TRUE	14.74	0.8	25
ANT3_HUMAN	EVPLNTIIFMGR.heavy	TRUE	700.385714	Unit	961.516317	Unit	TRUE	19.87	0.8	22.6
ANT3_HUMAN	EVPLNTIIFMGR.heavy	TRUE	700.385714	Unit	633.341647	Unit	TRUE	19.87	0.8	22.6
ANT3_HUMAN	EVPLNTIIFMGR.heavy	TRUE	700.385714	Unit	586.33021	Unit	TRUE	19.87	0.8	22.6
ANT3_HUMAN	EVPLNTIIFMGR.light	FALSE	695.38158	Unit	951.508048	Unit	TRUE	19.87	0.8	22.6
ANT3_HUMAN	EVPLNTIIFMGR.light	FALSE	695.38158	Unit	623.333378	Unit	TRUE	19.87	0.8	22.6
ANT3_HUMAN	EVPLNTIIFMGR.light	FALSE	695.38158	Unit	581.326076	Unit	TRUE	19.87	0.8	22.6
APOA_HUMAN	GTYSTTVTGR.heavy	TRUE	526.765955	Unit	731.392162	Unit	TRUE	4.35	0.8	17.2
APOA_HUMAN	GTYSTTVTGR.heavy	TRUE	526.765955	Unit	644.360134	Unit	TRUE	4.35	0.8	17.2
APOA_HUMAN	GTYSTTVTGR.heavy	TRUE	526.765955	Unit	543.312455	Unit	TRUE	4.35	0.8	17.2
APOA_HUMAN	GTYSTTVTGR.light	FALSE	521.76182	Unit	721.383893	Unit	TRUE	4.35	0.8	17.2
APOA_HUMAN	GTYSTTVTGR.light	FALSE	521.76182	Unit	634.351865	Unit	TRUE	4.35	0.8	17.2
APOA_HUMAN	GTYSTTVTGR.light	FALSE	521.76182	Unit	533.304186	Unit	TRUE	4.35	0.8	17.2
APOA1_HUMAN	VSFLSALEEYTK.heavy	TRUE	697.868299	Unit	1061.560466	Unit	TRUE	19.93	0.8	22.5
APOA1_HUMAN	VSFLSALEEYTK.heavy	TRUE	697.868299	Unit	948.476402	Unit	TRUE	19.93	0.8	22.5
APOA1_HUMAN	VSFLSALEEYTK.heavy	TRUE	697.868299	Unit	861.444374	Unit	TRUE	19.93	0.8	22.5
APOA1_HUMAN	VSFLSALEEYTK.light	FALSE	693.8612	Unit	1053.546267	Unit	TRUE	19.93	0.8	22.5
APOA1_HUMAN	VSFLSALEEYTK.light	FALSE	693.8612	Unit	940.462203	Unit	TRUE	19.93	0.8	22.5
APOA1_HUMAN	VSFLSALEEYTK.light	FALSE	693.8612	Unit	853.430175	Unit	TRUE	19.93	0.8	22.5
APOA2_HUMAN	EQLTPLIK.heavy	TRUE	475.294042	Unit	692.479637	Unit	TRUE	11.89	0.8	15.6
APOA2_HUMAN	EQLTPLIK.heavy	TRUE	475.294042	Unit	579.395573	Unit	TRUE	11.89	0.8	15.6
APOA2_HUMAN	EQLTPLIK.heavy	TRUE	475.294042	Unit	478.347895	Unit	TRUE	11.89	0.8	15.6
APOA2_HUMAN	EQLTPLIK.light	FALSE	471.286942	Unit	684.465438	Unit	TRUE	11.89	0.8	15.6
APOA2_HUMAN	EQLTPLIK.light	FALSE	471.286942	Unit	571.381374	Unit	TRUE	11.89	0.8	15.6
APOA2_HUMAN	EQLTPLIK.light	FALSE	471.286942	Unit	470.333696	Unit	TRUE	11.89	0.8	15.6
APOA4_HUMAN	LAPLAEDVR.heavy	TRUE	497.283783	Unit	809.439113	Unit	TRUE	9.92	0.8	16.3
APOA4_HUMAN	LAPLAEDVR.heavy	TRUE	497.283783	Unit	712.386349	Unit	TRUE	9.92	0.8	16.3
APOA4_HUMAN	LAPLAEDVR.heavy	TRUE	497.283783	Unit	599.302285	Unit	TRUE	9.92	0.8	16.3
APOA4_HUMAN	LAPLAEDVR.light	FALSE	492.279649	Unit	799.430844	Unit	TRUE	9.92	0.8	16.3
APOA4_HUMAN	LAPLAEDVR.light	FALSE	492.279649	Unit	702.37808	Unit	TRUE	9.92	0.8	16.3
APOA4_HUMAN	LAPLAEDVR.light	FALSE	492.279649	Unit	589.294016	Unit	TRUE	9.92	0.8	16.3
APOB_HUMAN	FSVPAGIVIPSFQALTAR.heavy	TRUE	942.534495	Unit	1212.697453	Unit	TRUE	19.99	0.8	30.1
APOB_HUMAN	FSVPAGIVIPSFQALTAR.heavy	TRUE	942.534495	Unit	1113.629039	Unit	TRUE	19.99	0.8	30.1
APOB_HUMAN	FSVPAGIVIPSFQALTAR.heavy	TRUE	942.534495	Unit	1000.544975	Unit	TRUE	19.99	0.8	30.1
APOB_HUMAN	FSVPAGIVIPSFQALTAR.light	FALSE	937.530361	Unit	1202.689184	Unit	TRUE	19.99	0.8	30.1
APOB_HUMAN	FSVPAGIVIPSFQALTAR.light	FALSE	937.530361	Unit	1103.62077	Unit	TRUE	19.99	0.8	30.1
APOB_HUMAN	FSVPAGIVIPSFQALTAR.light	FALSE	937.530361	Unit	990.536706	Unit	TRUE	19.99	0.8	30.1
APOC1_HUMAN	EFGNTLEDK.heavy	TRUE	530.755478	Unit	784.392673	Unit	TRUE	7.06	0.8	17.3
APOC1_HUMAN	EFGNTLEDK.heavy	TRUE	530.755478	Unit	613.328281	Unit	TRUE	7.06	0.8	17.3
APOC1_HUMAN	EFGNTLEDK.heavy	TRUE	530.755478	Unit	512.280603	Unit	TRUE	7.06	0.8	17.3
APOC1_HUMAN	EFGNTLEDK.light	FALSE	526.748378	Unit	776.378474	Unit	TRUE	7.06	0.8	17.3
APOC1_HUMAN	EFGNTLEDK.light	FALSE	526.748378	Unit	605.314082	Unit	TRUE	7.06	0.8	17.3
APOC1_HUMAN	EFGNTLEDK.light	FALSE	526.748378	Unit	504.266404	Unit	TRUE	7.06	0.8	17.3
APOC2_HUMAN	TAAQNLYEK.heavy	TRUE	523.273838	Unit	873.455607	Unit	TRUE	4.97	0.8	17.1
APOC2_HUMAN	TAAQNLYEK.heavy	TRUE	523.273838	Unit	802.418493	Unit	TRUE	4.97	0.8	17.1
APOC2_HUMAN	TAAQNLYEK.heavy	TRUE	523.273838	Unit	674.359916	Unit	TRUE	4.97	0.8	17.1
APOC2_HUMAN	TAAQNLYEK.light	FALSE	519.266738	Unit	865.441408	Unit	TRUE	4.97	0.8	17.1
APOC2_HUMAN	TAAQNLYEK.light	FALSE	519.266738	Unit	794.404294	Unit	TRUE	4.97	0.8	17.1
APOC2_HUMAN	TAAQNLYEK.light	FALSE	519.266738	Unit	666.345717	Unit	TRUE	4.97	0.8	17.1
APOC3_HUMAN	GWVTDGFSSLK.heavy	TRUE	602.808045	Unit	961.508037	Unit	TRUE	15.27	0.8	19.6
APOC3_HUMAN	GWVTDGFSSLK.heavy	TRUE	602.808045	Unit	862.439623	Unit	TRUE	15.27	0.8	19.6
APOC3_HUMAN	GWVTDGFSSLK.heavy	TRUE	602.808045	Unit	646.365001	Unit	TRUE	15.27	0.8	19.6
APOC3_HUMAN	GWVTDGFSSLK.light	FALSE	598.800945	Unit	953.493838	Unit	TRUE	15.27	0.8	19.6
APOC3_HUMAN	GWVTDGFSSLK.light	FALSE	598.800945	Unit	854.425424	Unit	TRUE	15.27	0.8	19.6
APOC3_HUMAN	GWVTDGFSSLK.light	FALSE	598.800945	Unit	638.350802	Unit	TRUE	15.27	0.8	19.6
APOD_HUMAN	NILTSNNIDVK.heavy	TRUE	619.845159	Unit	1011.55605	Unit	TRUE	11.04	0.8	20.1
APOD_HUMAN	NILTSNNIDVK.heavy	TRUE	619.845159	Unit	898.471986	Unit	TRUE	11.04	0.8	20.1
APOD_HUMAN	NILTSNNIDVK.heavy	TRUE	619.845159	Unit	797.424307	Unit	TRUE	11.04	0.8	20.1
APOD_HUMAN	NILTSNNIDVK.light	FALSE	615.838059	Unit	1003.541851	Unit	TRUE	11.04	0.8	20.1
APOD_HUMAN	NILTSNNIDVK.light	FALSE	615.838059	Unit	890.457787	Unit	TRUE	11.04	0.8	20.1
APOD_HUMAN	NILTSNNIDVK.light	FALSE	615.838059	Unit	789.410108	Unit	TRUE	11.04	0.8	20.1
APOE_HUMAN	AATVGSLAGQPLQER.heavy	TRUE	754.408763	Unit	908.482374	Unit	TRUE	10.22	0.8	24.2
APOE_HUMAN	AATVGSLAGQPLQER.heavy	TRUE	754.408763	Unit	837.445261	Unit	TRUE	10.22	0.8	24.2
APOE_HUMAN	AATVGSLAGQPLQER.heavy	TRUE	754.408763	Unit	652.365219	Unit	TRUE	10.22	0.8	24.2
APOE_HUMAN	AATVGSLAGQPLQER.light	FALSE	749.404629	Unit	898.474105	Unit	TRUE	10.22	0.8	24.2
APOE_HUMAN	AATVGSLAGQPLQER.light	FALSE	749.404629	Unit	827.436992	Unit	TRUE	10.22	0.8	24.2
APOE_HUMAN	AATVGSLAGQPLQER.light	FALSE	749.404629	Unit	642.35695	Unit	TRUE	10.22	0.8	24.2
APOH_HUMAN	VC[+57.0]PFAGILENGAVR.heavy	TRUE	756.896977	Unit	1253.687616	Unit	TRUE	17.24	0.8	24.3
APOH_HUMAN	VC[+57.0]PFAGILENGAVR.heavy	TRUE	756.896977	Unit	707.3628	Unit	TRUE	17.24	0.8	24.3
APOH_HUMAN	VC[+57.0]PFAGILENGAVR.heavy	TRUE	756.896977	Unit	627.347446	Unit	TRUE	17.24	0.8	24.3
APOH_HUMAN	VC[+57.0]PFAGILENGAVR.light	FALSE	751.892843	Unit	1243.679347	Unit	TRUE	17.24	0.8	24.3
APOH_HUMAN	VC[+57.0]PFAGILENGAVR.light	FALSE	751.892843	Unit	702.3586	Unit	TRUE	17.24	0.8	24.3
APOH_HUMAN	VC[+57.0]PFAGILENGAVR.light	FALSE	751.892843	Unit	622.343312	Unit	TRUE	17.24	0.8	24.3
APOL1_HUMAN	VTEPISAESGEQVER.heavy	TRUE	820.903708	Unit	1311.641454	Unit	TRUE	7.44	0.8	26.3
APOL1_HUMAN	VTEPISAESGEQVER.heavy	TRUE	820.903708	Unit	1101.504626	Unit	TRUE	7.44	0.8	26.3
APOL1_HUMAN	VTEPISAESGEQVER.heavy	TRUE	820.903708	Unit	943.435484	Unit	TRUE	7.44	0.8	26.3
APOL1_HUMAN	VTEPISAESGEQVER.light	FALSE	815.899573	Unit	1301.633185	Unit	TRUE	7.44	0.8	26.3
APOL1_HUMAN	VTEPISAESGEQVER.light	FALSE	815.899573	Unit	1091.496357	Unit	TRUE	7.44	0.8	26.3
APOL1_HUMAN	VTEPISAESGEQVER.light	FALSE	815.899573	Unit	933.427215	Unit	TRUE	7.44	0.8	26.3
APOM_HUMAN	FLLYNR.heavy	TRUE	418.238647	Unit	688.401605	Unit	TRUE	12.16	0.8	13.8

APOM_HUMAN	FLLYNR.heavy	TRUE	418.238647	Unit	575.317541	Unit	TRUE	12.16	0.8	13.8
APOM_HUMAN	FLLYNR.heavy	TRUE	418.238647	Unit	462.233477	Unit	TRUE	12.16	0.8	13.8
APOM_HUMAN	FLLYNR.light	FALSE	413.234513	Unit	678.393336	Unit	TRUE	12.16	0.8	13.8
APOM_HUMAN	FLLYNR.light	FALSE	413.234513	Unit	565.309272	Unit	TRUE	12.16	0.8	13.8
APOM_HUMAN	FLLYNR.light	FALSE	413.234513	Unit	452.225208	Unit	TRUE	12.16	0.8	13.8
B3AT_HUMAN	IDAYMAQSR.heavy	TRUE	532.757075	Unit	836.395868	Unit	TRUE	6.37	0.8	17.4
B3AT_HUMAN	IDAYMAQSR.heavy	TRUE	532.757075	Unit	602.295425	Unit	TRUE	6.37	0.8	17.4
B3AT_HUMAN	IDAYMAQSR.heavy	TRUE	532.757075	Unit	300.155397	Unit	TRUE	6.37	0.8	17.4
B3AT_HUMAN	IDAYMAQSR.light	FALSE	527.752941	Unit	826.387599	Unit	TRUE	6.37	0.8	17.4
B3AT_HUMAN	IDAYMAQSR.light	FALSE	527.752941	Unit	592.287156	Unit	TRUE	6.37	0.8	17.4
B3AT_HUMAN	IDAYMAQSR.light	FALSE	527.752941	Unit	300.155397	Unit	TRUE	6.37	0.8	17.4
C1QB_HUMAN	GNLC[+57.0]VNLMR.heavy	TRUE	543.774745	Unit	915.477823	Unit	TRUE	12.05	0.8	17.7
C1QB_HUMAN	GNLC[+57.0]VNLMR.heavy	TRUE	543.774745	Unit	802.393759	Unit	TRUE	12.05	0.8	17.7
C1QB_HUMAN	GNLC[+57.0]VNLMR.heavy	TRUE	543.774745	Unit	642.363111	Unit	TRUE	12.05	0.8	17.7
C1QB_HUMAN	GNLC[+57.0]VNLMR.heavy	TRUE	543.774745	Unit	543.294697	Unit	TRUE	12.05	0.8	17.7
C1QB_HUMAN	GNLC[+57.0]VNLMR.light	FALSE	538.770611	Unit	905.469554	Unit	TRUE	12.05	0.8	17.7
C1QB_HUMAN	GNLC[+57.0]VNLMR.light	FALSE	538.770611	Unit	792.38549	Unit	TRUE	12.05	0.8	17.7
C1QB_HUMAN	GNLC[+57.0]VNLMR.light	FALSE	538.770611	Unit	632.354842	Unit	TRUE	12.05	0.8	17.7
C1QB_HUMAN	GNLC[+57.0]VNLMR.light	FALSE	538.770611	Unit	533.286428	Unit	TRUE	12.05	0.8	17.7
C1QC_HUMAN	FQSVFTVTR.heavy	TRUE	547.797058	Unit	732.42782	Unit	TRUE	13.15	0.8	17.8
C1QC_HUMAN	FQSVFTVTR.heavy	TRUE	547.797058	Unit	633.359406	Unit	TRUE	13.15	0.8	17.8
C1QC_HUMAN	FQSVFTVTR.heavy	TRUE	547.797058	Unit	363.166296	Unit	TRUE	13.15	0.8	17.8
C1QC_HUMAN	FQSVFTVTR.light	FALSE	542.792923	Unit	722.419551	Unit	TRUE	13.15	0.8	17.8
C1QC_HUMAN	FQSVFTVTR.light	FALSE	542.792923	Unit	623.351137	Unit	TRUE	13.15	0.8	17.8
C1QC_HUMAN	FQSVFTVTR.light	FALSE	542.792923	Unit	363.166296	Unit	TRUE	13.15	0.8	17.8
C1R_HUMAN	YTTTMGVNTYK.heavy	TRUE	643.81247	Unit	1022.506657	Unit	TRUE	7.78	0.8	20.8
C1R_HUMAN	YTTTMGVNTYK.heavy	TRUE	643.81247	Unit	921.458978	Unit	TRUE	7.78	0.8	20.8
C1R_HUMAN	YTTTMGVNTYK.heavy	TRUE	643.81247	Unit	689.370815	Unit	TRUE	7.78	0.8	20.8
C1R_HUMAN	YTTTMGVNTYK.light	FALSE	639.80537	Unit	1014.492458	Unit	TRUE	7.78	0.8	20.8
C1R_HUMAN	YTTTMGVNTYK.light	FALSE	639.80537	Unit	913.444779	Unit	TRUE	7.78	0.8	20.8
C1R_HUMAN	YTTTMGVNTYK.light	FALSE	639.80537	Unit	681.356616	Unit	TRUE	7.78	0.8	20.8
C1S_HUMAN	TNFDNDIALVR.heavy	TRUE	644.331993	Unit	1072.566104	Unit	TRUE	13.26	0.8	20.8
C1S_HUMAN	TNFDNDIALVR.heavy	TRUE	644.331993	Unit	925.49769	Unit	TRUE	13.26	0.8	20.8
C1S_HUMAN	TNFDNDIALVR.heavy	TRUE	644.331993	Unit	581.400877	Unit	TRUE	13.26	0.8	20.8
C1S_HUMAN	TNFDNDIALVR.light	FALSE	639.327859	Unit	1062.557835	Unit	TRUE	13.26	0.8	20.8
C1S_HUMAN	TNFDNDIALVR.light	FALSE	639.327859	Unit	915.489421	Unit	TRUE	13.26	0.8	20.8
C1S_HUMAN	TNFDNDIALVR.light	FALSE	639.327859	Unit	571.392608	Unit	TRUE	13.26	0.8	20.8
C4BPA_HUMAN	EDVYVVGTVLR.heavy	TRUE	630.347112	Unit	753.485669	Unit	TRUE	14.74	0.8	20.4
C4BPA_HUMAN	EDVYVVGTVLR.heavy	TRUE	630.347112	Unit	654.417255	Unit	TRUE	14.74	0.8	20.4
C4BPA_HUMAN	EDVYVVGTVLR.heavy	TRUE	630.347112	Unit	555.348841	Unit	TRUE	14.74	0.8	20.4
C4BPA_HUMAN	EDVYVVGTVLR.light	FALSE	625.342977	Unit	743.4774	Unit	TRUE	14.74	0.8	20.4
C4BPA_HUMAN	EDVYVVGTVLR.light	FALSE	625.342977	Unit	644.408986	Unit	TRUE	14.74	0.8	20.4
C4BPA_HUMAN	EDVYVVGTVLR.light	FALSE	625.342977	Unit	545.340572	Unit	TRUE	14.74	0.8	20.4
CBG_HUMAN	GTWTQPFDLASTR.heavy	TRUE	745.369107	Unit	1145.5825	Unit	TRUE	15.81	0.8	24
CBG_HUMAN	GTWTQPFDLASTR.heavy	TRUE	745.369107	Unit	916.476226	Unit	TRUE	15.81	0.8	24
CBG_HUMAN	GTWTQPFDLASTR.heavy	TRUE	745.369107	Unit	666.3345	Unit	TRUE	15.81	0.8	24
CBG_HUMAN	GTWTQPFDLASTR.light	FALSE	740.364972	Unit	1135.5742	Unit	TRUE	15.81	0.8	24
CBG_HUMAN	GTWTQPFDLASTR.light	FALSE	740.364972	Unit	906.467957	Unit	TRUE	15.81	0.8	24
CBG_HUMAN	GTWTQPFDLASTR.light	FALSE	740.364972	Unit	661.3304	Unit	TRUE	15.81	0.8	24
CD5L_HUMAN	IWLDNVR.heavy	TRUE	463.260111	Unit	812.428882	Unit	TRUE	12.69	0.8	15.2
CD5L_HUMAN	IWLDNVR.heavy	TRUE	463.260111	Unit	626.349569	Unit	TRUE	12.69	0.8	15.2
CD5L_HUMAN	IWLDNVR.heavy	TRUE	463.260111	Unit	513.265505	Unit	TRUE	12.69	0.8	15.2
CD5L_HUMAN	IWLDNVR.light	FALSE	458.255977	Unit	802.420613	Unit	TRUE	12.69	0.8	15.2
CD5L_HUMAN	IWLDNVR.light	FALSE	458.255977	Unit	616.3413	Unit	TRUE	12.69	0.8	15.2
CD5L_HUMAN	IWLDNVR.light	FALSE	458.255977	Unit	503.257236	Unit	TRUE	12.69	0.8	15.2
CERU_HUMAN	DIASGLIGPLIIC[+57.0]K.heavy	TRUE	739.430544	Unit	921.568135	Unit	TRUE	19.95	0.8	23.8
CERU_HUMAN	DIASGLIGPLIIC[+57.0]K.heavy	TRUE	739.430544	Unit	808.484071	Unit	TRUE	19.95	0.8	23.8
CERU_HUMAN	DIASGLIGPLIIC[+57.0]K.heavy	TRUE	739.430544	Unit	751.462607	Unit	TRUE	19.95	0.8	23.8
CERU_HUMAN	DIASGLIGPLIIC[+57.0]K.light	FALSE	735.423444	Unit	913.553936	Unit	TRUE	19.95	0.8	23.8
CERU_HUMAN	DIASGLIGPLIIC[+57.0]K.light	FALSE	735.423444	Unit	800.469872	Unit	TRUE	19.95	0.8	23.8
CERU_HUMAN	DIASGLIGPLIIC[+57.0]K.light	FALSE	735.423444	Unit	743.448408	Unit	TRUE	19.95	0.8	23.8
CFAB_HUMAN	YGLVTYATYPK.heavy	TRUE	642.34172	Unit	950.507309	Unit	TRUE	12.65	0.8	20.8
CFAB_HUMAN	YGLVTYATYPK.heavy	TRUE	642.34172	Unit	851.438895	Unit	TRUE	12.65	0.8	20.8
CFAB_HUMAN	YGLVTYATYPK.heavy	TRUE	642.34172	Unit	334.176132	Unit	TRUE	12.65	0.8	20.8
CFAB_HUMAN	YGLVTYATYPK.light	FALSE	638.334621	Unit	942.49311	Unit	TRUE	12.65	0.8	20.8
CFAB_HUMAN	YGLVTYATYPK.light	FALSE	638.334621	Unit	843.424696	Unit	TRUE	12.65	0.8	20.8
CFAB_HUMAN	YGLVTYATYPK.light	FALSE	638.334621	Unit	334.176132	Unit	TRUE	12.65	0.8	20.8
CFAH_HUMAN	IDVHLVPDR.heavy	TRUE	358.53743	Unit	609.359406	Unit	TRUE	10.39	0.8	12.2
CFAH_HUMAN	IDVHLVPDR.heavy	TRUE	358.53743	Unit	496.275342	Unit	TRUE	10.39	0.8	12.2
CFAH_HUMAN	IDVHLVPDR.heavy	TRUE	358.53743	Unit	465.245609	Unit	TRUE	10.39	0.8	12.2
CFAH_HUMAN	IDVHLVPDR.light	FALSE	355.201341	Unit	599.351137	Unit	TRUE	10.39	0.8	12.2
CFAH_HUMAN	IDVHLVPDR.light	FALSE	355.201341	Unit	486.267073	Unit	TRUE	10.39	0.8	12.2
CFAH_HUMAN	IDVHLVPDR.light	FALSE	355.201341	Unit	465.245609	Unit	TRUE	10.39	0.8	12.2
CFAI_HUMAN	IVIEYVDR.heavy	TRUE	508.786159	Unit	804.412563	Unit	TRUE	11.19	0.8	16.6
CFAI_HUMAN	IVIEYVDR.heavy	TRUE	508.786159	Unit	691.328499	Unit	TRUE	11.19	0.8	16.6
CFAI_HUMAN	IVIEYVDR.heavy	TRUE	508.786159	Unit	562.285906	Unit	TRUE	11.19	0.8	16.6
CFAI_HUMAN	IVIEYVDR.light	FALSE	503.782024	Unit	794.404294	Unit	TRUE	11.19	0.8	16.6
CFAI_HUMAN	IVIEYVDR.light	FALSE	503.782024	Unit	681.32023	Unit	TRUE	11.19	0.8	16.6
CFAI_HUMAN	IVIEYVDR.light	FALSE	503.782024	Unit	552.277637	Unit	TRUE	11.19	0.8	16.6
CLUS_HUMAN	ASSIIDELFQDR.heavy	TRUE	702.355665	Unit	1045.51882	Unit	TRUE	19.87	0.8	22.6
CLUS_HUMAN	ASSIIDELFQDR.heavy	TRUE	702.355665	Unit	932.434756	Unit	TRUE	19.87	0.8	22.6

CLUS_HUMAN	ASSIIDELFQDR.heavy	TRUE	702.355665	Unit	575.281155	Unit	TRUE	19.87	0.8	22.6
CLUS_HUMAN	ASSIIDELFQDR.light	FALSE	697.351531	Unit	1035.510551	Unit	TRUE	19.87	0.8	22.6
CLUS_HUMAN	ASSIIDELFQDR.light	FALSE	697.351531	Unit	922.426487	Unit	TRUE	19.87	0.8	22.6
CLUS_HUMAN	ASSIIDELFQDR.light	FALSE	697.351531	Unit	565.272886	Unit	TRUE	19.87	0.8	22.6
CO2_HUMAN	AVISPGFDVFAK.heavy	TRUE	629.849713	Unit	975.502558	Unit	TRUE	17.39	0.8	20.4
CO2_HUMAN	AVISPGFDVFAK.heavy	TRUE	629.849713	Unit	888.470529	Unit	TRUE	17.39	0.8	20.4
CO2_HUMAN	AVISPGFDVFAK.heavy	TRUE	629.849713	Unit	444.738903	Unit	TRUE	17.39	0.8	20.4
CO2_HUMAN	AVISPGFDVFAK.light	FALSE	625.842613	Unit	967.488358	Unit	TRUE	17.39	0.8	20.4
CO2_HUMAN	AVISPGFDVFAK.light	FALSE	625.842613	Unit	880.45633	Unit	TRUE	17.39	0.8	20.4
CO2_HUMAN	AVISPGFDVFAK.light	FALSE	625.842613	Unit	440.731803	Unit	TRUE	17.39	0.8	20.4
CO3_HUMAN	IHWESASLLR.heavy	TRUE	611.334339	Unit	971.518426	Unit	TRUE	12.78	0.8	19.8
CO3_HUMAN	IHWESASLLR.heavy	TRUE	611.334339	Unit	785.439113	Unit	TRUE	12.78	0.8	19.8
CO3_HUMAN	IHWESASLLR.heavy	TRUE	611.334339	Unit	656.396519	Unit	TRUE	12.78	0.8	19.8
CO3_HUMAN	IHWESASLLR.light	FALSE	606.330204	Unit	961.510157	Unit	TRUE	12.78	0.8	19.8
CO3_HUMAN	IHWESASLLR.light	FALSE	606.330204	Unit	775.430844	Unit	TRUE	12.78	0.8	19.8
CO3_HUMAN	IHWESASLLR.light	FALSE	606.330204	Unit	646.38825	Unit	TRUE	12.78	0.8	19.8
CO5_HUMAN	TDAPDLPEENQAR.heavy	TRUE	733.343286	Unit	1178.567561	Unit	TRUE	7.1	0.8	23.6
CO5_HUMAN	TDAPDLPEENQAR.heavy	TRUE	733.343286	Unit	853.40379	Unit	TRUE	7.1	0.8	23.6
CO5_HUMAN	TDAPDLPEENQAR.heavy	TRUE	733.343286	Unit	589.787418	Unit	TRUE	7.1	0.8	23.6
CO5_HUMAN	TDAPDLPEENQAR.light	FALSE	728.339152	Unit	1168.559292	Unit	TRUE	7.1	0.8	23.6
CO5_HUMAN	TDAPDLPEENQAR.light	FALSE	728.339152	Unit	843.395521	Unit	TRUE	7.1	0.8	23.6
CO5_HUMAN	TDAPDLPEENQAR.light	FALSE	728.339152	Unit	584.783284	Unit	TRUE	7.1	0.8	23.6
CO6_HUMAN	IGESIELTC[+57.0]PK.heavy	TRUE	627.82812	Unit	955.500843	Unit	TRUE	10.69	0.8	20.3
CO6_HUMAN	IGESIELTC[+57.0]PK.heavy	TRUE	627.82812	Unit	755.384751	Unit	TRUE	10.69	0.8	20.3
CO6_HUMAN	IGESIELTC[+57.0]PK.heavy	TRUE	627.82812	Unit	626.342158	Unit	TRUE	10.69	0.8	20.3
CO6_HUMAN	IGESIELTC[+57.0]PK.light	FALSE	623.821021	Unit	947.486644	Unit	TRUE	10.69	0.8	20.3
CO6_HUMAN	IGESIELTC[+57.0]PK.light	FALSE	623.821021	Unit	747.370552	Unit	TRUE	10.69	0.8	20.3
CO6_HUMAN	IGESIELTC[+57.0]PK.light	FALSE	623.821021	Unit	618.327959	Unit	TRUE	10.69	0.8	20.3
CO7_HUMAN	VLFYVDSEK.heavy	TRUE	554.294239	Unit	895.428724	Unit	TRUE	12.84	0.8	18.1
CO7_HUMAN	VLFYVDSEK.heavy	TRUE	554.294239	Unit	748.36031	Unit	TRUE	12.84	0.8	18.1
CO7_HUMAN	VLFYVDSEK.heavy	TRUE	554.294239	Unit	585.296981	Unit	TRUE	12.84	0.8	18.1
CO7_HUMAN	VLFYVDSEK.light	FALSE	550.287139	Unit	887.414525	Unit	TRUE	12.84	0.8	18.1
CO7_HUMAN	VLFYVDSEK.light	FALSE	550.287139	Unit	740.346111	Unit	TRUE	12.84	0.8	18.1
CO7_HUMAN	VLFYVDSEK.light	FALSE	550.287139	Unit	577.282782	Unit	TRUE	12.84	0.8	18.1
CO8A_HUMAN	HTSLGPLEAK.heavy	TRUE	530.79748	Unit	923.528772	Unit	TRUE	7.36	0.8	17.3
CO8A_HUMAN	HTSLGPLEAK.heavy	TRUE	530.79748	Unit	835.430844	Unit	TRUE	7.36	0.8	17.3
CO8A_HUMAN	HTSLGPLEAK.heavy	TRUE	530.79748	Unit	822.481094	Unit	TRUE	7.36	0.8	17.3
CO8A_HUMAN	HTSLGPLEAK.light	FALSE	526.790381	Unit	915.514573	Unit	TRUE	7.36	0.8	17.3
CO8A_HUMAN	HTSLGPLEAK.light	FALSE	526.790381	Unit	835.430844	Unit	TRUE	7.36	0.8	17.3
CO8A_HUMAN	HTSLGPLEAK.light	FALSE	526.790381	Unit	814.466895	Unit	TRUE	7.36	0.8	17.3
CO9_HUMAN	LSPIYNLVPVK.heavy	TRUE	625.883555	Unit	1050.643742	Unit	TRUE	17.56	0.8	20.3
CO9_HUMAN	LSPIYNLVPVK.heavy	TRUE	625.883555	Unit	840.506915	Unit	TRUE	17.56	0.8	20.3
CO9_HUMAN	LSPIYNLVPVK.heavy	TRUE	625.883555	Unit	351.248181	Unit	TRUE	17.56	0.8	20.3
CO9_HUMAN	LSPIYNLVPVK.light	FALSE	621.876456	Unit	1042.629543	Unit	TRUE	17.56	0.8	20.3
CO9_HUMAN	LSPIYNLVPVK.light	FALSE	621.876456	Unit	832.492716	Unit	TRUE	17.56	0.8	20.3
CO9_HUMAN	LSPIYNLVPVK.light	FALSE	621.876456	Unit	343.233982	Unit	TRUE	17.56	0.8	20.3
CPN2_HUMAN	LSNNALSGLPQGVFGK.heavy	TRUE	805.443028	Unit	997.555656	Unit	TRUE	16.22	0.8	25.8
CPN2_HUMAN	LSNNALSGLPQGVFGK.heavy	TRUE	805.443028	Unit	740.4181	Unit	TRUE	16.22	0.8	25.8
CPN2_HUMAN	LSNNALSGLPQGVFGK.heavy	TRUE	805.443028	Unit	359.21688	Unit	TRUE	16.22	0.8	25.8
CPN2_HUMAN	LSNNALSGLPQGVFGK.light	FALSE	801.435929	Unit	989.541457	Unit	TRUE	16.22	0.8	25.8
CPN2_HUMAN	LSNNALSGLPQGVFGK.light	FALSE	801.435929	Unit	732.403901	Unit	TRUE	16.22	0.8	25.8
CPN2_HUMAN	LSNNALSGLPQGVFGK.light	FALSE	801.435929	Unit	351.202681	Unit	TRUE	16.22	0.8	25.8
F13A_HUMAN	STVLTIPEIIIK.heavy	TRUE	667.922878	Unit	1047.690358	Unit	TRUE	19.93	0.8	21.6
F13A_HUMAN	STVLTIPEIIIK.heavy	TRUE	667.922878	Unit	934.606294	Unit	TRUE	19.93	0.8	21.6
F13A_HUMAN	STVLTIPEIIIK.heavy	TRUE	667.922878	Unit	720.474552	Unit	TRUE	19.93	0.8	21.6
F13A_HUMAN	STVLTIPEIIIK.light	FALSE	663.915778	Unit	1039.676159	Unit	TRUE	19.93	0.8	21.6
F13A_HUMAN	STVLTIPEIIIK.light	FALSE	663.915778	Unit	926.592095	Unit	TRUE	19.93	0.8	21.6
F13A_HUMAN	STVLTIPEIIIK.light	FALSE	663.915778	Unit	712.460353	Unit	TRUE	19.93	0.8	21.6
FBLN1_HUMAN	TGYYFDGISR.heavy	TRUE	594.781605	Unit	867.423463	Unit	TRUE	11.94	0.8	19.3
FBLN1_HUMAN	TGYYFDGISR.heavy	TRUE	594.781605	Unit	704.360134	Unit	TRUE	11.94	0.8	19.3
FBLN1_HUMAN	TGYYFDGISR.heavy	TRUE	594.781605	Unit	322.139747	Unit	TRUE	11.94	0.8	19.3
FBLN1_HUMAN	TGYYFDGISR.light	FALSE	589.77747	Unit	857.415194	Unit	TRUE	11.94	0.8	19.3
FBLN1_HUMAN	TGYYFDGISR.light	FALSE	589.77747	Unit	694.351865	Unit	TRUE	11.94	0.8	19.3
FBLN1_HUMAN	TGYYFDGISR.light	FALSE	589.77747	Unit	322.139747	Unit	TRUE	11.94	0.8	19.3
FCN3_HUMAN	YGIDWASGR.heavy	TRUE	517.750108	Unit	701.324083	Unit	TRUE	11.62	0.8	16.9
FCN3_HUMAN	YGIDWASGR.heavy	TRUE	517.750108	Unit	586.29714	Unit	TRUE	11.62	0.8	16.9
FCN3_HUMAN	YGIDWASGR.heavy	TRUE	517.750108	Unit	400.217827	Unit	TRUE	11.62	0.8	16.9
FCN3_HUMAN	YGIDWASGR.light	FALSE	512.745973	Unit	691.315814	Unit	TRUE	11.62	0.8	16.9
FCN3_HUMAN	YGIDWASGR.light	FALSE	512.745973	Unit	576.288871	Unit	TRUE	11.62	0.8	16.9
FCN3_HUMAN	YGIDWASGR.light	FALSE	512.745973	Unit	390.209558	Unit	TRUE	11.62	0.8	16.9
FETUA_HUMAN	FSVVYAK.heavy	TRUE	411.235996	Unit	674.396301	Unit	TRUE	9.47	0.8	13.6
FETUA_HUMAN	FSVVYAK.heavy	TRUE	411.235996	Unit	587.364273	Unit	TRUE	9.47	0.8	13.6
FETUA_HUMAN	FSVVYAK.heavy	TRUE	411.235996	Unit	488.295859	Unit	TRUE	9.47	0.8	13.6
FETUA_HUMAN	FSVVYAK.light	FALSE	407.228896	Unit	666.382102	Unit	TRUE	9.47	0.8	13.6
FETUA_HUMAN	FSVVYAK.light	FALSE	407.228896	Unit	579.350074	Unit	TRUE	9.47	0.8	13.6
FETUA_HUMAN	FSVVYAK.light	FALSE	407.228896	Unit	480.28166	Unit	TRUE	9.47	0.8	13.6
FIBA_HUMAN	GSESGIFTNTK.heavy	TRUE	574.787309	Unit	875.471257	Unit	TRUE	7.78	0.8	18.7
FIBA_HUMAN	GSESGIFTNTK.heavy	TRUE	574.787309	Unit	788.439229	Unit	TRUE	7.78	0.8	18.7
FIBA_HUMAN	GSESGIFTNTK.heavy	TRUE	574.787309	Unit	618.333701	Unit	TRUE	7.78	0.8	18.7
FIBA_HUMAN	GSESGIFTNTK.light	FALSE	570.78021	Unit	867.457058	Unit	TRUE	7.78	0.8	18.7
FIBA_HUMAN	GSESGIFTNTK.light	FALSE	570.78021	Unit	780.42503	Unit	TRUE	7.78	0.8	18.7

FIBA_HUMAN	GSESGIFTNTK.light	FALSE	570.78021	Unit	610.319502	Unit	TRUE	7.78	0.8	18.7
FIBB_HUMAN	QGFGNVATNTDGK.heavy	TRUE	658.819672	Unit	714.350808	Unit	TRUE	12.1	0.8	30
FIBB_HUMAN	QGFGNVATNTDGK.heavy	TRUE	658.819672	Unit	643.313694	Unit	TRUE	12.1	0.8	30
FIBB_HUMAN	QGFGNVATNTDGK.heavy	TRUE	658.819672	Unit	333.155731	Unit	TRUE	12.1	0.8	30
FIBB_HUMAN	QGFGNVATNTDGK.light	FALSE	654.812573	Unit	706.336609	Unit	TRUE	12.1	0.8	21.3
FIBB_HUMAN	QGFGNVATNTDGK.light	FALSE	654.812573	Unit	635.299495	Unit	TRUE	12.1	0.8	21.3
FIBB_HUMAN	QGFGNVATNTDGK.light	FALSE	654.812573	Unit	333.155731	Unit	TRUE	12.1	0.8	21.3
FIBG_HUMAN	DNC[+57.0]C[+57.0]ILDER.heavy	TRUE	602.751664	Unit	655.364885	Unit	TRUE	8.2	0.8	19.5
FIBG_HUMAN	DNC[+57.0]C[+57.0]ILDER.heavy	TRUE	602.751664	Unit	542.280821	Unit	TRUE	8.2	0.8	19.5
FIBG_HUMAN	DNC[+57.0]C[+57.0]ILDER.heavy	TRUE	602.751664	Unit	429.196757	Unit	TRUE	8.2	0.8	19.5
FIBG_HUMAN	DNC[+57.0]C[+57.0]ILDER.light	FALSE	597.74753	Unit	645.356616	Unit	TRUE	8.2	0.8	19.5
FIBG_HUMAN	DNC[+57.0]C[+57.0]ILDER.light	FALSE	597.74753	Unit	532.272552	Unit	TRUE	8.2	0.8	19.5
FIBG_HUMAN	DNC[+57.0]C[+57.0]ILDER.light	FALSE	597.74753	Unit	419.188488	Unit	TRUE	8.2	0.8	19.5
FINC_HUMAN	SYTITGLQPGTDYK.heavy	TRUE	776.39267	Unit	1087.550964	Unit	TRUE	11.87	0.8	24.9
FINC_HUMAN	SYTITGLQPGTDYK.heavy	TRUE	776.39267	Unit	986.503286	Unit	TRUE	11.87	0.8	24.9
FINC_HUMAN	SYTITGLQPGTDYK.heavy	TRUE	776.39267	Unit	688.339181	Unit	TRUE	11.87	0.8	24.9
FINC_HUMAN	SYTITGLQPGTDYK.light	FALSE	772.38557	Unit	1079.536765	Unit	TRUE	11.87	0.8	24.9
FINC_HUMAN	SYTITGLQPGTDYK.light	FALSE	772.38557	Unit	978.489087	Unit	TRUE	11.87	0.8	24.9
FINC_HUMAN	SYTITGLQPGTDYK.light	FALSE	772.38557	Unit	680.324982	Unit	TRUE	11.87	0.8	24.9
GELS_HUMAN	AGALNSNDAFVLK.heavy	TRUE	664.358433	Unit	1015.529835	Unit	TRUE	13.08	0.8	21.5
GELS_HUMAN	AGALNSNDAFVLK.heavy	TRUE	664.358433	Unit	901.486907	Unit	TRUE	13.08	0.8	21.5
GELS_HUMAN	AGALNSNDAFVLK.heavy	TRUE	664.358433	Unit	814.454879	Unit	TRUE	13.08	0.8	21.5
GELS_HUMAN	AGALNSNDAFVLK.light	FALSE	660.351334	Unit	1007.515636	Unit	TRUE	13.08	0.8	21.5
GELS_HUMAN	AGALNSNDAFVLK.light	FALSE	660.351334	Unit	893.472708	Unit	TRUE	13.08	0.8	21.5
GELS_HUMAN	AGALNSNDAFVLK.light	FALSE	660.351334	Unit	806.44068	Unit	TRUE	13.08	0.8	21.5
GPX3_HUMAN	FLVGPDGIPIMR.heavy	TRUE	662.8697	Unit	965.511232	Unit	TRUE	18.76	0.8	21.4
GPX3_HUMAN	FLVGPDGIPIMR.heavy	TRUE	662.8697	Unit	908.489768	Unit	TRUE	18.76	0.8	21.4
GPX3_HUMAN	FLVGPDGIPIMR.heavy	TRUE	662.8697	Unit	526.304533	Unit	TRUE	18.76	0.8	21.4
GPX3_HUMAN	FLVGPDGIPIMR.light	FALSE	657.865565	Unit	955.502963	Unit	TRUE	18.76	0.8	21.4
GPX3_HUMAN	FLVGPDGIPIMR.light	FALSE	657.865565	Unit	898.481499	Unit	TRUE	18.76	0.8	21.4
GPX3_HUMAN	FLVGPDGIPIMR.light	FALSE	657.865565	Unit	516.296264	Unit	TRUE	18.76	0.8	21.4
HBA_HUMAN	VGAHAGEYGAEALER.heavy	TRUE	770.37492	Unit	1175.556662	Unit	TRUE	7.12	0.8	24.7
HBA_HUMAN	VGAHAGEYGAEALER.heavy	TRUE	770.37492	Unit	1104.519548	Unit	TRUE	7.12	0.8	24.7
HBA_HUMAN	VGAHAGEYGAEALER.heavy	TRUE	770.37492	Unit	365.193179	Unit	TRUE	7.12	0.8	24.7
HBA_HUMAN	VGAHAGEYGAEALER.light	FALSE	765.370786	Unit	1165.548393	Unit	TRUE	7.12	0.8	24.7
HBA_HUMAN	VGAHAGEYGAEALER.light	FALSE	765.370786	Unit	1094.511279	Unit	TRUE	7.12	0.8	24.7
HBA_HUMAN	VGAHAGEYGAEALER.light	FALSE	765.370786	Unit	365.193179	Unit	TRUE	7.12	0.8	24.7
HBD_HUMAN	LLGNVLVC[+57.0]VLAR.heavy	TRUE	668.904074	Unit	1110.632744	Unit	TRUE	19.96	0.8	28
HBD_HUMAN	LLGNVLVC[+57.0]VLAR.heavy	TRUE	668.904074	Unit	840.499939	Unit	TRUE	19.96	0.8	28
HBD_HUMAN	LLGNVLVC[+57.0]VLAR.heavy	TRUE	668.904074	Unit	628.347461	Unit	TRUE	19.96	0.8	28
HBD_HUMAN	LLGNVLVC[+57.0]VLAR.light	FALSE	663.89994	Unit	1100.624475	Unit	TRUE	19.96	0.8	28
HBD_HUMAN	LLGNVLVC[+57.0]VLAR.light	FALSE	663.89994	Unit	830.49167	Unit	TRUE	19.96	0.8	28
HBD_HUMAN	LLGNVLVC[+57.0]VLAR.light	FALSE	663.89994	Unit	618.339192	Unit	TRUE	19.96	0.8	28
HBE_HUMAN	LSELHC[+57.0]DK.heavy	TRUE	505.246766	Unit	896.402192	Unit	TRUE	3.21	0.8	16.5
HBE_HUMAN	LSELHC[+57.0]DK.heavy	TRUE	505.246766	Unit	680.32757	Unit	TRUE	3.21	0.8	16.5
HBE_HUMAN	LSELHC[+57.0]DK.heavy	TRUE	505.246766	Unit	567.243506	Unit	TRUE	3.21	0.8	16.5
HBE_HUMAN	LSELHC[+57.0]DK.light	FALSE	501.239666	Unit	888.387993	Unit	TRUE	3.21	0.8	16.5
HBE_HUMAN	LSELHC[+57.0]DK.light	FALSE	501.239666	Unit	672.313371	Unit	TRUE	3.21	0.8	16.5
HBE_HUMAN	LSELHC[+57.0]DK.light	FALSE	501.239666	Unit	559.229307	Unit	TRUE	3.21	0.8	16.5
HEMO_HUMAN	NFPSPVDAAFR.heavy	TRUE	615.810696	Unit	969.502775	Unit	TRUE	14.71	0.8	19.9
HEMO_HUMAN	NFPSPVDAAFR.heavy	TRUE	615.810696	Unit	785.417983	Unit	TRUE	14.71	0.8	19.9
HEMO_HUMAN	NFPSPVDAAFR.heavy	TRUE	615.810696	Unit	589.296805	Unit	TRUE	14.71	0.8	19.9
HEMO_HUMAN	NFPSPVDAAFR.light	FALSE	610.806562	Unit	959.494506	Unit	TRUE	14.71	0.8	19.9
HEMO_HUMAN	NFPSPVDAAFR.light	FALSE	610.806562	Unit	775.409714	Unit	TRUE	14.71	0.8	19.9
HEMO_HUMAN	NFPSPVDAAFR.light	FALSE	610.806562	Unit	579.288536	Unit	TRUE	14.71	0.8	19.9
HEP2_HUMAN	TLEAQLTPR.heavy	TRUE	519.794515	Unit	824.450012	Unit	TRUE	9.01	0.8	17
HEP2_HUMAN	TLEAQLTPR.heavy	TRUE	519.794515	Unit	695.407418	Unit	TRUE	9.01	0.8	17
HEP2_HUMAN	TLEAQLTPR.heavy	TRUE	519.794515	Unit	624.370305	Unit	TRUE	9.01	0.8	17
HEP2_HUMAN	TLEAQLTPR.light	FALSE	514.790381	Unit	814.441743	Unit	TRUE	9.01	0.8	17
HEP2_HUMAN	TLEAQLTPR.light	FALSE	514.790381	Unit	685.399149	Unit	TRUE	9.01	0.8	17
HEP2_HUMAN	TLEAQLTPR.light	FALSE	514.790381	Unit	614.362036	Unit	TRUE	9.01	0.8	17
HPT_HUMAN	VTSIQDWVQK.heavy	TRUE	606.329144	Unit	1011.53492	Unit	TRUE	12.21	0.8	19.7
HPT_HUMAN	VTSIQDWVQK.heavy	TRUE	606.329144	Unit	811.418828	Unit	TRUE	12.21	0.8	19.7
HPT_HUMAN	VTSIQDWVQK.heavy	TRUE	606.329144	Unit	683.36025	Unit	TRUE	12.21	0.8	19.7
HPT_HUMAN	VTSIQDWVQK.light	FALSE	602.322045	Unit	1003.520721	Unit	TRUE	12.21	0.8	19.7
HPT_HUMAN	VTSIQDWVQK.light	FALSE	602.322045	Unit	803.404629	Unit	TRUE	12.21	0.8	19.7
HPT_HUMAN	VTSIQDWVQK.light	FALSE	602.322045	Unit	675.346051	Unit	TRUE	12.21	0.8	19.7
HPTR_HUMAN	VGYVSGWGQSDNFK.heavy	TRUE	776.369529	Unit	1133.510162	Unit	TRUE	12.34	0.8	28
HPTR_HUMAN	VGYVSGWGQSDNFK.heavy	TRUE	776.369529	Unit	1046.478134	Unit	TRUE	12.34	0.8	28
HPTR_HUMAN	VGYVSGWGQSDNFK.heavy	TRUE	776.369529	Unit	320.160482	Unit	TRUE	12.34	0.8	28
HPTR_HUMAN	VGYVSGWGQSDNFK.light	FALSE	772.36243	Unit	1125.495963	Unit	TRUE	12.34	0.8	28
HPTR_HUMAN	VGYVSGWGQSDNFK.light	FALSE	772.36243	Unit	1038.463935	Unit	TRUE	12.34	0.8	28
HPTR_HUMAN	VGYVSGWGQSDNFK.light	FALSE	772.36243	Unit	320.160482	Unit	TRUE	12.34	0.8	28
HRG_HUMAN	GGEGTGYFVDFSVR.heavy	TRUE	750.85329	Unit	1099.54464	Unit	TRUE	16.07	0.8	24.1
HRG_HUMAN	GGEGTGYFVDFSVR.heavy	TRUE	750.85329	Unit	879.459848	Unit	TRUE	16.07	0.8	24.1
HRG_HUMAN	GGEGTGYFVDFSVR.heavy	TRUE	750.85329	Unit	633.32302	Unit	TRUE	16.07	0.8	24.1
HRG_HUMAN	GGEGTGYFVDFSVR.light	FALSE	745.849155	Unit	1089.536371	Unit	TRUE	16.07	0.8	24.1
HRG_HUMAN	GGEGTGYFVDFSVR.light	FALSE	745.849155	Unit	869.451579	Unit	TRUE	16.07	0.8	24.1
HRG_HUMAN	GGEGTGYFVDFSVR.light	FALSE	745.849155	Unit	623.314751	Unit	TRUE	16.07	0.8	24.1
IC1_HUMAN	GVTSVSQIFHSPDLAIR.heavy	TRUE	612.999581	Unit	790.426956	Unit	TRUE	16.84	0.8	19.8
IC1_HUMAN	GVTSVSQIFHSPDLAIR.heavy	TRUE	612.999581	Unit	781.444198	Unit	TRUE	16.84	0.8	19.8

IC1_HUMAN	GVTSVSQIFHSPDLAIR.heavy	TRUE	612.999581	Unit	697.376735	Unit	TRUE	16.84	0.8	19.8
IC1_HUMAN	GVTSVSQIFHSPDLAIR.light	FALSE	609.663492	Unit	785.422822	Unit	TRUE	16.84	0.8	19.8
IC1_HUMAN	GVTSVSQIFHSPDLAIR.light	FALSE	609.663492	Unit	771.435929	Unit	TRUE	16.84	0.8	19.8
IC1_HUMAN	GVTSVSQIFHSPDLAIR.light	FALSE	609.663492	Unit	692.3726	Unit	TRUE	16.84	0.8	19.8
IGHA1_HUMAN	DASGVTFTWTPSSGK.heavy	TRUE	774.874644	Unit	871.439957	Unit	TRUE	13.78	0.8	24.9
IGHA1_HUMAN	DASGVTFTWTPSSGK.heavy	TRUE	774.874644	Unit	584.312966	Unit	TRUE	13.78	0.8	24.9
IGHA1_HUMAN	DASGVTFTWTPSSGK.heavy	TRUE	774.874644	Unit	483.265287	Unit	TRUE	13.78	0.8	24.9
IGHA1_HUMAN	DASGVTFTWTPSSGK.light	FALSE	770.867545	Unit	863.425758	Unit	TRUE	13.78	0.8	24.9
IGHA1_HUMAN	DASGVTFTWTPSSGK.light	FALSE	770.867545	Unit	576.298767	Unit	TRUE	13.78	0.8	24.9
IGHA1_HUMAN	DASGVTFTWTPSSGK.light	FALSE	770.867545	Unit	475.251088	Unit	TRUE	13.78	0.8	24.9
IGHA2_HUMAN	DASGATFTWTPSSGK.heavy	TRUE	760.858994	Unit	1119.55605	Unit	TRUE	11.96	0.8	24.5
IGHA2_HUMAN	DASGATFTWTPSSGK.heavy	TRUE	760.858994	Unit	584.312966	Unit	TRUE	11.96	0.8	24.5
IGHA2_HUMAN	DASGATFTWTPSSGK.heavy	TRUE	760.858994	Unit	483.265287	Unit	TRUE	11.96	0.8	24.5
IGHA2_HUMAN	DASGATFTWTPSSGK.light	FALSE	756.851895	Unit	1111.541851	Unit	TRUE	11.96	0.8	24.5
IGHA2_HUMAN	DASGATFTWTPSSGK.light	FALSE	756.851895	Unit	576.298767	Unit	TRUE	11.96	0.8	24.5
IGHA2_HUMAN	DASGATFTWTPSSGK.light	FALSE	756.851895	Unit	475.251088	Unit	TRUE	11.96	0.8	24.5
IGHG1_HUMAN	GPSVFPLAPSSK.heavy	TRUE	597.834063	Unit	854.486179	Unit	TRUE	13.84	0.8	19.4
IGHG1_HUMAN	GPSVFPLAPSSK.heavy	TRUE	597.834063	Unit	707.417765	Unit	TRUE	13.84	0.8	19.4
IGHG1_HUMAN	GPSVFPLAPSSK.heavy	TRUE	597.834063	Unit	426.243823	Unit	TRUE	13.84	0.8	19.4
IGHG1_HUMAN	GPSVFPLAPSSK.light	FALSE	593.826963	Unit	846.47198	Unit	TRUE	13.84	0.8	19.4
IGHG1_HUMAN	GPSVFPLAPSSK.light	FALSE	593.826963	Unit	699.403566	Unit	TRUE	13.84	0.8	19.4
IGHG1_HUMAN	GPSVFPLAPSSK.light	FALSE	593.826963	Unit	418.229624	Unit	TRUE	13.84	0.8	19.4
IGHG2_HUMAN	GLPAPIEK.heavy	TRUE	416.754553	Unit	662.396301	Unit	TRUE	8.69	0.8	13.8
IGHG2_HUMAN	GLPAPIEK.heavy	TRUE	416.754553	Unit	565.343538	Unit	TRUE	8.69	0.8	13.8
IGHG2_HUMAN	GLPAPIEK.heavy	TRUE	416.754553	Unit	494.306424	Unit	TRUE	8.69	0.8	13.8
IGHG2_HUMAN	GLPAPIEK.light	FALSE	412.747453	Unit	654.382102	Unit	TRUE	8.69	0.8	13.8
IGHG2_HUMAN	GLPAPIEK.light	FALSE	412.747453	Unit	557.329339	Unit	TRUE	8.69	0.8	13.8
IGHG2_HUMAN	GLPAPIEK.light	FALSE	412.747453	Unit	486.292225	Unit	TRUE	8.69	0.8	13.8
IGHG3_HUMAN	WYVDGVEVHNAK.heavy	TRUE	475.57313	Unit	976.493784	Unit	TRUE	10.24	0.8	18
IGHG3_HUMAN	WYVDGVEVHNAK.heavy	TRUE	475.57313	Unit	861.466841	Unit	TRUE	10.24	0.8	18
IGHG3_HUMAN	WYVDGVEVHNAK.heavy	TRUE	475.57313	Unit	804.445377	Unit	TRUE	10.24	0.8	18
IGHG3_HUMAN	WYVDGVEVHNAK.light	FALSE	472.901731	Unit	968.479585	Unit	TRUE	10.24	0.8	18
IGHG3_HUMAN	WYVDGVEVHNAK.light	FALSE	472.901731	Unit	853.452642	Unit	TRUE	10.24	0.8	18
IGHG3_HUMAN	WYVDGVEVHNAK.light	FALSE	472.901731	Unit	796.431178	Unit	TRUE	10.24	0.8	18
IGHG4_HUMAN	TTPPVLDSDGSFFLYSR.heavy	TRUE	956.471758	Unit	1416.66694	Unit	TRUE	18.68	0.8	30.5
IGHG4_HUMAN	TTPPVLDSDGSFFLYSR.heavy	TRUE	956.471758	Unit	1303.582876	Unit	TRUE	18.68	0.8	30.5
IGHG4_HUMAN	TTPPVLDSDGSFFLYSR.heavy	TRUE	956.471758	Unit	1188.555933	Unit	TRUE	18.68	0.8	30.5
IGHG4_HUMAN	TTPPVLDSDGSFFLYSR.light	FALSE	951.467623	Unit	1406.658671	Unit	TRUE	18.68	0.8	30.5
IGHG4_HUMAN	TTPPVLDSDGSFFLYSR.light	FALSE	951.467623	Unit	1293.574607	Unit	TRUE	18.68	0.8	30.5
IGHG4_HUMAN	TTPPVLDSDGSFFLYSR.light	FALSE	951.467623	Unit	1178.547664	Unit	TRUE	18.68	0.8	30.5
IGHM_HUMAN	QVGSGVTTDQVQAEAK.heavy	TRUE	813.414665	Unit	1398.695062	Unit	TRUE	6.18	0.8	26.1
IGHM_HUMAN	QVGSGVTTDQVQAEAK.heavy	TRUE	813.414665	Unit	1098.551693	Unit	TRUE	6.18	0.8	26.1
IGHM_HUMAN	QVGSGVTTDQVQAEAK.heavy	TRUE	813.414665	Unit	997.504014	Unit	TRUE	6.18	0.8	26.1
IGHM_HUMAN	QVGSGVTTDQVQAEAK.light	FALSE	809.407565	Unit	1390.680863	Unit	TRUE	6.18	0.8	26.1
IGHM_HUMAN	QVGSGVTTDQVQAEAK.light	FALSE	809.407565	Unit	1090.537494	Unit	TRUE	6.18	0.8	26.1
IGHM_HUMAN	QVGSGVTTDQVQAEAK.light	FALSE	809.407565	Unit	989.489815	Unit	TRUE	6.18	0.8	26.1
IGJ_HUMAN	SSEDPNEDIVER.heavy	TRUE	700.314194	Unit	981.487519	Unit	TRUE	6.15	0.8	22.6
IGJ_HUMAN	SSEDPNEDIVER.heavy	TRUE	700.314194	Unit	641.349235	Unit	TRUE	6.15	0.8	22.6
IGJ_HUMAN	SSEDPNEDIVER.heavy	TRUE	700.314194	Unit	491.247398	Unit	TRUE	6.15	0.8	22.6
IGJ_HUMAN	SSEDPNEDIVER.light	FALSE	695.31006	Unit	971.47925	Unit	TRUE	6.15	0.8	22.6
IGJ_HUMAN	SSEDPNEDIVER.light	FALSE	695.31006	Unit	631.340966	Unit	TRUE	6.15	0.8	22.6
IGJ_HUMAN	SSEDPNEDIVER.light	FALSE	695.31006	Unit	486.243263	Unit	TRUE	6.15	0.8	22.6
ITIH1_HUMAN	AAISGENAGLVR.heavy	TRUE	584.321428	Unit	912.477289	Unit	TRUE	7.91	0.8	19
ITIH1_HUMAN	AAISGENAGLVR.heavy	TRUE	584.321428	Unit	825.445261	Unit	TRUE	7.91	0.8	19
ITIH1_HUMAN	AAISGENAGLVR.heavy	TRUE	584.321428	Unit	639.381204	Unit	TRUE	7.91	0.8	19
ITIH1_HUMAN	AAISGENAGLVR.light	FALSE	579.317294	Unit	902.46902	Unit	TRUE	7.91	0.8	19
ITIH1_HUMAN	AAISGENAGLVR.light	FALSE	579.317294	Unit	815.436992	Unit	TRUE	7.91	0.8	19
ITIH1_HUMAN	AAISGENAGLVR.light	FALSE	579.317294	Unit	629.372935	Unit	TRUE	7.91	0.8	19
ITIH2_HUMAN	IQPSGGTNINEALLR.heavy	TRUE	796.935145	Unit	1351.720373	Unit	TRUE	12.33	0.8	25.5
ITIH2_HUMAN	IQPSGGTNINEALLR.heavy	TRUE	796.935145	Unit	725.417983	Unit	TRUE	12.33	0.8	25.5
ITIH2_HUMAN	IQPSGGTNINEALLR.heavy	TRUE	796.935145	Unit	676.363824	Unit	TRUE	12.33	0.8	25.5
ITIH2_HUMAN	IQPSGGTNINEALLR.light	FALSE	791.931011	Unit	1341.712104	Unit	TRUE	12.33	0.8	25.5
ITIH2_HUMAN	IQPSGGTNINEALLR.light	FALSE	791.931011	Unit	715.409714	Unit	TRUE	12.33	0.8	25.5
ITIH2_HUMAN	IQPSGGTNINEALLR.light	FALSE	791.931011	Unit	671.35969	Unit	TRUE	12.33	0.8	25.5
ITIH4_HUMAN	LGVYELLLK.heavy	TRUE	528.333167	Unit	942.574994	Unit	TRUE	19.1	0.8	17.3
ITIH4_HUMAN	LGVYELLLK.heavy	TRUE	528.333167	Unit	786.485117	Unit	TRUE	19.1	0.8	17.3
ITIH4_HUMAN	LGVYELLLK.heavy	TRUE	528.333167	Unit	623.421788	Unit	TRUE	19.1	0.8	17.3
ITIH4_HUMAN	LGVYELLLK.light	FALSE	524.326068	Unit	934.560795	Unit	TRUE	19.1	0.8	17.3
ITIH4_HUMAN	LGVYELLLK.light	FALSE	524.326068	Unit	778.470918	Unit	TRUE	19.1	0.8	17.3
ITIH4_HUMAN	LGVYELLLK.light	FALSE	524.326068	Unit	615.407589	Unit	TRUE	19.1	0.8	17.3
KLKB1_HUMAN	IAYGTQGSSGYSLR.heavy	TRUE	735.366564	Unit	1122.541346	Unit	TRUE	8.84	0.8	23.6
KLKB1_HUMAN	IAYGTQGSSGYSLR.heavy	TRUE	735.366564	Unit	964.472204	Unit	TRUE	8.84	0.8	23.6
KLKB1_HUMAN	IAYGTQGSSGYSLR.heavy	TRUE	735.366564	Unit	836.413626	Unit	TRUE	8.84	0.8	23.6
KLKB1_HUMAN	IAYGTQGSSGYSLR.light	FALSE	730.36243	Unit	1112.533077	Unit	TRUE	8.84	0.8	23.6
KLKB1_HUMAN	IAYGTQGSSGYSLR.light	FALSE	730.36243	Unit	954.463935	Unit	TRUE	8.84	0.8	23.6
KLKB1_HUMAN	IAYGTQGSSGYSLR.light	FALSE	730.36243	Unit	826.405357	Unit	TRUE	8.84	0.8	23.6
KNG1_HUMAN	YFIDFVAR.heavy	TRUE	520.775594	Unit	730.41217	Unit	TRUE	16.9	0.8	17
KNG1_HUMAN	YFIDFVAR.heavy	TRUE	520.775594	Unit	617.328106	Unit	TRUE	16.9	0.8	17
KNG1_HUMAN	YFIDFVAR.heavy	TRUE	520.775594	Unit	502.301162	Unit	TRUE	16.9	0.8	17
KNG1_HUMAN	YFIDFVAR.light	FALSE	515.77146	Unit	720.403901	Unit	TRUE	16.9	0.8	17
KNG1_HUMAN	YFIDFVAR.light	FALSE	515.77146	Unit	607.319837	Unit	TRUE	16.9	0.8	17

KNG1_HUMAN	YFIDFVAR.light	FALSE	515.77146	Unit	492.292893	Unit	TRUE	16.9	0.8	17
MBL2_HUMAN	FQASVATPR.heavy	TRUE	493.7683	Unit	711.402333	Unit	TRUE	6.99	0.8	16.2
MBL2_HUMAN	FQASVATPR.heavy	TRUE	493.7683	Unit	640.365219	Unit	TRUE	6.99	0.8	16.2
MBL2_HUMAN	FQASVATPR.heavy	TRUE	493.7683	Unit	454.264777	Unit	TRUE	6.99	0.8	16.2
MBL2_HUMAN	FQASVATPR.light	FALSE	488.764166	Unit	701.394064	Unit	TRUE	6.99	0.8	16.2
MBL2_HUMAN	FQASVATPR.light	FALSE	488.764166	Unit	630.35695	Unit	TRUE	6.99	0.8	16.2
MBL2_HUMAN	FQASVATPR.light	FALSE	488.764166	Unit	444.256508	Unit	TRUE	6.99	0.8	16.2
PEDF_HUMAN	ELLDTVTAPQK.heavy	TRUE	611.842085	Unit	867.466172	Unit	TRUE	10.47	0.8	19.8
PEDF_HUMAN	ELLDTVTAPQK.heavy	TRUE	611.842085	Unit	552.323136	Unit	TRUE	10.47	0.8	19.8
PEDF_HUMAN	ELLDTVTAPQK.heavy	TRUE	611.842085	Unit	380.238344	Unit	TRUE	10.47	0.8	19.8
PEDF_HUMAN	ELLDTVTAPQK.light	FALSE	607.834985	Unit	859.451973	Unit	TRUE	10.47	0.8	19.8
PEDF_HUMAN	ELLDTVTAPQK.light	FALSE	607.834985	Unit	544.308937	Unit	TRUE	10.47	0.8	19.8
PEDF_HUMAN	ELLDTVTAPQK.light	FALSE	607.834985	Unit	372.224145	Unit	TRUE	10.47	0.8	19.8
PGRP2_HUMAN	AGLLRPDYALLGHR.heavy	TRUE	521.299414	Unit	745.926926	Unit	TRUE	13.19	0.8	17.1
PGRP2_HUMAN	AGLLRPDYALLGHR.heavy	TRUE	521.299414	Unit	605.375724	Unit	TRUE	13.19	0.8	17.1
PGRP2_HUMAN	AGLLRPDYALLGHR.heavy	TRUE	521.299414	Unit	492.29166	Unit	TRUE	13.19	0.8	17.1
PGRP2_HUMAN	AGLLRPDYALLGHR.light	FALSE	517.963324	Unit	740.922792	Unit	TRUE	13.19	0.8	16.9
PGRP2_HUMAN	AGLLRPDYALLGHR.light	FALSE	517.963324	Unit	595.367455	Unit	TRUE	13.19	0.8	16.9
PGRP2_HUMAN	AGLLRPDYALLGHR.light	FALSE	517.963324	Unit	482.283391	Unit	TRUE	13.19	0.8	16.9
PLF4_HUMAN	IC[+57.0]LDLQAPLYK.heavy	TRUE	671.369955	Unit	1068.617922	Unit	TRUE	16.57	0.8	21.7
PLF4_HUMAN	IC[+57.0]LDLQAPLYK.heavy	TRUE	671.369955	Unit	955.533858	Unit	TRUE	16.57	0.8	21.7
PLF4_HUMAN	IC[+57.0]LDLQAPLYK.heavy	TRUE	671.369955	Unit	528.327159	Unit	TRUE	16.57	0.8	21.7
PLF4_HUMAN	IC[+57.0]LDLQAPLYK.light	FALSE	667.362856	Unit	1060.603723	Unit	TRUE	16.57	0.8	21.7
PLF4_HUMAN	IC[+57.0]LDLQAPLYK.light	FALSE	667.362856	Unit	947.519659	Unit	TRUE	16.57	0.8	21.7
PLF4_HUMAN	IC[+57.0]LDLQAPLYK.light	FALSE	667.362856	Unit	520.31296	Unit	TRUE	16.57	0.8	21.7
PLMN_HUMAN	HSIFTPETNPR.heavy	TRUE	654.83216	Unit	1171.598133	Unit	TRUE	7.97	0.8	21.1
PLMN_HUMAN	HSIFTPETNPR.heavy	TRUE	654.83216	Unit	1084.566104	Unit	TRUE	7.97	0.8	21.1
PLMN_HUMAN	HSIFTPETNPR.heavy	TRUE	654.83216	Unit	971.48204	Unit	TRUE	7.97	0.8	21.1
PLMN_HUMAN	HSIFTPETNPR.light	FALSE	649.828026	Unit	1161.589864	Unit	TRUE	7.97	0.8	21.1
PLMN_HUMAN	HSIFTPETNPR.light	FALSE	649.828026	Unit	1074.557835	Unit	TRUE	7.97	0.8	21.1
PLMN_HUMAN	HSIFTPETNPR.light	FALSE	649.828026	Unit	961.473771	Unit	TRUE	7.97	0.8	21.1
PON1_HUMAN	LLIGTVFHK.heavy	TRUE	518.325676	Unit	922.560013	Unit	TRUE	15.45	0.8	16.9
PON1_HUMAN	LLIGTVFHK.heavy	TRUE	518.325676	Unit	639.370421	Unit	TRUE	15.45	0.8	16.9
PON1_HUMAN	LLIGTVFHK.heavy	TRUE	518.325676	Unit	439.254329	Unit	TRUE	15.45	0.8	16.9
PON1_HUMAN	LLIGTVFHK.light	FALSE	514.318577	Unit	914.545814	Unit	TRUE	15.45	0.8	16.9
PON1_HUMAN	LLIGTVFHK.light	FALSE	514.318577	Unit	631.356222	Unit	TRUE	15.45	0.8	16.9
PON1_HUMAN	LLIGTVFHK.light	FALSE	514.318577	Unit	431.24013	Unit	TRUE	15.45	0.8	16.9
RET4_HUMAN	FSGTWYAMAK.heavy	TRUE	585.280609	Unit	1022.485527	Unit	TRUE	13.22	0.8	19
RET4_HUMAN	FSGTWYAMAK.heavy	TRUE	585.280609	Unit	935.453499	Unit	TRUE	13.22	0.8	19
RET4_HUMAN	FSGTWYAMAK.heavy	TRUE	585.280609	Unit	591.305044	Unit	TRUE	13.22	0.8	19
RET4_HUMAN	FSGTWYAMAK.light	FALSE	581.273509	Unit	1014.471328	Unit	TRUE	13.22	0.8	19
RET4_HUMAN	FSGTWYAMAK.light	FALSE	581.273509	Unit	927.4393	Unit	TRUE	13.22	0.8	19
RET4_HUMAN	FSGTWYAMAK.light	FALSE	581.273509	Unit	583.290845	Unit	TRUE	13.22	0.8	19
SAA4_HUMAN	EALQGVGDMGR.heavy	TRUE	571.778539	Unit	829.386031	Unit	TRUE	8.37	0.8	18.6
SAA4_HUMAN	EALQGVGDMGR.heavy	TRUE	571.778539	Unit	701.327454	Unit	TRUE	8.37	0.8	18.6
SAA4_HUMAN	EALQGVGDMGR.heavy	TRUE	571.778539	Unit	545.237576	Unit	TRUE	8.37	0.8	18.6
SAA4_HUMAN	EALQGVGDMGR.light	FALSE	566.774405	Unit	819.377762	Unit	TRUE	8.37	0.8	18.6
SAA4_HUMAN	EALQGVGDMGR.light	FALSE	566.774405	Unit	691.319185	Unit	TRUE	8.37	0.8	18.6
SAA4_HUMAN	EALQGVGDMGR.light	FALSE	566.774405	Unit	535.229307	Unit	TRUE	8.37	0.8	18.6
SEPP1_HUMAN	LPTDSELAPR.heavy	TRUE	554.797255	Unit	995.503169	Unit	TRUE	8.64	0.8	18
SEPP1_HUMAN	LPTDSELAPR.heavy	TRUE	554.797255	Unit	898.450406	Unit	TRUE	8.64	0.8	18
SEPP1_HUMAN	LPTDSELAPR.heavy	TRUE	554.797255	Unit	682.375784	Unit	TRUE	8.64	0.8	18
SEPP1_HUMAN	LPTDSELAPR.light	FALSE	549.79312	Unit	985.4949	Unit	TRUE	8.64	0.8	18
SEPP1_HUMAN	LPTDSELAPR.light	FALSE	549.79312	Unit	888.442137	Unit	TRUE	8.64	0.8	18
SEPP1_HUMAN	LPTDSELAPR.light	FALSE	549.79312	Unit	672.367515	Unit	TRUE	8.64	0.8	18
SHBG_HUMAN	IALGGLLFPASNLR.heavy	TRUE	726.434053	Unit	927.528596	Unit	TRUE	19.97	0.8	23.4
SHBG_HUMAN	IALGGLLFPASNLR.heavy	TRUE	726.434053	Unit	814.444532	Unit	TRUE	19.97	0.8	23.4
SHBG_HUMAN	IALGGLLFPASNLR.heavy	TRUE	726.434053	Unit	667.376118	Unit	TRUE	19.97	0.8	23.4
SHBG_HUMAN	IALGGLLFPASNLR.light	FALSE	721.429918	Unit	917.520327	Unit	TRUE	19.97	0.8	23.4
SHBG_HUMAN	IALGGLLFPASNLR.light	FALSE	721.429918	Unit	804.436263	Unit	TRUE	19.97	0.8	23.4
SHBG_HUMAN	IALGGLLFPASNLR.light	FALSE	721.429918	Unit	657.367849	Unit	TRUE	19.97	0.8	23.4
STOM_HUMAN	YLQTLTTIAAEK.heavy	TRUE	680.384117	Unit	955.554987	Unit	TRUE	13.15	0.8	22
STOM_HUMAN	YLQTLTTIAAEK.heavy	TRUE	680.384117	Unit	854.507309	Unit	TRUE	13.15	0.8	22
STOM_HUMAN	YLQTLTTIAAEK.heavy	TRUE	680.384117	Unit	741.423245	Unit	TRUE	13.15	0.8	22
STOM_HUMAN	YLQTLTTIAAEK.light	FALSE	676.377017	Unit	947.540788	Unit	TRUE	13.15	0.8	22
STOM_HUMAN	YLQTLTTIAAEK.light	FALSE	676.377017	Unit	846.49311	Unit	TRUE	13.15	0.8	22
STOM_HUMAN	YLQTLTTIAAEK.light	FALSE	676.377017	Unit	733.409046	Unit	TRUE	13.15	0.8	22
TETN_HUMAN	LDTLAQEVALLK.heavy	TRUE	661.394484	Unit	879.538943	Unit	TRUE	18.06	0.8	21.4
TETN_HUMAN	LDTLAQEVALLK.heavy	TRUE	661.394484	Unit	808.501829	Unit	TRUE	18.06	0.8	21.4
TETN_HUMAN	LDTLAQEVALLK.heavy	TRUE	661.394484	Unit	330.165962	Unit	TRUE	18.06	0.8	21.4
TETN_HUMAN	LDTLAQEVALLK.light	FALSE	657.387385	Unit	871.524744	Unit	TRUE	18.06	0.8	21.4
TETN_HUMAN	LDTLAQEVALLK.light	FALSE	657.387385	Unit	800.48763	Unit	TRUE	18.06	0.8	21.4
TETN_HUMAN	LDTLAQEVALLK.light	FALSE	657.387385	Unit	330.165962	Unit	TRUE	18.06	0.8	21.4
THBG_HUMAN	NALALFVLPK.heavy	TRUE	547.346609	Unit	908.6059	Unit	TRUE	19.92	0.8	17.8
THBG_HUMAN	NALALFVLPK.heavy	TRUE	547.346609	Unit	795.521836	Unit	TRUE	19.92	0.8	17.8
THBG_HUMAN	NALALFVLPK.heavy	TRUE	547.346609	Unit	724.484723	Unit	TRUE	19.92	0.8	17.8
THBG_HUMAN	NALALFVLPK.light	FALSE	543.339509	Unit	900.591701	Unit	TRUE	19.92	0.8	17.8
THBG_HUMAN	NALALFVLPK.light	FALSE	543.339509	Unit	787.507637	Unit	TRUE	19.92	0.8	17.8
THBG_HUMAN	NALALFVLPK.light	FALSE	543.339509	Unit	716.470524	Unit	TRUE	19.92	0.8	17.8
THRB_HUMAN	TATSEYQTFFNPR.heavy	TRUE	786.371846	Unit	1082.529325	Unit	TRUE	13.72	0.8	25.2
THRB_HUMAN	TATSEYQTFFNPR.heavy	TRUE	786.371846	Unit	919.465996	Unit	TRUE	13.72	0.8	25.2

THRB_HUMAN	TATSEYQTFFNPR.heavy	TRUE	786.371846	Unit	282.18	Unit	TRUE	13.72	0.8	25.2
THRB_HUMAN	TATSEYQTFFNPR.light	FALSE	781.367712	Unit	1072.521056	Unit	TRUE	13.72	0.8	25.2
THRB_HUMAN	TATSEYQTFFNPR.light	FALSE	781.367712	Unit	909.457727	Unit	TRUE	13.72	0.8	25.2
THRB_HUMAN	TATSEYQTFFNPR.light	FALSE	781.367712	Unit	272.1717	Unit	TRUE	13.72	0.8	25.2
TotalIGHG	DTLMISR.heavy	TRUE	423.22488	Unit	629.367862	Unit	TRUE	8.74	0.8	14
TotalIGHG	DTLMISR.heavy	TRUE	423.22488	Unit	516.283798	Unit	TRUE	8.74	0.8	14
TotalIGHG	DTLMISR.heavy	TRUE	423.22488	Unit	385.243313	Unit	TRUE	8.74	0.8	14
TotalIGHG	DTLMISR.light	FALSE	418.220745	Unit	619.359593	Unit	TRUE	8.74	0.8	14
TotalIGHG	DTLMISR.light	FALSE	418.220745	Unit	506.275529	Unit	TRUE	8.74	0.8	14
TotalIGHG	DTLMISR.light	FALSE	418.220745	Unit	375.235044	Unit	TRUE	8.74	0.8	14
TRFE_HUMAN	EGYYGYTGAFR.heavy	TRUE	647.292337	Unit	944.450012	Unit	TRUE	11.41	0.8	20.9
TRFE_HUMAN	EGYYGYTGAFR.heavy	TRUE	647.292337	Unit	781.386683	Unit	TRUE	11.41	0.8	20.9
TRFE_HUMAN	EGYYGYTGAFR.heavy	TRUE	647.292337	Unit	561.301891	Unit	TRUE	11.41	0.8	20.9
TRFE_HUMAN	EGYYGYTGAFR.light	FALSE	642.288202	Unit	934.441743	Unit	TRUE	11.41	0.8	20.9
TRFE_HUMAN	EGYYGYTGAFR.light	FALSE	642.288202	Unit	771.378414	Unit	TRUE	11.41	0.8	20.9
TRFE_HUMAN	EGYYGYTGAFR.light	FALSE	642.288202	Unit	551.293622	Unit	TRUE	11.41	0.8	20.9
TTHY_HUMAN	GSPAINVAVHVFR.heavy	TRUE	459.593939	Unit	738.428488	Unit	TRUE	14.1	0.8	20
TTHY_HUMAN	GSPAINVAVHVFR.heavy	TRUE	459.593939	Unit	568.322961	Unit	TRUE	14.1	0.8	20
TTHY_HUMAN	GSPAINVAVHVFR.heavy	TRUE	459.593939	Unit	284.665118	Unit	TRUE	14.1	0.8	20
TTHY_HUMAN	GSPAINVAVHVFR.light	FALSE	456.257849	Unit	728.420219	Unit	TRUE	14.1	0.8	20
TTHY_HUMAN	GSPAINVAVHVFR.light	FALSE	456.257849	Unit	558.314692	Unit	TRUE	14.1	0.8	20
TTHY_HUMAN	GSPAINVAVHVFR.light	FALSE	456.257849	Unit	279.660984	Unit	TRUE	14.1	0.8	20
VTDB_HUMAN	HLSLLTTLSNR.heavy	TRUE	632.866003	Unit	1127.665818	Unit	TRUE	13.38	0.8	20.5
VTDB_HUMAN	HLSLLTTLSNR.heavy	TRUE	632.866003	Unit	1014.581754	Unit	TRUE	13.38	0.8	20.5
VTDB_HUMAN	HLSLLTTLSNR.heavy	TRUE	632.866003	Unit	701.381598	Unit	TRUE	13.38	0.8	20.5
VTDB_HUMAN	HLSLLTTLSNR.light	FALSE	627.861869	Unit	1117.657549	Unit	TRUE	13.38	0.8	20.5
VTDB_HUMAN	HLSLLTTLSNR.light	FALSE	627.861869	Unit	1004.573485	Unit	TRUE	13.38	0.8	20.5
VTDB_HUMAN	HLSLLTTLSNR.light	FALSE	627.861869	Unit	691.373329	Unit	TRUE	13.38	0.8	20.5
VTNC_HUMAN	FEDGVLDPDYPR.heavy	TRUE	716.834566	Unit	885.434027	Unit	TRUE	12.74	0.8	23.1
VTNC_HUMAN	FEDGVLDPDYPR.heavy	TRUE	716.834566	Unit	772.349963	Unit	TRUE	12.74	0.8	23.1
VTNC_HUMAN	FEDGVLDPDYPR.heavy	TRUE	716.834566	Unit	657.32302	Unit	TRUE	12.74	0.8	23.1
VTNC_HUMAN	FEDGVLDPDYPR.light	FALSE	711.830431	Unit	875.425758	Unit	TRUE	12.74	0.8	23.1
VTNC_HUMAN	FEDGVLDPDYPR.light	FALSE	711.830431	Unit	762.341694	Unit	TRUE	12.74	0.8	23.1
VTNC_HUMAN	FEDGVLDPDYPR.light	FALSE	711.830431	Unit	647.314751	Unit	TRUE	12.74	0.8	23.1
ZA2G_HUMAN	AYLEEEC[+57.0]PATLR.heavy	TRUE	731.349526	Unit	1114.507269	Unit	TRUE	10.24	0.8	23.5
ZA2G_HUMAN	AYLEEEC[+57.0]PATLR.heavy	TRUE	731.349526	Unit	985.464676	Unit	TRUE	10.24	0.8	23.5
ZA2G_HUMAN	AYLEEEC[+57.0]PATLR.heavy	TRUE	731.349526	Unit	567.348841	Unit	TRUE	10.24	0.8	23.5
ZA2G_HUMAN	AYLEEEC[+57.0]PATLR.light	FALSE	726.345391	Unit	1104.499	Unit	TRUE	10.24	0.8	23.5
ZA2G_HUMAN	AYLEEEC[+57.0]PATLR.light	FALSE	726.345391	Unit	975.456407	Unit	TRUE	10.24	0.8	23.5
ZA2G_HUMAN	AYLEEEC[+57.0]PATLR.light	FALSE	726.345391	Unit	557.340572	Unit	TRUE	10.24	0.8	23.5

Other settings: Fragmentor: 380; Cell accelerator voltage: 4; Polarity: positive; Peptides highlighted in grey are not part of the final PlasmaDive kit (Biognosys, CH)

SUPPLEMENTAL TABLE 3:

				Nanoflow in human plasma digest				Standard flow in human plasma digest				Standard flow in LC solution	
UniProt Entry Name	UniProt ID	Protein Name	Peptide	LOD (ug/mL)	LOQ (ug/mL)	Linear_Range_Start (ug/mL)	Linear_Range_End (ug/mL)	LOD (ug/mL)	LOQ (ug/mL)	Linear_Range_Start (ug/mL)	Linear_Range_End (ug/mL)	LOD (ug/mL)	LOQ (ug/mL)
A1AG1_HUMAN	P02763	Alpha-1-acid glycoprotein 1 (Orosomucoid-1)	SDVVYTDWK	0.226	0.543	1.566	156.610	0.602	1.650	15.661	156.610	0.048	0.134
A1AG2_HUMAN	P19652	Alpha-1-acid glycoprotein 2 (Orosomucoid-2)	EHVAHLLFLR	0.741	1.652	4.363	436.274	2.843	7.752	43.627	436.274	0.034	0.078
A1AT_HUMAN	P01009	Alpha-1-antitrypsin	SVLGQLGITK	0.106	0.259	1.472	147.163	0.081	0.203	1.472	147.163	0.162	0.380
A1BG_HUMAN	P04217	Alpha-1B-glycoprotein	LLELTGPK	0.229	0.439	0.679	67.865	0.356	0.746	6.786	67.865	0.035	0.054
A2AP_HUMAN	P08697	Alpha-2-antiplasmin (Serpin F2)	LFGPDLK	0.185	0.406	1.171	117.108	0.368	0.899	1.171	117.108	0.070	0.149
A2GL_HUMAN	P02750	Leucine-rich alpha-2-glycoprotein (LRG)	VAAGAFQGLR	0.127	0.300	1.022	102.199	0.099	0.233	1.022	102.199	0.067	0.175
A2MG_HUMAN	P01023	Alpha-2-macroglobulin (Alpha-2-M)	AIGYLNTGYQR	0.858	2.300	12.699	1269.924	0.631	1.843	12.699	1269.924	0.781	1.893
AACT_HUMAN	P01011	Alpha-1-antichymotrypsin (ACT)	EIGELYLPK	0.350	0.774	2.672	267.158	0.111	0.284	2.672	267.158	0.114	0.244
AFAM_HUMAN	P43652	Afamin (Alpha-albumin)	AESPEVCFNEESPK	0.416	1.139	2.262	2261.951	0.940	2.544	22.620	2261.951	2.844	7.608
ALBU_HUMAN	P02768	Serum albumin	YLYEIAR	0.527	0.912	1.111	111.100	0.148	0.363	1.111	111.100	0.122	0.323
AMBP_HUMAN	P02760	Protein AMBP	TVAACNLPIVR	0.061	0.132	0.167	166.982	0.054	0.144	1.670	166.982	0.138	0.356
ANGT_HUMAN	P01019	Angiotensinogen (Serpin A8)	ALQDQLVLVAAK	NA	NA	NA	NA	0.167	0.406	0.646	646.418	0.395	0.712
ANT3_HUMAN	P01008	Antithrombin-III (Serpin C1)	EVPLNTIIFMGR	0.330	0.801	2.750	275.008	0.947	2.347	27.501	275.008	0.009	0.023
APOA_HUMAN	P08519	Apolipoprotein(a)	GTYSTTVTGR	8.153	18.704	53.125	5312.484	5.898	10.244	53.125	5312.484	2.980	4.998
APOA1_HUMAN	P02647	Apolipoprotein A-I	VSFLSALEEYTK	0.055	0.122	0.166	166.494	0.190	0.394	1.665	166.494	0.045	0.125
APOA2_HUMAN	P02652	Apolipoprotein A-II	EQLTPLIK	0.039	0.059	0.092	9.232	0.106	0.215	0.923	9.232	0.005	0.016
APOA4_HUMAN	P06727	Apolipoprotein A-IV	LAPLAEDVR	1.164	2.183	1.938	193.807	0.072	0.167	1.938	193.807	0.131	0.317
APOB_HUMAN	P04114	Apolipoprotein B-100	FSVPAGIVIPSFQALTAR	0.571	1.079	0.304	3038.832	9.813	22.779	303.883	3038.832	NA	NA
APOC1_HUMAN	P02654	Apolipoprotein C-I	EFGNTLEDK	2.346	5.613	10.646	106.461	0.123	0.229	1.065	106.461	0.163	0.401
APOC2_HUMAN	P02655	Apolipoprotein C-II	TAAQNLYEK	0.128	0.217	0.782	78.181	0.032	0.072	0.078	78.181	0.034	0.045
APOC3_HUMAN	P02656	Apolipoprotein C-III	GWVTDGFSSLK	0.540	1.064	0.855	85.466	0.061	0.153	0.855	85.466	0.007	0.017
APOD_HUMAN	P05090	Apolipoprotein D	NILTSNNIDVK	0.140	0.385	2.334	233.369	0.035	0.090	0.233	233.369	0.161	0.338
APOE_HUMAN	P02649	Apolipoprotein E	AATVGSLAGQPLQER	0.056	0.121	0.236	236.096	0.254	0.701	2.361	236.096	0.470	1.253
APOH_HUMAN	P02749	Apolipoprotein H	VCPFAGILENGAVR	0.043	0.112	0.332	332.212	0.241	0.552	3.322	332.212	0.348	0.867
APOL1_HUMAN	O14791	Apolipoprotein L1	VTEPISAESGEQVER	0.297	0.763	0.939	938.894	1.532	4.132	9.389	938.894	1.070	2.377
APOM_HUMAN	O95445	Apolipoprotein M	FLLYNR	0.031	0.058	0.294	29.369	0.036	0.090	0.294	29.369	0.045	0.127
BTD_HUMAN	P43251	Biotinidase	SHLIIAQVAK	0.361	0.720	2.392	239.183	0.711	1.515	2.392	239.183	0.530	1.496
C1QA_HUMAN	P02745	Complement C1q subcomponent subunit A	SLGFCDTTNK	0.334	0.714	1.198	119.795	0.100	0.160	1.198	119.795	0.200	0.508
C1QB_HUMAN	P02746	Complement C1q subcomponent subunit B	GNLCVNLMR	0.180	0.452	1.130	113.040	0.119	0.350	1.130	113.040	0.003	0.006
C1QC_HUMAN	P02747	Complement C1q subcomponent subunit C	FQSVFTVTR	0.212	0.380	0.429	42.854	0.098	0.240	0.429	42.854	0.063	0.162
C1R_HUMAN	P00736	Complement C1r subcomponent	GLTLHLK	2.783	4.691	28.483	284.834	0.897	2.135	2.848	284.834	0.607	1.651
C1S_HUMAN	P09871	Complement C1s subcomponent	TNFDNDIALVR	3.019	5.337	6.390	638.983	3.439	8.845	63.898	638.983	0.942	2.448
C4BPA_HUMAN	P04003	C4b-binding protein alpha chain	GYILVGQAK	0.567	1.228	4.468	446.815	0.316	0.744	4.468	446.815	0.185	0.417
CBG_HUMAN	P08185	Corticosteroid-binding globulin (Serpin A6)	GTWTQPFDLASTR	0.303	0.586	2.004	200.422	1.903	3.655	20.042	200.422	0.041	0.107
CD5L_HUMAN	O43866	CD5 antigen-like (CT-2) (SP-alpha)	IWLDNVR	0.162	0.397	0.450	45.012	0.253	0.494	4.501	45.012	0.015	0.043
CERU_HUMAN	P00450	Ceruloplasmin (Ferroxidase)	DIASGLIGPLIICK	0.367	0.678	0.903	903.245	0.740	1.712	9.032	903.245	0.262	0.598
CFAB_HUMAN	P00751	Complement factor B	YGLVTYATYPK	0.557	1.317	0.312	311.592	0.404	0.987	3.116	311.592	0.198	0.476
CFAH_HUMAN	P08603	Complement factor H (H factor 1)	IDVHLVPDR	5.867	10.403	13.508	1350.785	1.549	4.380	13.508	1350.785	0.584	1.491
CFAI_HUMAN	P05156	Complement factor I	IVIEYVDR	0.499	1.303	1.365	136.496	0.363	0.707	1.365	136.496	0.111	0.259
CHLE_HUMAN	P06276	Cholinesterase (EC 3.1.1.8)	IFFPGVSEFGK	1.653	2.196	2.050	205.002	1.376	3.420	20.500	205.002	0.365	0.854
CLUS_HUMAN	P10909	Clusterin (Aging-associated gene 4 protein) (Apolipoprotein J)	ASSIIDELFQDR	0.114	0.246	0.368	367.879	0.272	0.547	3.679	367.879	0.267	0.665
CO2_HUMAN	P06681	Complement C2	AVISPGFDVFAK	0.147	0.297	0.368	368.034	0.147	0.384	3.680	368.034	0.214	0.446
CO3_HUMAN	P01024	Complement C3	GYTQQLAFR	0.843	2.104	7.444	744.370	1.398	3.309	7.444	744.370	0.721	2.019
CO4A_HUMAN	P0C0L4	Complement C4-A	PVAFSVVPTAAAAVSLK	1.384	3.471	1.859	1859.068	1.034	2.376	18.591	1859.068	1.797	4.367
CO5_HUMAN	P01031	Complement C5	TDAPDLPEENQAR	0.771	1.993	9.195	919.542	0.749	1.853	9.195	919.542	1.135	2.997
CO8A_HUMAN	P07357	Complement component C8 alpha chain	HTSLGPLEAK	1.395	3.339	5.993	599.335	4.545	8.725	59.934	599.335	0.433	1.281
CO9_HUMAN	P02748	Complement component C9	LSPIYNLVPVK	0.342	0.667	1.760	176.048	0.166	0.378	1.760	176.048	0.161	0.327
CXCL7_HUMAN	P02775	Platelet basic protein (C-X-C motif chemokine 7)	NIQSLEVIGK	0.362	0.677	1.525	152.528	0.298	0.760	1.525	152.528	0.228	0.576
F13A_HUMAN	P00488	Coagulation factor XIII A chain	STVLTIPEIIIK	0.470	0.919	0.475	474.596	0.199	0.375	4.746	474.596	0.235	0.399
F13B_HUMAN	P05160	Coagulation factor XIII B chain	IAQYYYTFK	0.965	2.222	6.941	694.134	0.423	1.144	6.941	694.134	2.524	6.469
FA10_HUMAN	P00742	Coagulation factor X	ACIPTGPYPCGK	0.136	0.324	0.326	326.053	0.120	0.291	3.261	326.053	0.352	0.788
FA9_HUMAN	P00740	Coagulation factor IX	SALVLQYLR	0.031	0.078	0.107	106.734	0.127	0.296	1.067	106.734	0.074	0.120
FBLN1_HUMAN	P23142	Fibulin-1	TGYYFDGISR	0.636	1.614	3.227	322.717	0.297	0.773	3.227	322.717	0.005	0.012
FETUA_HUMAN	P02765	Alpha-2-HS-glycoprotein	FSVVYAK	0.129	0.243	0.016	163.393	0.096	0.208	1.634	163.393	0.169	0.375
FETUB_HUMAN	Q9UGM5	Fetuin-B	LVVLPFPK	0.022	0.056	0.533	53.284	0.013	0.032	0.053	53.284	0.027	0.048
FIBA_HUMAN	P02671	Fibrinogen alpha chain	GSESGIFTNTK	1.015	2.280	3.973	397.331	0.408	0.691	3.973	397.331	0.445	1.078
FIBG_HUMAN	P02679	Fibrinogen gamma chain	DNCCILDER	1.127	1.741	0.979	978.581	0.544	1.354	9.786	978.581	2.540	6.830
FINC_HUMAN	P02751	Fibronectin (FN)	SYTITGLQPGTDYK	1.356	3.728	25.602	2560.181	2.126	4.997	25.602	2560.181	1.948	4.584
GELS_HUMAN	P06396	Gelsolin (Actin-depolymerizing factor)	AGALNSNDAFVLK	0.352	0.605	0.726	725.669	0.193	0.500	7.257	725.669	0.597	1.462
GPX3_HUMAN	P22352	Glutathione peroxidase 3	FLVGPDGIPIMR	0.061	0.110	0.087	87.274	0.158	0.368	0.873	87.274	0.113	0.294
HBB_HUMAN	P68871	Hemoglobin subunit beta	VNVDEVGGEALGR	0.021	0.050	0.073	72.694	0.020	0.055	0.727	72.694	0.014	0.042
HBD_HUMAN	P02042	Hemoglobin subunit delta (Delta-globin)	LLGNVLVCVLAR	0.031	0.062	0.043	43.273	0.964	1.892	4.327	43.273	0.062	0.174
HEMO_HUMAN	P02790	Hemopexin (Beta-1B-glycoprotein)	NFPSPVDAAFR	0.353	0.821	1.419	141.919	3.079	5.998	14.192	141.919	0.202	0.487
HEP2_HUMAN	P05546	Heparin cofactor 2	TLEAQLTPR	0.206	0.471	1.423	142.336	0.423	1.024	1.423	142.336	0.194	0.537
HPT_HUMAN	P00738	Haptoglobin	VTSIQDWVQK	1.257	2.523	2.810	280.985	0.416	1.009	2.810	280.985	0.002	0.005
HPTR_HUMAN	P00739	Haptoglobin-related protein	VGYVSGWGQSDNFK	0.356	0.897	1.935	193.534	0.167	0.489	1.935	193.534	0.287	0.848
HRG_HUMAN	P04196	Histidine-rich glycoprotein	GGEGTGYFVDFSVR	0.892	1.874	0.747	746.640	1.913	4.432	7.466	746.640	NA	NA
IC1_HUMAN	P05155	Plasma protease C1 inhibitor	LLDSLPSDTR	0.214	0.430	1.194	119.450	0.016	0.040	0.119	119.450	0.138	0.375
IGHA1_HUMAN	P01876	Ig alpha-1 chain C region	TPLTATLSK	0.306	0.536	0.902	90.164	0.130	0.294	0.902	90.164	0.204	0.576
IGHA2_HUMAN	P01877	Ig alpha-2 chain C region	DASGATFTWTPSSGK	0.176	0.416	0.460	459.580	0.596	1.433	4.596	459.580	0.014	0.034

IGHG1_HUMAN	P01857	Ig gamma-1 chain C region	GPSVFPLAPSSK	0.338	0.534	0.951	95.073	0.079	0.161	0.951	95.073	0.098	0.246
IGHG2_HUMAN	P01859	Ig gamma-2 chain C region	GLPAPIEK	0.380	0.758	1.208	120.768	0.104	0.262	1.208	120.768	0.072	0.180
IGHG3_HUMAN	P01860	Ig gamma-3 chain C region (HDC)	WYVDGVEVHNAK	0.559	1.416	1.916	1915.760	19.191	38.241	191.576	1915.760	0.055	0.125
IGHM_HUMAN	P01871	Ig mu chain C region	YAATSQVLLPSK	0.685	1.353	1.886	188.575	0.254	0.650	1.886	188.575	0.111	0.225
IPSP_HUMAN	P05154	Plasma serine protease inhibitor	TLYLADTFPTNFR	0.226	0.457	0.442	441.829	0.224	0.587	4.418	441.829	0.333	0.716
ITIH1_HUMAN	P19827	Inter-alpha-trypsin inhibitor heavy chain H1	AAISGENAGLVR	0.137	0.341	0.285	285.340	0.588	1.290	2.853	285.340	0.421	1.043
ITIH2_HUMAN	P19823	Inter-alpha-trypsin inhibitor heavy chain H2	FYNQVSTPLLR	0.533	1.244	1.279	127.856	0.762	1.920	12.786	127.856	0.121	0.351
ITIH4_HUMAN	Q14624	Inter-alpha-trypsin inhibitor heavy chain H4	ILDDLSPR	1.951	3.980	19.220	192.197	0.665	1.474	1.922	192.197	0.130	0.356
KAIN_HUMAN	P29622	Kallistatin (Kallikrein inhibitor)	LGFTDLFSK	1.599	3.175	3.407	340.747	0.182	0.400	3.407	340.747	0.222	0.485
KLKB1_HUMAN	P03952	Plasma kallikrein	IAYGTQGSSGYSLR	0.767	1.768	6.996	699.563	2.808	8.323	69.956	699.563	1.358	3.813
KNG1_HUMAN	P01042	Kininogen-1	YFIDFVAR	0.342	0.725	0.513	512.520	0.341	0.509	5.125	512.520	0.214	0.460
PEDF_HUMAN	P36955	Pigment epithelium-derived factor (PEDF)	ELLDTVTAPQK	0.374	0.941	1.680	167.968	0.707	1.842	16.797	167.968	0.486	1.112
PGRP2_HUMAN	Q96PD5	N-acetylmuramoyl-L-alanine amidase	AGLLRPDYALLGHR	2.527	5.333	21.019	210.192	4.702	12.254	21.019	210.192	0.028	0.078
PLF4_HUMAN	P02776	Platelet factor 4 (Oncostatin-A)	ICLDLQAPLYK	0.095	0.168	0.093	93.030	0.084	0.210	0.930	93.030	0.048	0.086
PLMN_HUMAN	P00747	Plasminogen	HSIFTPETNPR	1.162	2.522	13.376	1337.575	3.092	7.606	13.376	1337.575	1.762	4.632
PON1_HUMAN	P27169	Serum paraoxonase	LLIGTVFHK	2.290	4.871	16.754	167.541	3.225	5.661	16.754	167.541	0.245	0.524
PRG4_HUMAN	Q92954	Proteoglycan 4	GLPNVVTSAISLPNIR	1.697	2.759	1.349	1348.583	0.703	1.631	13.486	1348.583	0.903	1.813
RET4_HUMAN	P02753	Retinol-binding protein 4	FSGTWYAMAK	0.738	1.440	2.765	276.495	0.262	0.675	2.765	276.495	0.079	0.220
SAA4_HUMAN	P35542	Serum amyloid A-4 protein	EALQGVGDMGR	0.277	0.508	0.687	68.684	0.143	0.292	0.687	68.684	0.135	0.379
SEPP1_HUMAN	P49908	Selenoprotein P	LPTDSELAPR	0.316	0.620	2.114	211.412	0.324	0.642	2.114	211.412	0.196	0.477
SHBG_HUMAN	P04278	Sex hormone-binding globulin	IALGGLLFPASNLR	0.043	0.102	0.094	94.024	0.582	1.441	9.402	94.024	0.059	0.170
TETN_HUMAN	P05452	Tetranectin	LDTLAQEVALLK	0.122	0.296	1.329	132.863	0.043	0.072	0.133	132.863	0.047	0.099
THBG_HUMAN	P05543	Thyroxine-binding globulin (Serpin A7)	NALALFVLPK	0.130	0.297	0.232	232.488	0.083	0.204	2.325	232.488	0.193	0.431
THRB_HUMAN	P00734	Prothrombin	TATSEYQTFFNPR	0.536	1.356	1.477	1476.843	2.370	5.991	14.768	1476.843	3.096	8.583
TRFE_HUMAN	P02787	Serotransferrin	EGYYGYTGAFR	1.032	2.190	3.144	314.394	2.008	4.891	31.439	314.394	0.823	2.082
TTHY_HUMAN	P02766	Transthyretin	AADDTWEPFASGK	NA	NA	NA	NA	0.689	1.600	5.424	54.236	0.357	0.944
VTDB_HUMAN	P02774	Vitamin D-binding protein	HLSLLTTLSNR	0.370	0.779	2.021	202.141	0.525	1.455	2.021	202.141	0.443	1.317
VTNC_HUMAN	P04004	Vitronectin	FEDGVLDPDYPR	0.464	0.968	2.193	219.265	1.494	3.209	21.927	219.265	0.804	1.981
VWF_HUMAN	P04275	von Willebrand factor	ILAGPAGDSNVVK	0.732	1.711	2.920	2920.271	0.773	2.026	29.203	2920.271	2.336	6.136
ZA2G_HUMAN	P25311	Zinc-alpha-2-glycoprotein	AYLEEECPATLR	0.209	0.420	0.437	437.112	0.261	0.742	4.371	437.112	0.313	0.847
			MEDIAN	0.359	0.768			0.349	0.745			0.195	0.439
			AVERAGE	0.721	1.514			1.063	2.409			0.459	1.139

SUPPLEMENTAL TABLE 4:

	Nanoflow concentration (ug/mL)				Standard flow concentration (ug/mL)			
Proteins	**Average**	**SD**	**Min**	**Max**	**Average**	**SD**	**Min**	**Max**
A1AG1_HUMAN	273.978	97.386	88.176	767.027	289.685	109.295	83.121	820.878
A1AG2_HUMAN	153.128	42.185	54.665	276.891	160.734	48.612	55.326	314.885
A1AT_HUMAN	931.652	236.862	371.225	2102.659	997.558	264.572	369.888	2248.086
A1BG_HUMAN	112.953	22.911	45.416	195.347	103.775	22.689	36.332	180.305
A2AP_HUMAN	21.367	3.218	10.621	32.340	16.839	2.533	8.009	26.412
A2GL_HUMAN	14.400	5.382	4.420	53.817	12.527	4.880	4.035	47.748
A2MG_HUMAN				SIS missing				
AACT_HUMAN	191.167	48.326	72.469	730.090	182.711	48.254	69.375	740.588
ABCF1_HUMAN	3.753	1.403	1.038	8.915	2.329	1.084	0.355	10.573
AFAM_HUMAN	116.585	27.288	51.535	264.362	120.085	27.157	50.699	258.232
ALBU_HUMAN	29847.877	3611.924	17521.812	43305.750	35796.752	4732.333	22358.763	50593.131
AMBP_HUMAN	80.284	12.821	36.413	137.023	73.938	12.915	36.530	129.616
ANGT_HUMAN	48.553	13.383	2.384	154.880	40.914	11.542	18.169	136.694
ANT3_HUMAN	261.567	49.219	111.993	465.956	263.320	57.484	121.743	493.690
APOA_HUMAN	250.800	286.845	7.948	1859.563	220.425	266.944	4.794	1801.360
APOA1_HUMAN	2243.625	489.132	1134.769	4235.591	2484.866	608.083	1147.605	5255.154
APOA2_HUMAN	28.420	6.251	13.242	58.098	27.208	6.411	11.797	55.651
APOA4_HUMAN	56.129	15.445	18.127	136.960	52.817	15.021	14.577	136.566
APOB_HUMAN	1151.470	345.354	390.548	2466.532	1103.702	363.772	353.831	2526.697
APOC1_HUMAN	29.898	7.100	12.001	55.689	25.901	6.452	8.419	46.910
APOC2_HUMAN	16.248	6.968	2.795	58.254	13.928	6.307	2.324	52.773
APOC3_HUMAN	64.199	25.232	15.464	218.282	61.870	25.480	13.738	228.689
APOD_HUMAN	32.926	8.516	15.259	76.250	28.750	7.990	14.495	76.757
APOE_HUMAN	28.240	9.194	8.340	82.644	26.683	9.310	7.639	93.999
APOH_HUMAN		SIS peak problem			163.322	38.532	55.906	281.233
APOL1_HUMAN	16.628	4.562	5.391	36.497	14.743	3.951	4.804	32.756
APOM_HUMAN	13.193	2.681	5.234	23.442	11.269	2.437	5.134	20.091
B3AT_HUMAN	2.613	0.817	0.677	6.269	0.282	0.140	0.050	1.613
C1QB_HUMAN	16.767	2.988	5.649	41.273	16.724	3.077	5.852	30.569
C1QC_HUMAN	27.825	4.823	10.863	45.960	21.536	4.034	8.022	36.660
C1R_HUMAN	24.622	5.033	10.588	44.386	23.419	3.781	13.146	35.836
C1S_HUMAN	34.865	5.840	21.960	58.999	18.992	2.915	10.307	30.548
C4BPA_HUMAN	105.135	25.810	35.994	213.332	98.871	25.504	29.638	195.253
CBG_HUMAN	5.476	1.694	2.265	19.013	4.658	1.570	1.976	20.570
CD5L_HUMAN	15.180	7.886	2.975	78.019	13.800	7.590	2.598	80.200
CERU_HUMAN	1068.045	264.910	461.717	2367.225	1052.695	287.467	392.997	2083.961
CFAB_HUMAN	117.625	25.065	46.638	220.970	110.950	25.266	38.194	214.336
CFAH_HUMAN	161.337	52.426	28.562	456.069	189.738	34.407	111.013	296.185
CFAI_HUMAN	14.404	3.208	5.497	25.471	11.780	2.694	4.126	23.702
CLUS_HUMAN	134.876	21.284	61.655	198.616	127.653	23.121	61.348	203.888
CO2_HUMAN	23.261	4.060	10.222	35.937	16.760	3.035	6.444	28.749
CO3_HUMAN	1240.971	303.537	526.868	2892.228	1263.522	332.920	446.616	3127.835
CO5_HUMAN	58.367	10.732	26.470	105.652	51.658	9.467	21.083	92.208
CO6_HUMAN	26.280	5.965	6.368	44.627	23.130	4.821	8.462	40.623
CO7_HUMAN	56.616	26.515	3.668	369.429	49.430	25.484	2.960	399.596
CO8A_HUMAN	15.139	2.752	5.198	25.233	13.281	2.474	5.076	23.462
CO9_HUMAN	43.024	13.905	8.714	118.699	38.193	13.042	7.666	110.605
CPN2_HUMAN	26.062	6.188	11.870	54.602	21.535	5.364	8.983	43.613
F13A_HUMAN	18.849	5.276	5.071	43.477	15.246	4.349	4.481	36.728
FBLN1_HUMAN	9.912	3.175	1.928	22.797	7.228	2.184	1.989	16.286
FCN3_HUMAN	11.553	3.291	2.887	24.697	6.444	1.917	0.042	14.163
FETUA_HUMAN	175.930	29.978	75.445	276.129	166.563	29.148	69.220	268.305
FIBA_HUMAN	1461.558	371.805	179.064	3374.523	1597.170	424.602	184.489	3587.873
FIBB_HUMAN	1504.306	361.873	163.570	3263.127		wrong RT window		
FIBG_HUMAN	1085.956	267.720	128.788	2378.050	1153.478	297.871	112.881	2733.730
FINC_HUMAN	343.940	189.990	59.499	2538.839	320.357	195.786	45.230	2913.630
GELS_HUMAN	111.256	16.741	66.008	173.464	80.432	14.779	37.423	140.750

GPX3_HUMAN	4.716	0.956	2.355	7.586	3.723	0.760	1.731	6.822
HBA_HUMAN	22.509	23.172	3.013	271.033	24.906	26.341	3.247	294.509
HBD_HUMAN	2.599	2.301	0.516	24.153	2.153	1.939	0.247	21.033
HBE_HUMAN	0.993	3.186	0.134	31.789	0.525	0.109	0.267	1.105
HEMO_HUMAN	664.943	118.796	259.786	1025.541	646.288	121.821	222.314	1019.497
HEP2_HUMAN	47.783	9.729	18.168	80.693	41.571	9.132	14.822	72.280
HPT_HUMAN	1250.269	562.361	23.080	3855.210	1433.929	676.850	16.530	4985.870
HPTR_HUMAN	40.711	17.940	5.073	250.097	39.316	18.556	4.410	262.325
HRG_HUMAN	189.931	47.869	69.507	407.688	196.549	52.839	70.584	473.516
IC1_HUMAN	277.867	55.000	116.329	520.620	289.834	58.272	115.833	546.196
IGHA1_HUMAN	956.036	456.464	61.592	4339.298	1294.456	656.539	71.237	6705.435
IGHA2_HUMAN	127.000	77.929	13.826	757.461	112.845	79.103	0.766	779.548
IGHG1_HUMAN	5557.499	1886.299	2040.760	25013.172	6254.303	2223.804	2201.105	28236.605
IGHG2_HUMAN	2241.876	872.258	405.498	5345.709	2305.817	954.463	399.473	6083.937
IGHG3_HUMAN	577.374	245.615	166.819	2341.727	545.872	245.723	120.910	2306.035
IGHG4_HUMAN	797.155	686.325	3.363	4997.327	895.961	799.821	7.041	6297.100
IGHM_HUMAN	865.949	632.629	145.548	9182.313	944.944	759.086	156.260	12047.425
IGJ_HUMAN	34.798	18.469	7.294	210.097	33.563	19.134	7.488	230.792
ITIH1_HUMAN	92.540	16.074	1.848	141.905	86.612	16.168	0.378	136.352
ITIH2_HUMAN	248.962	44.436	102.898	408.489	246.662	50.109	84.643	426.426
ITIH4_HUMAN	226.744	71.299	22.076	447.146	223.637	72.469	20.231	458.562
KLKB1_HUMAN	31.731	7.155	6.645	60.502	30.247	6.529	7.100	55.877
KNG1_HUMAN	176.877	29.257	111.625	319.207	166.871	28.358	102.994	332.672
MBL2_HUMAN	0.349	0.220	0.038	1.475	0.267	0.171	0.024	1.193
PEDF_HUMAN	16.531	3.949	6.793	32.835	10.938	2.704	3.855	23.073
PGRP2_HUMAN	54.927	9.489	32.825	94.089	33.701	6.058	18.155	52.141
PLF4_HUMAN	0.612	0.406	0.137	5.556	0.384	0.349	0.056	4.122
PLMN_HUMAN	153.924	25.179	23.527	265.009	154.423	25.607	24.967	253.143
PON1_HUMAN	31.670	9.547	8.318	73.051		wrong RT window		
RET4_HUMAN	49.548	14.642	17.654	156.953	45.673	13.944	10.879	145.573
SAA4_HUMAN	26.766	7.331	1.074	52.762	25.101	7.271	0.511	56.253
SEPP1_HUMAN	4.365	0.936	1.895	8.316	3.702	0.734	1.388	5.965
SHBG_HUMAN	5.628	2.701	1.071	17.535	5.243	2.472	1.342	18.410
STOM_HUMAN	0.998	0.448	0.259	3.109	0.173	0.138	0.002	1.889
TETN_HUMAN	6.796	1.242	3.062	10.846	6.117	1.137	2.987	9.418
THBG_HUMAN	10.618	2.630	2.640	23.888	8.970	2.210	2.471	17.271
THRB_HUMAN	136.630	27.319	46.466	265.002	145.120	29.609	43.610	259.316
Total IGHG	9050.800	2197.207	2995.452	22761.999	10136.147	2582.882	3398.767	24142.232
TRFE_HUMAN	1686.141	294.745	793.800	2915.196	1793.694	327.922	987.705	3063.628
TTHY_HUMAN	56.336	18.314	15.944	131.699	44.653	15.820	9.640	119.418
VTDB_HUMAN	345.845	66.240	171.631	559.691	368.598	74.985	188.409	662.881
VTNC_HUMAN	154.421	26.624	75.181	254.593	149.864	27.323	73.685	269.201
ZA2G_HUMAN	32.305	6.274	15.506	76.090	28.541	6.000	12.947	71.777